Submerged Fossil Corals: Archives of Diagenesis, Subsidence and Sea level

A DISSERTATION
SUBMITTED TO THE FACULTY OF THE GRADUATE SCHOOL
OF THE UNIVERSITY OF MINNESOTA
BY

Kristin Emigh Riker-Coleman

IN PARTIAL FULFILLMENT OF THE REQUIREMENTS
FOR THE DEGREE OF
DOCTOR OF PHILOSOPHY

Dr. Christina Gallup

December 2008

© Kristin Emigh Riker-Coleman 2008

Acknowledgements

This work began with a quick email/phone call exchange with my advisor, Dr. Christina Gallup; I never dreamed it would be such a long journey. I'd like to acknowledge her support of my pursuit of a career and a family. Christina was willing to train me herself in the lab, to run samples when I couldn't and to remind me to just sit down and do it. Thanks to Christina for her work as my graduate advisor – it couldn't have been an easy job.

There are numerous people I'd like to acknowledge here that interacted along this very long journey. My friends from UMD provided countless hours of conversation, inspiration to get out and enjoy life in Northern Minnesota and to ask questions about the science: Nick Lang, Leah Gruhn, Jere Mohr, Joy Turnbull, Keely Pearson, and John Swenson. Dean Peterson and Deb Rausch, and their daughter Elizabeth have opened their home and their hearts to both my family and me. Carol Koos, Miranda Pilon and Stephanie Carlson are my nonscientist friends -- without their love, support and childcare I wouldn't have been able to finish this project. Stacy Holden brought love and light to Duluth and challenged me to develop a sense of community wherever I am, whatever I am doing. Anne Pilli provided me with a mantra for answering my self-doubt: "Kristin you *can* do this, you *are doing* this."

Erik, my husband, who in the beginning was so willing to follow me to Duluth to begin this crazy degree program and in the end was so willing to push me out the door to get to work at the lab, thank you for your love and support. Our daughter Erin, who challenges me to be "more" in every aspect of parenting her, taught me how to be a good parent. Our daughter Leah is a constant reminder of the nurturing person I hope to be as a parent. Without my family I'm not sure I would be the whole person that I am.

My mom, Carol, got me interested in science and my dad, Chris, taught me to keep working at something, even if it is hard.

My research in Papua New Guinea was supported by a grant from the National Science Foundation to Christina and Dr. Eli Silver and Dr. Don Potts from the University of California Santa Cruz. Dr. Jody Webster collected the samples from New Britain and provided numerous hours of conversation about the corals from each of my sites. My work in Hawaii was supported by the Monterey Bay Aquarium Research Institute. Dr. David Clague's research group collected the samples. I received a small block grant from the graduate school. Dr. Hai Cheng helped me with the technical aspects of running samples on the mass spectrometer and Dr. Penny Morton, Dr. Andy Breckenridge, and Abby Hudler helped with Xray diffraction.

Dedication

This dissertation is dedicated to Erin, Leah and Erik.

Abstract

Corals are well suited as absolute markers of sea-level. Given the modern elevation of the coral, the age of coral, sea level at the coral's time of death, and the paleogrowth position of a fossil corals allow one to compute a vertical tectonic rate of motion; if the tectonic rate is known then one can use the sample's location, paleogrowth position, and age to compute a paleosea level. I studied the uranium-series isotopic composition of fossil corals from three settings: New Britain, Papua New Guinea, Hawaii and the Huon Gulf, Papua New Guinea. These three settings are distinct in their tectonic setting: New Britain corals are emergent as a result of tectonic uplift and the Hawaiian and Huon corals are submergent.

Corals samples from uplifted terraces in New Britain are highly altered due high rainfall rates in the area. The measured ^{230}Th ages of corals from the Holocene terrace are between 4.3 ± 0.03 ka to 9.0 ± 0.16 ka. Using these ages, their present elevation and the corresponding paleo sea level, I computed an average uplift rate of 1.6 ±0.4 m/ka.

Uranium-series isotopic compositions of submerged corals are not better preserved than their subaerially exposed counterparts, although their diagenetic signatures differ. I report ^{230}Th ages of three fossil reefs from the northwestern coast of Hawaii: the -400 m reef at Mahukona (136.7 ± 0.9 ka to 151.8 ± 1.7 ka), the –1000 m terrace off eastern Kohala (377.2 +13.4/-12.2 ka and 392.5 +20.5/-17.9 ka) and the -1000 m reef off northwestern Kohala (286.5 ± 1.4 ka to 342.8 ± 1.4 ka). From the submerged Hawaiian samples I identify three main trends in uranium-series isotopic composition: (1.) An increase in both 230Th/238U and 234U/238U; (2.) an increase in

230Th/238U with little change in 234U/238U; and (3.) low 230Th/238U with both low and high 234U/238U.

Measured ^{230}Th ages of submergent coral samples from the Huon Gulf range from 60 ka to infinite age (>600 ka). The measured ^{230}Th ages of coral samples are older than we expected, but broadly increase in age with depth. Corals from three terraces (-1280 m, -1650 m, and -1950 m) represent material from Stage 11, suggesting that the model of terrace development is likely more complex than the original idea of a distinct sea-level rise event per terrace. Although I am able to identify three main trends in the uranium-series isotopic compositions of the Hawaiian samples, no clear trend emerges in the Huon Gulf setting. The subsidence rate (m/ka) computed from the most reliable ages of the deepest terraces suggests that the subsidence in the Huon Gulf averages 4 m/ka.

Table of Contents

Chapter 1: Introduction	1
1.2 Modeling:	6
1.3 Dissertation Design:	8
1.4 Study Site: Tectonic Setting of Huon Gulf, Papua New Guinea	8
1.5 Study Site: Geologic Setting of NB, PNG	10
1.6 Study Site: Geologic Setting of Hawaii	11
1.7 Organization of this Document	11
1.8 References in the Introduction	13
Chapter 2: New Britain	20
Chapter 3: Uranium series data from Submerged Coral Reefs of Hawaii: Diagenetic Changes, Sea Level, and Subsidence	34
Abstract:	34
1.0 Introduction:	35
1.1 Geologic Setting:	36
1.2 Previous Work:	37
2.0 Sample Sites:	40
3.0 Methods and Results:	41
4.0 Discussion:	44
4.1 Diagenesis: Calcite Content	44
4.2 Trends in Isotopic Composition	47
4.2.1 Modeling Trends in Isotopic Composition	48
4.3 Discussion: Timing of Reef Drowning	54
4.4 Discussion: Subsidence:	54
4.5 Discussion: Magnitudes of Sea Level	56
5.0 Conclusions	57
6.0 Acknowledgements	58
7.0 References	58
Chapter 4: A riddle wrapped up in an enigma: uranium series data (and a few) ^{230}Th ages of corals from the Huon Gulf	69
1.0 Introduction	69
2. Setting of the Huon Gulf	70
2.1 Tectonic Setting of the Huon Gulf	70
2.2 Models of reef development	70
3. Sample Collection and Methods	72
3.1 Samples	72
3.2 Methods	73
4 Results	75

4.1 Hand sample/subsampling observations:	75
4.2 Uranium-series measurements:	76
5. Discussion of Initial Results	79
6 Experimenting With Chemical Cleaning Protocols	80
6.1 EDTA Pre-cleaning	80
6.2 Foram cleaning protocol/Deep Sea Coral Protocol:	82
6.3 Selective Dissolution	84
6.4 Grain Size experiment	87
6.5 Final Sampling Protocol	90
7.1 Discussion: Geochemistry	93
7.1.1 Thorium Content	94
7.1.2 Calcite Content	96
7.1.3 Other Trends in U-Series Data – Lack of trends in U-Series Data	98
7.2 Discussion: Resolving the Age of the Samples	99
7.3 Discussion: Subsidence	102
7.4 Discussion: Documentation of Stage 11	104
8.0 Conclusions	105
9.0 References	106
Chapter 5: Conclusions	129
Bibliography	134

List of Tables

3.1	Age data from Hawaiian coals	67
3.2	Modeling results from Hawaii	68
4.1	Results from Huon Gulf	124
4.2	Protactinium data	127
4.3	Predicted and observed terrace locations	128

Table of Figures

1. 1	Sea level records from coral	18
1. 2	Tectonic setting of Huon Gulf and New Britain.	19
2.1	(a) Tectonic setting of New Britain. (b) Sample locations in the Jacquinot Bay field area.	32
2.2	Cross section of regional seismicity	33
3.1	Hawaii and offshore bathymetry, showing sample locations	62
3.2	$^{234}U/^{238}U$ activity vs. $^{230}Th/^{238}U$ activity for Hawaiian corals.	63
3.3	Age vs. relative age difference between modeled age and theoretical age for calcite-replacement model	65
3.4	A). July insolation at 65°N [44]. B). Our reliable ages and their errors. C). Siddall et al. sea level record based on a Red Sea salinity record of $\delta_{18}O$.	66
4.1	Tectonic Setting of the Huon Gulf	110
4.2	Data from the deepwater coral cleaning protocol	111
4.3	Data from the grainsize experiments	115
4.4	Data from the selective dissolution experiments	118
4.5	Evolution Plot for all samples measured from Huon Gulf	121
4.6	Depth vs. measured age for samples from the Huon Gulf	122
4.7	Bathymetry of the Huon Gulf	123

Chapter 1: Introduction

As sea-level markers with absolute chronologies, reef-building or hermatypic corals are well suited for determining the timing of rapid changes in global ice volume. Coral skeletons that grew in the last ~40 ka can be dated using radiocarbon techniques and those that grew in the last ~650 ka can be dated, in principle, using uranium-series methods. Because hermatypic corals contain symbiotic yellow-green algae, called zooxanthellae, within their cells, the growth range of hermatypic corals is generally restricted to depths of less than 100 meters (within the photic zone) and to tropical and subtropical waters. Different species of hermatypic corals thrive in different environments, resulting in a characteristic zonation of species within a reef environment according to water depth and distance from the reef crest (e.g. Goreau, 1959). Coral species that grow in a narrow depth range and near the sea surface provide the best sea-level markers.

Uranium-series dating of fossil corals has made it possible to document both tectonic rates and sea-level change. Tectonic constraints from fossil corals allow for evaluation of the direction of motion coupled with an absolute chronometer to provide a rate of motion. Studies such as (Hilman Natawidjaja et al., 2007) have evaluated uplift rates from coral terraces in the context of GPS data to evaluate three-dimensional tectonic rates of motion. Other studies such as Ota et al. (1996) and Taylor et al. (1987) document magnitudes of coseismic uplift associated with earthquake events. Likewise, coral records document rate of subsidence for the island of Hawaii (Ludwig et al., 1991).

Studies going as far back as the 1960s (e.g. Broecker, 1963; Broecker et al., 1968) show that fossil corals provide a sea level record that can be used to test theories for the ice ages. The major theory for what drives the glacial cycles is called the Milankovitch Theory. This theory proposes that the amount of summer insolation received at high northern latitudes is the dominant control on the advance and retreat of Earth's ice-sheets. Variations in the Earth's eccentricity, axial tilt, and precession collectively control the amount of insolation received by the Earth and these three dominant cycles are collectively known as the Milankovitch Cycles, after Milutin Milankovitch, the Serbian astronomer who is generally credited with calculating their magnitude. A geologic record of ice volume oscillations on a high-precision, absolute timescale is required to reliably test the Milankovitch Theory. Numerous researchers (e.g Broecker and van Donk, 1970; Hays, 1976) have documented Milankovitch frequencies in marine sediment data. Since there is no reliable, precise chronometer for these types of records beyond the limits of radiocarbon (roughly 60,000 years), corals are better suited than other marine sediments for testing the Milankovitch Theory.

Whether for sea level or tectonic studies, corals are excellent sea-level markers because they provide a dateable snapshot of relative sea level on a tectonically active shoreline. The modern elevation of a fossil coral sample is a function of age, uplift rate and sea level and can be represented by the equation: $H_i = u_i T_i + (SL_i + PG)$, where H_i = the present elevation of coral i (m), u_i = uplift or subsidence rate of coral i averaged over the time period since the reef grew (m/ka), T_i is the age of the coral (ka), SL_i is the eustatic sea level at which coral i grew (m), and PG is the paleowater depth of the coral

(given in meters relative to sea level). Given a well-constrained uplift/subsidence rate, then the equation can be solved to compute a paleo sea-level:

$$SL_i = H_i\text{-}PG - u_i T_i \ .$$

If the tectonic rate is not well-constrained and the paleo sea-level at T_i, the time at which the coral i grew, is well-constrained, one can solve for the tectonic rate:

$$u_i = (H_i\text{-}PG - SL)/ T_i.$$

If neither sea-level nor tectonic rate are constrained, then it is necessary to use data from more than one terrace. If two corals, i and j, are both from the same shoreline yet differ in age and elevation and if sea-level is constrained for coral i, then it is possible to solve for a tectonic rate using coral i and to then use that tectonic rate to find a paleo sea-level for coral j. In the absence of both a well-constrained subsidence rate and a well-constrained sea level, the argument becomes circular: one cannot compute both a subsidence rate and a paleo sea-level from one data point.

Whether one can gain paleo sea-level information, tectonic rate, or both from a suite of coral sample ages must be determined on an individual basis. In this study, I present one case (New Britain, Chapter # 2) where sea level (SL) is well constrained for the time period of interest. Using the age of the New Britain corals (T_i) and their paleogrowth depth (PG) I can compute an uplift rate (u_i). For one of my study areas (Hawaii, Chapter # 3), I use coral ages from one terrace to compute a subsidence rate and then apply that subsidence rate to another terrace to compute a paleo sea level. And finally, for my third study location (Huon Gulf, PNG, Chapter # 4), I could potentially follow the same technique as Hawaii but the Huon Gulf may present a more complicated tectonic history than what preliminary modeling would suggest.

The best sea level records come from tectonically active shorelines because the tectonic motion helps to separate corals of different ages into distinct terraces, rather than superimpose corals of different ages on the same location. Much of the record of the timing and magnitude of sea-level changes associated with glacial cycles comes from uplifted corals exposed on tectonically emergent coastlines, mainly from Barbados (Bard et al., 1990; Bender et al., 1979; Edwards et al., 1987; Gallup et al., 2002) and from Papua New Guinea (PNG) (Chappell, 1974; Chappell, 1996; Cutler, 2003; Esat et al., 1999; Stein, 1993). Oscillating sea level superimposed on the slowly rising shoreline produces coral terraces. Reefs grow during periods of stable relative sea level; continuous tectonic uplift separates the reefs into a series of coral terraces. Edwards et al. (2003) summarize the best of the fossil coral sea-level record for the last 450 ka (see Figure 1). High sea-level events recorded by fossil corals support the Milankovitch theory's predictions: high sea-level events coincide with or postdate the timing of summer insolation at high latitudes. The emergent coral record is biased toward high sea-level events – high sea level today means that corals growing during low or intermediate sea level are below sea level and not easily accessible.

Under conditions of slowly varying eustatic sea level, the growth rate of corals on a subsiding margin can match the rise in relative sea level and generate a large carbonate platform, even on a rapidly subsiding margin (Galewsky, 1996; Wallace, 2002; Webster et al., accepted, in revision). However, when eustatic sea-level rise is very rapid, the corals drown because relative sea-level rise is too rapid for skeletal growth to keep up and the corals move out of the photic zone. A subsiding margin

continues moving the (now drowned) coral platform still further from the photic zone. A new platform establishes itself in the new photic zone window of depth.

Unlike the fossil coral record from stable (e.g., Great Barrier Reef) and uplifted settings (e.g., Huon Peninsula, Barbados), submerged reefs from the Huon Gulf, Papua New Guinea and from Hawaii are thought to be mainly glacial reefs that developed in response to rapid subsidence (~2-6 m/kyr) (Galewsky, 1996; Ludwig et al., 1991; Wallace, 2002; Webster et al., accepted, in revision). Submerged reefs develop during periods of Earth's sea level and climate history (i.e., glacial periods, early deglaciations), that are inadequately sampled by reefs in stable and uplifting tectonic settings. Depending upon the relationship between eustatic sea-level changes and reef growth, rapid subsidence ensures accommodation space is continually created, thus generating greatly expanded stratigraphic sections compared to reefs from stable and uplifting tectonic settings. Moreover, the tops of the terraces may represent material that was growing during or just immediately prior to a glacial termination – a time period representing the transition from glacial to interglacial conditions (a period of time when relative sea-level rise (due to the combination of subsidence and eustatic sea-level rise) exceeds the growth rate of the coral).

One of the biggest challenges that coral sea-level studies have faced is demonstrating the accuracy of the uranium-series ages. It was recognized early on (Bender et al., 1979) that exposure to meteoric waters has altered many emergent (exposed) corals, resulting in their shifted uranium-series isotopic compositions. Several studies have suggested that submerged fossil corals that have never been subaerially exposed are far more likely to be pristine than those that have been exposed (Edwards et

al., 1993; Edwards et al., 1991). My dissertation project represents the first large-scale test of the hypothesis that submerged fossil corals remain better preserved with regards to their uranium-series isotopes than emergent fossil corals do.

Demonstration of the accuracy of uranium-series coral ages requires confidence in the assumption that the coral has remained a closed system to the uranium-series isotopes in question. Previous workers (e.g. Cutler, 2003; Gallup et al., 2002; Gallup et al., 1994; Henderson and Slowey, 2000; Thurber et al., 1965) have used a selection of specific criteria for deciding whether an age is reliable (and to evaluate that closed-system behavior). These criteria include: coral has <2% calcite, a uranium concentration within range of modern corals (2-3 ppm), a $^{230}Th/^{232}Th$ activity ratio less than 20, and a $\delta^{234}U_i$ values within error of modern seawater (145.8 ± 1.7 ‰) (Cheng et al., 2000). Corals are originally deposited as aragonite. Thurber et al. (1965) suggested that a measureable amount of calcite (generally 2-3%) indicates that the sample has been recrystallized to some degree and that the ^{230}Th age may not be reliable. Calcite content can either come from recrystallization of original skeletal material or from addition of new material (such as cements). Based upon my work in Hawaii (see Section 2 of this thesis), I suggest that the <2% criterion might be expanded to <20% in some submerged settings. Additionally some workers (Cutler, 2003) have used high-precision techniques for ^{231}Pa dating to test ^{230}Th ages for concordancy.

1.2 Modeling:

Collecting, subsampling, and measuring a coral's isotopic composition is a huge task; yet a large number of coral samples that appear to look unaltered do not meet the

reliability criteria listed above. In an effort to better understand the geochemical alteration of these corals and to evaluate their usefulness as geochronometers, a variety of open-system models have been developed. Gallup et al. (1994) were the first to include diagenetic addition terms in the differential equations describing U-series decay. Gallup et al. estimated the rate of addition of ^{234}U and ^{230}Th using the U/He age and U/Th isotopic composition of a coral with $^{234}U/^{238}U$ and $^{230}Th/^{238}U$ ratios that could not be explained by closed-system evolution. Henderson et al. (2002; 2001) showed that alpha-recoil had significant effects on the isotopic composition of marine carbonate sediments, and made the first attempt to quantify the physical process of alpha-recoil in U-series decay equations. Combining these two ideas, Thompson et al. (2003) derived equations to account for the coupled addition of ^{234}U and ^{230}Th to fossil corals. The Thompson model uses the systematics of U-series decay with appropriate physical and geochemical constraints, not the empirical assessment of model parameters from selected data (which distinguishes their approach from Gallup et al.). Villement and Feuillet (2003) proposed a similar, yet slightly different model of alpha recoil controlled diagenesis that accounts for continuous selective redistribution (gain or loss) of ^{234}U, ^{234}Th and ^{230}Th and also can include excess initial ^{230}Th. Both the Thompson et al. and Villement and Feuillet models show that recoil processes tend to increase $^{234}U/^{238}U$ and $^{230}Th/^{234}U$ ratios with time, leading to an overestimation of the apparent age of the sample. These models present an alternative way to date old reef terraces with systematic alteration. However, Andersen et al. (2008) provide evidence to suggest that both the Villemant and Feuillet model and the Thompson model are limited for older samples, indicating additional diagenetic mechanisms at work beyond alpha recoil. I

applied the Villemant and Feuillet model to the submerged coral data from Hawaii in order to try to model diagenetic alteration

1.3 Dissertation Design:

My dissertation research project was designed to use submerged coral platforms to construct a high-precision, absolute chronology for glacial terminations during the last 400 ka. My aim was to use data from a suite of corals of varying age to look specifically at the existing theories regarding the timing of glacial terminations. My project set out to test whether submerged corals are better preserved than their uplifted counterparts and to document the timing of the past several glacial terminations. To do so, I selected one primary location: the Huon Gulf, Papua New Guinea. Several months after we collected corals from Huon Gulf, I began working on the samples from Hawaii, a second submerged site. Finally, as commonly happens when scientists gather, they often begin talking about scientific ideas and proposing new projects: my work on New Britain is an outgrowth of the Huon Gulf project –Dr. Jody Webster (now at the University of Sydney, then at the University of Papua New Guinea) collected these corals on a preliminary assessment of the terraces of New Britain.

1.4 Study Site: Tectonic Setting of Huon Gulf, Papua New Guinea

In August and September 2001, I was part of a team of scientists from the University of Minnesota Duluth (UMD), the University of California at Santa Cruz (UCSC), and the University of Papua New Guinea that collected reef material, including many fossil corals, from a series of submerged coral platforms in the Huon

Gulf, Papua New Guinea (PNG). These corals are the submerged counterparts to the well-studied corals on the Huon Peninsula (Chappell, 1974; Esat et al., 1999). We collected over two tons of samples from the tops of nine carbonate platforms between 300 and 2600 meters of water depth. These samples were collected, in part, because the unique combination of tectonic subsidence and sea level oscillations in this area was thought to be promising for recording glacial terminations.

PNG occupies the eastern half of the larger island of New Guinea. Much of the island sits on the northern margin of the Australian plate, which is actively colliding with the Huon-Finisterre terrane (Abbott et al., 1994) (Figure 2). Onshore this collision manifests itself in the Ramu-Markham fault; offshore collision is a subduction zone, located in the Huon Gulf. The modern tip of collision lies in the western Solomon Sea at about 147°E (Crook, 1989; Davies et al., 1987; Silver, 1991). West of 147°E (the western portion of the country of PNG) consists of an actively growing mountain system where the Bismarck forearc has thrust over the Australian continental margin (Abbott et al., 1994). The Huon-Finisterre Mountains, with present elevations of 4 km, and the Huon Peninsula, where a series of highly studied reefs are found (e.g. Chappell, 1974; Esat et al., 1999), are direct products of this collision.

Galewsky et al. (1996) and Wallace (2002) modeled the development of these reefs and suggest that under conditions of slowly varying eustatic sea level, the growth rate of corals on the subsiding Australian plate can match the rise in relative sea level and generate a large carbonate platform. However, during glacial terminations, the corals drown because sea-level rise is too rapid for skeletal growth to keep up. Following sea level rise, continued subsidence moves the drowned coral out of the

photic zone and a new platform establishes itself in the new photic zone window of depth. Each major glacial termination should in turn produce a carbonate terrace, the tops of which contain material documenting the beginning of the glacial termination. Thus looking at the timing of drowning of the terraces from the tops of the terraces could provide information about a series of glacial terminations.

The Huon Gulf represents an area with the prospect of obtaining very good control on tectonic rates. Uplift rates from Huon Peninsua on the Huon-Finisterre terrane (e.g.Chappell, 1974; Esat et al., 1999) and convergence rates between the South Bismarck plate and the Australian plate (76 km/Ma at the Huon Gulf based upon recent GPS observations (Tregoning, 1999; Wallace, 2004)) are well constrained. Submerged coral samples could provide the missing subsidence rate and allow for comparison between the uplift rate, the subsidence rate, and the convergence rate.

1.5 Study Site: Geologic Setting of NB, PNG

New Britain (NB) is an elongate 450 km long island in the Papua New Guinea archipelago paralleling the New Britain Trench (Figure 2). The coastline of NB and the coastlines of most of the islands of PNG including those of the Huon Peninsula (HP), contain a series of raised carbonate terraces. The HP and NB terraces are both likely the result of tectonic uplift but, while tectonic uplift of the HP is due to collision between the Finisterre volcanic arc and the continental New Guinea Highlands (Pigram, 1987), uplift in eastern NB is likely due to processes related to subduction of the oceanic Solomon Sea Plate beneath the South Bismarck Plate along the NB Trench.

1.6 Study Site: Geologic Setting of Hawaii

The Hawaiian Archipelago is a northwest to southeast trending group of nineteen islands and atolls located in the center of the Pacific Plate, of which Hawaii is the southernmost and youngest island (Figure 3). Hawaii is a composite of at least five young volcanic mountains, two of which are currently active (Campbell and Erlandson, 1981; Webster et al., 2007). Lithospheric loading associated with continued volcanism over the Hawaiian hotspot during the last 500 ky is thought to generate the subsidence that Hawaii is currently experiencing (Campbell and Erlandson, 1981; Moore, 1987).

The island of Hawaii is surrounded in coral terraces. Models of formation suggest that the terraces form during lowstands preceding glacial periods and the corals continue to persist so long as the rate of relative sea-level change is less than the vertical growth rate of the coral (Moore and Campbell, 1987; Moore and Fornari, 1984; Webster et al., 2007). Similar to the Huon Gulf model of formation, corals drown during rapid sea-level rise. Following a drowning event, coral reestablishes itself landward of the drowned terrace, while the original terrace continues to move to deeper water.

1.7 Organization of this Document

Finally, I include a note on the structure of this work. It is organized into three main sections, followed by a conclusion. The first two sections are intended as journal articles in their entirety. The first section, on emergent corals from New Britain, Papua New Guinea, was published in 2006 in *Geophysical Research Letters* (Riker-Coleman et al., 2006). Dr. Jody Webster collected the coral samples with the help of two

undergraduate students from the University of Papua New Guinea. Dr. Laura Wallace, of GNS Science, New Zealand, provided the tectonic expertise and Dr. Webster identified the coral samples and provided the sedimentological setting. The second section is an article about submerged corals from the island of Hawaii, to be submitted to the *Journal of Earth and Planetary Science Letters*. Researchers in Dr. David Clague's research group at the Monterey Bay Aquarium Research Institute collected the Hawaiian corals. Dr. Jody Webster spent a considerable amount of time placing them into a sedimentological setting, and with the help of Dr. Don Potts (from the University of California at Santa Cruz, UCSC), identifying their taxonomy. Dr. George Burr at the NSF Arizona AMS Laboratory at the University of Arizona did the radiocarbon dating on those samples. One subset of those samples (from the -150 m reef) was published (Webster et al., 2004a), linking the drowning of the -150 m reef to Meltwater Pulse 1A. Additionally Webster and Wallace (2007) numerically modeled the growth and drowning of the Hawaiian reefs over the last 250,000 years, using my preliminary data as a very rough test of their model. The third section of my dissertation represents a summary of my work on submerged corals from the Huon Gulf, Papua New Guinea. This third section is a summary of my work thus far, including detailed description of laboratory experiments I have done. Dr. Hai Cheng (University of Minnesota) measured the protactinium isotopic composition of six of the Huon samples and Dr. Christina Gallup (University of Minnesota Duluth) performed one of the preliminary laboratory experiments on the Huon samples. The Huon corals were collected as a part of a larger cooperative project, some of which has already been published. In 2004, Webster took the lead on a discussion of the sedimentology of the reefs and their drowning signature

(Webster et al., 2004b; Webster et al., 2004c). The preliminary (modeled) age data from Hawaii and the Huon Gulf, coupled with their sedimentological records was used to characterize coral reef evolution on rapidly subsiding margins (Webster et al., accepted, in revision). These models are premature because they do not include my best estimates of age, which are included within this dissertation.

In the conclusions of the individual chapters I make some comments on what we learn in each instance from the fossil coral record. In the overall conclusion section of my dissertation, I summarize the differences I identify between working on emergent corals and submerged corals and I attempt to answer the question: *Are submerged corals better preserved than their emergent counterparts?*

References in the Introduction

Abbott, L.D., Silver, E.A., and Galewsky, J., Silver, E.A., Gallup, C.D., Edwards, R.L., and Potts, D.C., 1994, Structural evolution of a modern arc-continent collision in Papua New Guinea: Tectonics, v. 13, p. 1007-1034.

Andersen, M.B., Stirling, C.H., Potter, E.-K., Halliday, A.N., Blake, S.G., McCulloch, M.T., Aylin, B.F., and O'Leary, M., 2008, High-precision U-series measurements of more than 500,000 year old fossil corals: Earth and Planetary Science Letters, v. 265, p. 229-245.

Bard, E., Hamelin, B., and Fairbanks, R.G., 1990, U-Th ages obtained by mass spectrometry in corals from Barbados: sea level during the past 130,000 years: Nature, v. 346, p. 456-458.

Bender, M.L., Fairbanks, R., Taylor, F.W., Matthews, R.K., Goddard, J.G., and Broecker, W., 1979, Uranium-series dating of the Pleistocene reef tracts of Barbados, West Indies: Geological Society of America Bulletin, v. 90, p. 577-594.

Berger, A., and Loutre, M.F., 1991, Insolation values for the climate of the last 10 million years: Quaternary Science Reviews, v. 10, p. 297-318.

Broecker, W., 1963, A preliminary evaluation of uranium series inequilibrium as a tool for absolute age measurements on marine carbonates: J Geophysical Research, v. 68, p. 2817-2834.

Broecker, W., Thurber, D., Ku, J.G.T.-l., Matthews, R.K., and Mesolella, K.J., 1968, Milankovitch Hypothesis Supported by Precise Dating of Coral Reefs and Deep-Sea Sediments: Science, v. 159, p. 297-300.

Broecker, W., and van Donk, J., 1970, Insolation changes, ice volumes and the 18O record in deep-sea cores: Rev. Geophys., Space Phys., v. 8, p. 169-197.

Campbell, J.F., and Erlandson, D.L., 1981, Geology of the Kohala submarine terrace, Hawaii: Marine Geology, v. 41, p. 63-72.

Chappell, J., 1974, Geology of coral terraces, Huon Peninsula, New Guinea: A study of Quaternary tectonic movements and sea-level changes: Geological Society of American Bulletin, v. 85, p. 553-570.

—, 1996, Reconciliation of late Quaternary sea levels derived from coral terraces at Huon Peninsula with deep sea oxygen isotope records: Earth and Planetary Science Letters, v. 141, p. 227-236.

Cheng, H., Edwards, R.L., Hoff, J., Gallup, C.D., Richards, D.A., and Asmerom, Y., 2000, The half-lives of uranium-234 and thorium-230: Chemical Geology, v. 169, p. 17-33.

Crook, K., 1989, Suturing history of an allochthonous terrane at a modern plate boundary traced by flysch-to-molasse facies transitions: Sedimentary Geology, v. 61, p. 49-79.

Cutler, K., 2003, Rapid sea-level fall and deep-ocean temperature change since the last interglacial period Earth and Planetary Science Letters, v. 206, p. 253-271.

Davies, H., Honza, E., Tiffin, D., Lock, J., Okuda, Y., Keene, J., Murakami, F., and Kishimoto, K., 1987, Regional setting and structure of the western Solomon Sea: Geo-marine letters, v. 6, p. 181-191.

Edwards, R.L., Beck, J., Burr, G.S., Donahue, D.J., Chappell, J.M., Bloom, A.L., Druffel, E.R.M., and Taylor, F.W., 1993, A large drop in atmospheric 14C/12C and reduced melting in the Younger Dryas, documented with 230Th ages of corals: Science, v. 260, p. 962-968.

Edwards, R.L., Chen, J.H., and Wasserburg, G.J., 1987, U-238-U-234-Th-230-Th-232 systematics and the precise measurement of time over the past 500,000 years.: Earth and Planetary Science Letters.

Edwards, R.L., Gallup, C.D., and Cheng, H., 2003, Uranium-series dating of marine and lacustrine carbonates, *in* Bourdon, B., Henderson, G.M., Lundstrom, C.C., and Turner, S.P., eds., Uranium-series Geochemistry, Volume 52: Reviews in Mineralogy and Geochemistry, p. 363-405.

Edwards, R.L., Gallup, C.D., Taylor, F.W., and Quinn, T.M., 1991, 230Th/238U and 234U/238U in submarine corals: Evidence for Diagenetic Leaching of 234U: Eos (Transactions, American Geophysical Union), v. 72, p. 535.

Esat, T.M., McCulloch, M.T., Chappell, J., Pillans, B., and Omura, A., 1999, Rapid fluctuations in sea level recorded at Huon Peninsua during the penultimate deglaciation: Science, v. 283, p. 197-201.

Galewsky, J., Silver, E.A., Gallup, C.D., Edwards, R.L., and Potts, D.C. , 1996, Foredeep tectonics and carbonate platform dynamics in the Huon Gulf, Papua New Guinea: Geology, v. 24, p. 819-822.

Gallup, C.D., 1997, High-precision uranium-series analyses of fossil corals and Nicaragua Rise sediments: The timing of high sea levels and the marine delta U-234 Value, University of Minnesota.
Gallup, C.D., Cheng, H., Speed, R., Taylor, F.W., and Edwards, R.L., 2002, Direct Determination of the Timing of Sea Level Change During Termination II: Science, v. 295, p. 310-314.
Gallup, C.D., Edwards, R.L., and Johnson, R.G., 1994, The timing of high sea level over the past 200,000 years: Science, v. 263, p. 796-800.
Goreau, T., 1959, The ecology of Jamaican coral reefs. 1. Species composition and zonation: Ecology, v. 40, p. 67-90.
Hays, J., Imbrie, J., and Shackleton, N., 1976, Variations in the Earth's orbit: Pacemaker of the ice ages: Science, v. 194, p. 1121-1132.
Henderson, G., and Slowey, N., 2000, Evidence from U-Th dating against Northern Hemisphere forcing of the penultimate deglaciation: Nature, v. 404, p. 61-66.
Henderson, G.M., 2002, Seawater (234U/238U) during the last 800 thousand years: Earth and Planetary Science Letters, v. 199, p. 97-110.
Henderson, G.M., Slowey, N.C., and Fleisher, M.Q., 2001, U–Th dating of carbonate platform and slope sediments: Geochim. Cosmochim. Acta, v. 65, p. 2757-2770.
Hilman Natawidjaja, D., Sieh , K., Galetzka, J., Suwargadis, B.W., Cheng, H., Edwards, R.L., and Chilfeh, M., 2007, Interseismic deformation above the Sunda Megathrust recorded in coral microatolls of the Mentawai islands, West Sumatra: Journal of Geophysical Research, v. 112, p. B02404.1-B02404.27.
Ludwig, K.R., Szabo, B.J., Moore, J.G., and Simmons, K.R., 1991, Crustal subsidence rate off Hawaii determined from 234U/238U ages of drowned coral reefs: Geology, v. 19, p. 171-174.
Moore, J., and Campbell, J.F., 1987, Age of tilted reefs, Hawaii: Journal of Geophysical Research, v. 92, p. 2641-2646.
Moore, J., and Fornari, D.J., 1984, Drowned reefs as indicators of the rate of subsidence of the island of Hawaii: Journal of Geology, v. 92, p. 753-759.
Moore, J.G., 1987, Subsidence of the Hawaiian Ridge, *in* Decker, R.W., Wright, T.L., and Staufer, P.H., eds., Volcanism in Hawaii U.S. Geological Survey Professional Paper: Washington DC, p. 85-100.
Ota, Y., and J. Chappell 1996, Late Quaternary coseismic uplift events on the Huon Peninsula, Papua New Guinea, deduced from coral terrace data: Journal of Geophysical Research, B, Solid Earth and Planets, v. 101, p. 6071-6082.
Pigram, C.J.a.D., H.L, 1987, Terranes and accretion history of the New Guinea orogen: BMR Journal of Australian Geology and Geophysics, v. 19, p. 55-76.
Riker-Coleman, K.E., Gallup, C.D., Wallace, L.M., Webster, J.M., Cheng, H., and Edwards, R.L., 2006, Evidence of Holocene uplift in east New Britain, Papua New Guinea: Geophys. Res. Letters, v. 33, p. L18612
Silver, E.A., Abbott, L.D., Kirchoff-Stein, K.S., Reed, D.L., Bernstein-Taylor, B., and Hilyard, D. , 1991, Collision propagation in Papua New Guinea and the Solomon Sea: Tectonics, v. 10, p. 863-874.

Stein, M., Wasserburg, G.J., Aharon, P., Chen, J.H., Zhu, Z.R., Bloom, A., and Chappell, J., 1993, TIMS U-series dating and stable isotopes of the last interglacial event in Papua New Guinea: Geochimica et Cosmochimica Acta, v. 57, p. 2541-2554.

Stirling, C.H., Esat, T.M., Lambeck, K., McCulloch, M.T., Blake, S.G., Lee, D.-C., and Halliday, A.N., 2001, Orbital forcing of the marine isotope stage 9 interglacial: Science, v. 291, p. 290-293.

Taylor, F.W., Frohlich, C., Lecolle, J., and Strecker, M., 1987, Analysis of Partially Emerged Corals and Reef Terraces in the Central Vanuatu Arc: Comparison of Contemporary Coseismic and Nonseismic With Quaternary Vertical Movements Journal of Geophysical Research, v. 92, p. 4905-4933.

Thompson, W.G., Spiegelman, M.W., Goldstein, S.L., and Speed, R.C., 2003, An open-system model for U-series age determinations of fossil corals: Earth and Planetary Science Letters, v. 210, p. 365-381.

Thurber, I.D., broeker, S.W., Blanchard, R.L., and Potratz, H.A., 1965, Uranium-series ages of Pacific atoll coral.: Science, v. 149, p. 55-59.

Tregoning, P., Jackson, R.J., McQueen, H., Lambeck, K., Stevens, C., Little, R.P., Curley, R., Rosa, R., 1999, Motion of the South Bismarck plate, Papua New Guinea: Geophys. Res. Letters, v. 26, p. 3517-3520.

Villemant, B., and Feuillet, N., 2003, Dating open systems by the 238U-234U-230Th method: application to Quaternary reef terraces: Earth and Planetary Science Letter, v. 210, p. 105-118.

Wallace, L.M., 2002, Tectonics and arc-continent collision in Papua New Guinea: Insights from geodetic, geophysical and geologic data: Santa Cruz, California, University of California.

Wallace, L.M., Stevens, C., Silver, E., McCaffrey, R., Loratung, W., Hasiata, S., Stanaway, R., Curely, R., Rosa, R., Taugaloidi, J., 2004, GPS and seismological constraints on active tectonics and arc-continent collision in Papua New Guinea: Implications for mechanics of microplate rotations in a plate boundary zone: Journal of Geophysical Research, v. 109, p. B05404.

Webster, J.M., Braga, J.C., Clague, D.A., Gallup, C.D., hein, J.R., Potts, D.C., Renema, W., Riding, R., Riker-Coleman, K., Silver, E., and Wallace, L.M., accepted, in revision, Coral Reef Evolution on Rapidly Subsiding Margins: Global and Planetary Change, Special Issue.

Webster, J.M., Clague, D.A., Riker-Coleman, K., Gallup, C., Braga, J.C., Potts, D., Moore, J.G., Winterer, E.L., and Paull, C.K., 2004a, Drowning of the -150 m reef off Hawaii: A casualty of global meltwater pulse 1A?: Geology, v. 32, p. 249-252.

Webster, J.M., Wallace, L., Silver, E., Applegate, B., Potts, D., Braga, J.C., Riker-Coleman, K., and Gallup, C., 2004b, Drowned carbonate platforms in the Huon Gulf, Papua New Guinea: Geochemistry, Geophysics, Geosystems, v. Volume 5.

Webster, J.M., Wallace, L., Silver, E., Potts, D., Braga, J.C., Renema, W., Riker-Coleman, K., and Gallup, C., 2004c, Coralgal composition of drowned carbonate platforms in the Huon Gulf, Papua New Guinea ; implications for lowstand reef development and drowning Marine Geology, v. 204, p. 59-89.

Webster, J.M., Wallace, L.M., Clague, D.A., and Braga, J.C., 2007, Numerical modeling of the growth and drowning of Hawaiian coral reefs during the last two glacial cycles (0–250 kyr): Geochemistry, Geophysics, Geosystems, v. 8, p. Q03011.

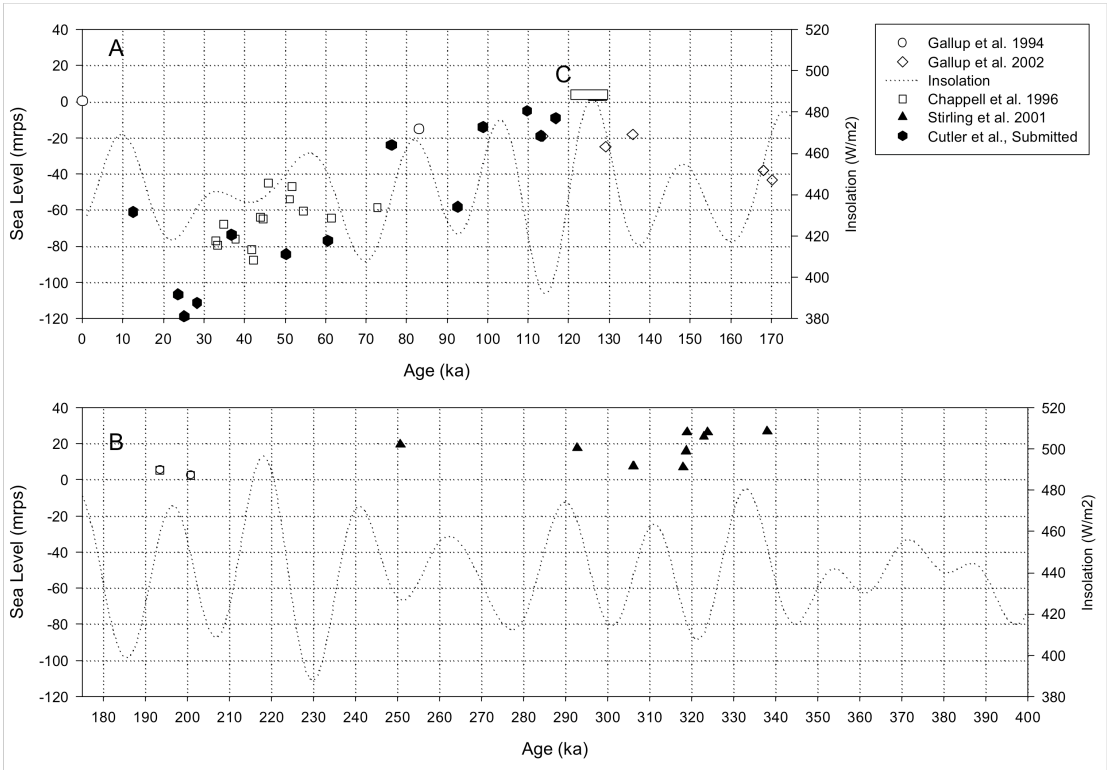

Figure 1. Sea level records from coral and insolation for 0 to 175 ka (A) and 175 to 400 ka (B). Data from (Chappell, 1996; Gallup, 1997; Gallup et al., 2002; Stirling, 2001). Insolation from (Berger and Loutre, 1991).

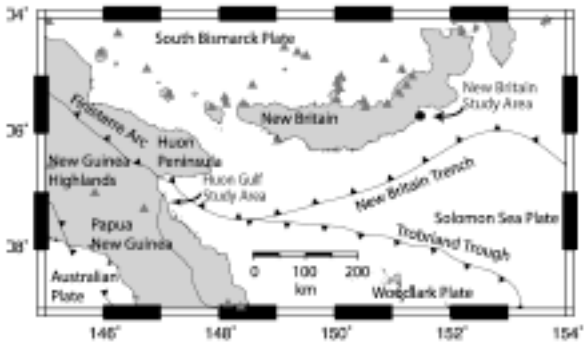

Figure 2. Tectonic setting of Huon Gulf and New Britain. Grey triangles show location of active volcanic arc. Study locations are shown with arrows.

Chapter 2: Evidence of Holocene uplift in east New Britain, Papua New Guinea
K. E. Riker-Coleman, C. D. Gallup, L. M. Wallace, J. M. Webster, H. Cheng, and R. L. Edwards

Abstract: We present the first published evidence of uplift along the eastern coast of New Britain, Papua New Guinea based upon 230Th dating of uplifted Holocene coral reefs. Although uplift rates of the nearby Huon Peninsula are well constrained (2–3 m/ka), little is known about vertical motion along the eastern margin of New Britain. Based upon relative sea-level curves for Papua New Guinea, present sample elevations, and estimates of paleowater depth of four in-situ Holocene corals we calculate an average uplift rate of 1.6 ± 0.4 m/ka for the southeast coast of New Britain. We suggest underplating of subducted sediment as a possible mechanism for uplift of the reefs.

1. Introduction

Raised coral reef terraces are prevalent on the coastlines of the islands of Papua New Guinea (PNG). Fossil corals from the nearby Huon Peninsula (HP) in PNG have provided an extensive record of tectonic uplift and sea level change over the last 300,000 years [Bloom et al., 1974; Chappell, 1974; McCulloch et al., 1999; Cutler et al., 2003]. Coral terraces are also present on islands east of the mainland of New Guinea, such as those on New Britain (NB) (Figure 1), although there is no published data on NB terraces. The HP and NB terraces are both likely the result of tectonic uplift but, while tectonic uplift of the HP is due to collision between the Finisterre volcanic arc and the continental New Guinea Highlands [e.g., Pigram and Davies, 1987], uplift in eastern NB (ENB) is likely due to processes related to subduction of the oceanic Solomon Sea Plate beneath the South Bismarck Plate along the NB Trench. We provide the first estimate of the uplift rate of ENB from uranium-series dating of raised terraces there, and suggest some potential mechanisms for the uplift, including the possible role of sediment underplating.

2. Tectonic Setting of East New Britain

PNG is an island nation, north of Australia in the Pacific Ocean, where the Australian Plate, Pacific Plate and many microplates meet (Figure 1a). The west-southwest convergent motion of the Pacific Plate (~110 mm/yr) relative to the Australian Plate [DeMets et al., 1994] is the dominant tectonic motion in the region, although the existence of several rapidly rotating microplates has led to a wide variety of tectonic settings throughout the region [e.g., Wallace et al., 2004]. Interactions between the Pacific and Australian plates have made PNG the site of orogenic events since at least the Oligocene [Dow, 1977; Pigram and Davies, 1987]. Active arc-continent collision currently occurs in the Markham Valley, where the New Guinea Highlands and Finisterre Volcanic arc converge. As a consequence of the Finisterre collision, the Finisterre range has grown to elevations of 4 km, and the Huon Peninsula (HP) has uplifted rapidly, allowing preservation of a series of highly studied uplifted reefs [Chappell, 1974; Esat et al., 1999; Stirling et al., 1998], yielding uplift rates from 1–4 m/ka. The Finisterre collision has propagated east with time, and the modern tip of collision lies in the western Solomon Sea at about 147 E [Davies et al., 1987; Silver et al., 1991]. To the east of the Finisterre collision, the Solomon Sea Plate subducts beneath the South Bismarck Plate at the NB trench (Figure 1a, Figure 2).

NB is the largest island in PNG, apart from the mainland of New Guinea. It is an elongate east-west island (~450 km long) that parallels the NB Trench (Figure 1a). Based on GPS data, Tregoning et al. [1999] and Wallace et al. [2004] found that convergence along the NB Trench should increase from ~55 mm/yr at 147.5 E to ~130 mm/yr at 151.5 E. The Jacquinot Bay (JB) area is on the southeastern coast of NB, ~100

km north of the most rapid convergence at the NB Trench. Limited geologic work has been done in east NB, and very little is known about active upper plate faulting in the JB region. Initially mapped from aerial photos by the Australian government, the carbonate terraces of NB are covered with dense jungle vegetation, making exploration difficult.

3. Data and Analysis

We have conducted a preliminary field survey of the uplifted coral reef terraces of the JB area (Figure 1b). We selected this area because aerial photos indicated possible well-defined terraces, similar in morphology to those seen on the HP and because of the proximity to an airstrip. We identified six terraces and number them Terrace 1 (T1) as the terrace closest to the ocean, Terrace 2 (T2) as the next highest in elevation, and so on (Figure 1). Only the lower three appear to be well developed and traceable throughout the study area. We measured the elevations of T1-T3 using Abney leveling and we used handheld GPS to roughly estimate the elevations of T4–T6. The reef crests of T1, T2, and T3 are at 2 m, 35 m, and 65 m above sea level, respectively. We estimate the approximate elevations of T4, T5, and T6 to be 120 m, 200 m, and 270 m. At the base of T1 we identify a contact between the mudstone substrate and the coral reef material.

Field and laboratory investigations of the coralgal assemblages within T1, T2, and T3 indicate deposition within generally shallow, high-energy reef environments (i.e., reef crest, slope and/or flat) on the basis of comparisons with similar modern [e.g., Nakamori et al., 1994; Pandolfi and Minchin, 1995] and fossil [e.g., Webster et al., 2004] analogues in PNG [Riker-Coleman et al., 2004].

Due to the combination of high rainfall and dense vegetation covering the carbonate terraces, conditions at JB are not ideal for coral preservation for the purpose of uranium series dating. Many corals in situ showed very clear signs of recyrstallization (i.e., calcite sparkles, dissolution cavities and staining with iron and/or organic material). We collected 27 samples of shallow-water corals from T1, T2, and T3.

We measured the U-Th isotopic composition and calcite/aragonite composition of 15 coral samples, limiting our measurements to samples with minimal visible alteration in hand sample. We measured eight corals from T1, two from T2 and four from T3. We follow other workers [Cutler et al., 2003; Gallup et al., 2002] in determining criteria for deciding whether an age is reliable. The criteria we use are: coral has <2% calcite, a uranium concentration within range of modern corals (2–3 ppm) and a d234Ui values within error of modern seawater (145.8 ± 1.7%) [Cheng et al., 2000]. All samples meeting all of the reliability conditions are from T1 and range in age from 4.3 ± 0.03 ka to 9.0 ± 0.16 ka (d234U: 143.8 to 147.0) (Complete data table is available in the auxiliary material1). None of the corals from T2 or T3 were less than 90% calcite. With the exception of NB7, coral samples from T2 and T3 were low in 238U concentration (<1ppm), likely indicating loss of uranium either during or after re-crystallization.

The present elevation of a coral sample is a function of age, uplift rate and sea level as represented by the equation: Hi = uiTi + (SLi + PG), where Hi = the present elevation of terrace i (m), ui = uplift rate of terrace I averaged over the time period since the reef grew (m/ka), Ti is the age of the terrace (ka), SLi is the eustatic sea level at

which terrace i grew (m), and PG is the paleowater depth of the coral (given in meters relative to sea level). Since the last glacial maximum, the sea level record is virtually continuous and data from at least five distinct locations provide similar sea level curves [Edwards et al., 2003]. We used present elevation, an estimate of average paleowater depth, 230Th ages (see auxiliary material), and paleosea level to compute a local uplift rate for each sample from T1. Paleowater depths were determined using modern analogues for coral and coralline algal species assemblages at each sample location. We use the Lambeck and Chappell [2001] reconstruction of relative sea level for PNG, which is based upon the HP reef terraces and differs from other records due to isostatic effects [Lambeck et al., 2002]. Uplift rates from Holocene coral samples with reliable ages are: NB21: 0.4 to 1.6 m/ka; NB17: 1.4 to 1.8 m/ka; NB18a: 1.4 to 1.8 m/ka; NB29 1.7 to 2.1 m/ka. The expressed uplift ranges include calculated uncertainties in age, paleosea level, elevation (0.5 m) and paleowater depth.

4. Discussion

Corals from the Holocene terrace (T1) in the JB area yield reliable ages that likely bracket the life of the reef. The oldest measured sample, NB29 (230Th age = 9.0 ± 0.16 ka; d234Ui = 147.5 ± 1.6), was collected on the contact between a basal mudstone substrate and the very base of T1, likely representing initiation of reef growth. Sample NB21 is the youngest measured sample (230Th age = 4.3 ± 0.03 ka; d234Ui = 148.4 ± 1.9), the most seaward sample, and likely represents the very last stage of reef growth just before the reef emerged. The average uplift rate of the samples,

1.6 ± 0.4 m/ka, and the presence of a series of uplifted terraces suggests that uplift is occurring in ENB.

In tectonic environments with more than one uplifted terrace, it is customary to use the last interglacial (LI) terrace to calculate a long-term local uplift rate. We are unable to determine which terrace is the LI terrace because none of the samples from T2 or T3 (the most likely candidates) produce reliable 230Th ages. We used the modern elevation of the reef crest, an age of 125 ka, paleowater depth of 0 m, and a paleo sea level of +5 m to estimate a possible range of uplift rates (assuming T2, T3 and T4 were LI). Estimated uplift rates are 0.3 m/ka, 0.5 m/ka, and 0.9 m/ka, assuming T2, T3 and T4 (respectively) are the LI terrace. All are within the range of uplift rates computed from the Holocene terrace corals.

Computed uplift rates from ENB are comparable to those from other similar tectonic settings. The range of uplift rates estimated for the HP (1.0–4.0 m/ka [Chappell, 1974; Ota and Chappell, 1996; Cutler et al., 2003]) encompasses those from JB (1.6 ± 0.4 m/ka). Several studies of coral terraces from Indonesia document uplift of the Banda Island Arc [Chappell and Veeh, 1978; Bard et al., 1996; Pirazzoli et al., 1993; Hantoro et al., 1994]. The uplift rates from terraces in Indonesia are similar to our Holocene uplift rate for ENB. Uplift in the Banda Island Arc ranges from 0.4 to 0.5 m/ka for Atauro Island, [Chappell and Veeh, 1978] to 1.0 m/ka for Alor Island[Hantoro et al., 1994] and 0.2 to 0.5 m/ka for Sumba Island [Bard et al., 1996; Pirazzoli et al., 1993]. However, the uplift in the Banda and Sunda Arcs is more likely related to collision of the Australian continent with the Sunda and Banda arcs since ~3 Ma [e.g., Johnston and Bowin, 1981] rather than subduction-related processes.

Arc volcanism in NB is located on the northern side of the island, 80–100 km to the north of JB, while subduction of the Solomon Sea Plate at the NB Trench occurs 100 km to the south of JB. The large distance of the uplifted JB terraces (80–100 km) from the obvious potential sources of uplift for the region (e.g., plate convergence and arc volcanism) begs the question, why is the JB area actively uplifting? Uplift of the JB terraces is not likely to be related to subduction interface earthquakes, as modeling of GPS velocities show no evidence for interseismic coupling on the portion of the subduction interface near JB [Tregoning et al., 1999; Wallace et al., 2004]. If the subduction interface undergoes interseismic coupling in this region, it is likely to occur beneath the offshore region to the south of JB, and coseismic rupture of this part of the subduction interface would lead to subsidence at JB. One reason for the observed tectonic uplift may be that ENB is more intensely faulted than regions to the west [e.g., Johnson, 1979], and the uplift of the JB terraces is due to local faulting. However, other raised reefs (up to 300 m high) are apparent all along the south coast of NB and Johnson [1979] suggested that the entire island has a regional northwest tilt. If the entire south coast of NB is actively uplifting, it is possible that the uplift of JB this study reveals is due to some regional tectonic phenomenon and cannot be explained by local faulting in ENB.

We suggest that underplating of subducted sediments beneath NB could cause the observed regional uplift, as is thought to occur in the rapidly uplifting Raukumara peninsula of northeastern New Zealand [Walcott, 1987] (the Raukumara peninsula is in a similar position as JB relative to the trench and active arc). Little or no accretionary wedge is associated with subduction at the NB trench east of 149 E [Galewsky and

Silver, 1997]. Thus, it is likely that all sediment on the downgoing plate is being subducted (at a rapid rate of ~130 mm/yr) and may become subsequently underplated, although it is currently unknown if sediment underplating beneath NB occurs. Further studies on the JB terraces and other uplifted reef terraces along the NB coast are required to help distinguish between possible mechanisms for uplift of the JB terraces.

5. Conclusions

We identified six major coral reef terraces in the JB area of ENB, similar to those studied from tropical, uplifted settings worldwide. Uranium-series dating of four coral samples from the terrace closest to the sea (T1) brackets it as Holocene in age (4.3 ± 0.03 ka to 9.0 ± 0.16 ka). We collected samples from the next two terraces in elevation, but the samples are too altered to provide reliable age data.

We present the first Holocene uplift rates from ENB. Uplift ranges from 0.4 to 2.1 m/ka based upon 230Th ages from Holocene corals, with an average uplift rate of 1.6 ± 0.4 m/ka. One way to test the long-term uplift rate would be to evaluate the rate of uplift using the last interglacial (LI) terrace. Collection of less-altered samples from terraces T2–T6 may make identification of the LI terrace possible in the future.

We suggest that regional uplift of the south coast of NB may be due to underplating of sediment subducted at the NB trench. An expanded field campaign in ENB and comparison to terraces in Western NB would assist us in adequately constraining any spatial and temporal variability in uplift rates, and help us to distinguish between possible mechanisms for tectonic uplift of ENB.

Acknowledgments. We thank D. Potts for help in coral identification; the University of Papua New Guinea, M. Baloiloi and the local government and people of Jacquinot Bay for assistance with fieldwork; P. Morton for help with XRD analyses; and Aron Meltzer and one anonymous reviewer for helpful reviews. LW acknowledges helpful discussions with K. Berryman and M. Reyners. Financial support for this project was from the National Science Foundation (Grant OCE-9907869) and from the University of Minnesota Duluth.

6.0 References

Bard, E., C. Jouannic, B. Hamelin, P. Pirazzoli, M. Arnold, G. Faure, P. Sumosusastro, and Syaefudin (1996), Pleistocene sea levels and tectonic uplift based on dating of corals from Sumba Island, Indonesia, Geophys. Res. Lett., 23, 1473–1476.

Bloom, A. J., W. S. Broecker, J. Chappell, R. K. Matthews, and K. J. Mesolella (1974), Quaternary sea level fluctuations on a tectonic coast: New 230Th/234U dates from the Huon Peninsula, New Guinea, Quat. Res., 4, 185–205.

Chappell, J. (1974), Geology of coral terraces, Huon Peninsula, New Guinea: A study of Quaternary tectonic movements and sea-level changes, Geol. Soc. Am. Bull., 85, 553– 570.

Chappell, J., and H. H. Veeh (1978), Late Quaternary tectonic movements and sea-level changes at Timor and Atauro Island, Geol. Soc. Am. Bull.,89, 356–368.

Cheng, H., R. L. Edwards, J. Hoff, C. D. Gallup, D. A. Richards, and V. Asmerom (2000), The half-lives of uranium-234 and thorium-230,Chem. Geol., 169, 17– 33.

Cutler, K. B., R. L. Edwards, F. W. Taylor, H. Cheng, J. Adkins, C. D. Gallup, P. M. Cutler, G. S. Burr, J. Chappell, and A. L. Bloom (2003), Rapid sea-level fall and deep-ocean temperature change since the last interglacial period, Earth Planet. Sci. Lett., 206, 253– 271.

Davies, H. L., E. Honza, D. L. Tiffin, J. Lock, Y. Okuda, J. B. Keene, F. Murakami, and K. Kisimota (1987), Regional setting and structure of the western Solomon Sea, Geo Mar. Lett., 7, 153– 160.

DeMets, C., R. G. Gordon, D. F. Argus, and S. Stein (1994), Effects of recent revisions to the geomagnetic reversal time scale on estimates of current plate motions, Geophys. Res. Lett., 21, 2191–2194.

Dow, D. B. (1977), A geological synthesis of Papua New Guinea, Bur. Miner. Resour. Aust. Bull., 201, 1 –41.

Edwards, R. L., K. B. Cutler, H. Cheng, and C. D. Gallup (2003), Geochemical evidence for Quaternary sea-level changes, in Treatise on Geochemistry: The Oceans and Marine Geochemistry, edited by H. D. H. a. K. K. Turekian, pp. 343– 364, Elsevier, New York.

Esat, T. M., M. T. McCulloch, J. Chappell, B. Pillans, and A. S. Omura (1999), Rapid fluctuations in sea level recorded at Huon Peninsula during the penultimate deglaciation, Science, 283, 197–204.

Gallup, C. D., H. Cheng, R. Speed, F. W. Taylor, and R. L. Edwards (2002),Direct determination of the timing of sea level change during Termination II, Science, 295, 310–313.

Galewsky, J., and E. A. Silver (1997), Tectonic controls on facies transitionsin an oblique collision: The western Solomon Sea, Papua New Guinea, Geol. Soc. Am. Bull., 109, 1266–1278.

Hantoro, W. S., P. A. Pirazzoli, C. Jouannic, H. Faure, C. T. Hoang, U. Radtke, C. Causse, M. Borel Best, S. Bieda, and K. Lambeck (1994), Quaternary uplifted coral reef terraces on Alor Island, East Indonesia, Coral Reefs, 13, 215–223.

Johnson, R. W. (1979), Geotectonics and volcanism in Papua New Guinea: A review of the late Cainozoic, BMR J. Aust. Geol. Geophys., 4, 181– 207.

Johnston, C. R., and C. O. Bowin (1981), Crustal reactions resulting from the mid-Pliocene to recent continent-island arc collision in the Timor region, BMR J. Aust. Geol. Geophys., 6, 223– 243.

Lambeck, K., and J. Chappell (2001), Sea level change through the last glacial cycle, Science, 292, 679– 686.

Lambeck, K., Y. Yokoyama, and T. Purcell (2002), In to and out of the LastGlacial Maximum: Sea-level change during Oxygen Isotope Stages 3 and2, Quat. Sci. Rev., 21, 343– 360.

McCulloch, M., A. W. Tudhope, T. M. Esat, G. E. Mortimer, J. Chappell, B. Pilans, A. R. Chivas, and A. Omura (1999), Coral record of equatorial sea-surface temperature during the penultimate deglaciation at Huon Peninsula, Science, 283, 202–204.

Nakamori, T., E. Wallensky, and C. Campbell (1994), Recent hermatypic coral assemblages at Huon Peninsula, Contrib. Int. Geol. Correlation Prog., 274, 111 –116.

Ota, Y., and J. Chappell (1996), Late Quaternary coseismic uplift events on the Huon Peninsula, Papua New Guinea, deduced from coral terrace data, J. Geophys. Res., 101, 6071– 6082.

Pandolfi, J. M., and P. R. Minchin (1995), A comparison of taxanomic composition and diversity between reef coral life and death assemblages in Madang Lagoon, Papua New Guinea, Palaeogeogr. Palaeoclimatol. Palaeoecol., 119, 321–341.

Pigram, C. J., and H. L. Davies (1987), Terranes and the accretion history of the New Guinea orogen, BMR J. Aust. Geol. Geophys., 10, 193– 211.

Pirazzoli, P. A., et al. (1993), A one million-year-long sequence of marine terraces on Sumba Island, Indonesia, Mar. Geol., 109, 221– 236.

Riker-Coleman, K., J. M. Webster, C. D. Gallup, L. M. Wallace, and E. A. Silver (2004), Evidence of rapid tectonic uplift in East New Britain, Papua New Guinea, GSA Abstr. Prog., 36(5), 215– 231.

Silver, E. A., L. Kirchoff-Stein, K. S. Reed, B. L. Bernstein, and D. Hilyard (1991), Collision propagation in Papua New Guinea and the Solomon Sea, Tectonics, 10, 863–874.

Stirling, C. H., T. M. Esat, K. Lambeck, and M. T. McCulloch (1998), Timing and duration of the Last Interglacial: Evidence for a restricted interval of widespread coral reef growth, Earth Planet. Sci. Lett., 160, 745– 762.

Tregoning, P., R. J. Jackson, H. McQueen, K. Lambeck, C. Stevens, R. P. Little, R. Curley, and R. Rosa (1999), Motion of the South Bismarck Plate, Papua New Guinea, Geophys. Res. Lett., 26, 3517– 3520.

Walcott, R. I. (1987), Geodetic strain and the deformational history of the North Island of New Zealand during the late Cainozoic, Philos. Trans. R. Soc. London, Ser. A, 321, 163–181.

Wallace, L. M., C. Stevens, E. Silver, R. McCaffrey, W. Loratung, S. Hasiata, R. Stanaway, R. Curley, R. Rosa, and J. Taugaloidi (2004), GPS and seismological constraints on active tectonics and arc-continent collision in Papua New Guinea: Implications for mechanics of microplate rotations in a plate boundary zone, J. Geophys. Res., 109, B05404, doi:10.1029/2003JB002481.

Webster, J. M., L. Wallace, E. Silver, D. Potts, J. C. Braga, W. Renema, K. Riker-Coleman, and C. D. Gallup (2004), Coralgal composition of drowned carbonate platforms in the Huon Gulf, Papua New Guinea: Implications for lowstand reef development and drowning, Mar. Geol., 204, 59– 89.

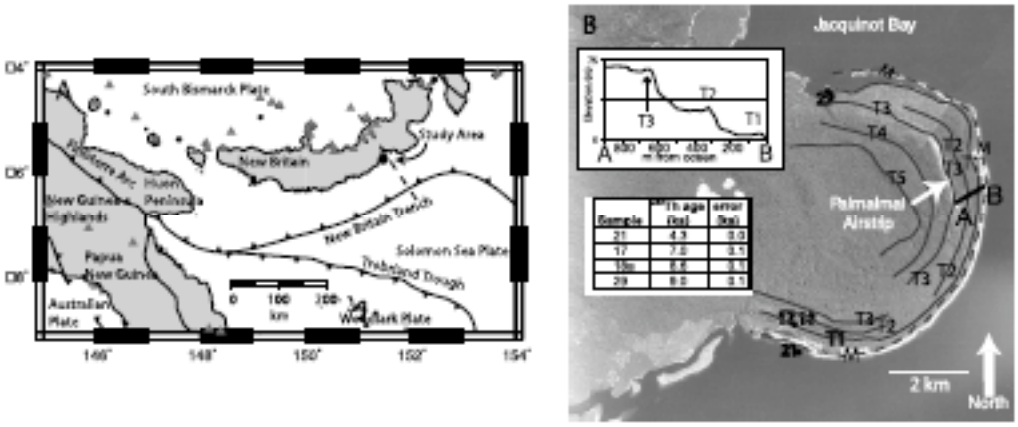

Figure 1. (a) Tectonic setting of New Britain. Black dot indicates location of Jacquinot Bay study area, and grey triangles show location of active volcanic arc. Dashed line shows location of seismicity profile in Figure 2b. (b) Sample locations in the Jacquinot Bay field area. T1–T5 indicate identified locations of coral terraces, T6 is not shown. M identifies location of modern reef. Approximate sample locations are indicated with sample numbers. Sample 21 is from T1 on a small offshore island, Samples 17 and 18 are from the same location. Top inset is topographic cross section of Figures 1a and 1b and bottom inset is sample ages and their 2-sigma errors.

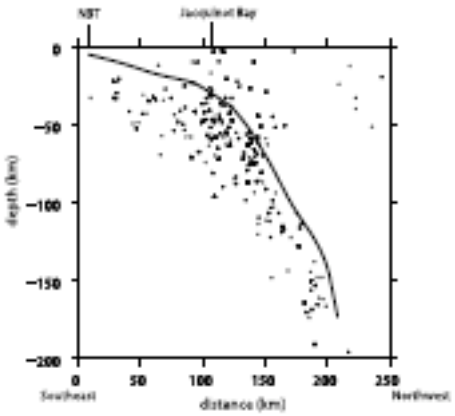

Figure 2. Cross-section of regional seismicity (1964– 2005; Mw > 5.5) projected onto profile line shown in Figure 1a. JB = Jacquinot Bay; NBT = New Britain Trench. Solid line shows inferred location of subduction interface. Earthquake locations from the IRIS website (http://www.iris.edu/quakes/eventsrch.htm).

Chapter 3: Uranium series data from Submerged Coral Reefs of Hawaii: Diagenetic Changes, Sea Level, and Subsidence

Kristin Riker-Coleman[1]
Christina Gallup[1]
Jody Webster[2,3]
George Burr[4]
David Clague[2]
Larry Edwards[5]
Hai Cheng[5]

1. Dept. of Geological Sciences, University of Minnesota Duluth, Duluth, MN 55812
2. Monterey Bay Aquarium Research Institute, Moss Landing, CA 95039
3. School of Earth Sciences, James Cook University, Townsville, QLD 4811, Australia
4. NSF-Arizona AMS Laboratory, University of Arizona, Tucson, AZ 85721-0081
5. Department of Geology and Geophysics, University of Minnesota, Minneapolis, MN 55455

Abstract:

We report new ages of submerged coral samples from three locations in Hawaii: ^{230}Th ages for the –400 m reef terrace at Mahukona, ^{230}Th ages for the –1000 m reef terrace at east and northwest Kohala, and new ^{14}C ages for five of the samples from the -150 m reef terrace. We identify three main trends in the isotopic composition of submerged coral samples from Hawaii: an increase in both ^{230}Th/^{238}U and ^{234}U/^{238}U; an increase in ^{230}Th/^{238}U with little change in ^{234}U/^{238}U; and low ^{230}Th/^{238}U with both low and high ^{234}U/^{238}U. We use open-system modeling to explain these trends in the data and to give us confidence in the samples that meet age reliability criteria. Based on these reliable ages, we find that the -400 m terrace drowned at 136.7 ± 1.0 ka, while the -1000 m terrace initiated growth 365.0-412.4 ka. We compute a long-term subsidence rate of -2.3 ± 0.4 m/ka from the -1000 m terrace. Using this subsidence rate and coral samples from the –400 m terrace, we compute a paleo-sea level at 136.7 ± 1.0 ka below –56 m; this result suggests reef drowning after rapid sea-level rise at ~137 ka during the penultimate glacial termination.

1.0 Introduction:

The tectonic process of subsidence of volcanic islands is closely linked to the evolution of coral reefs in tropical areas. Fossil reefs preserved offshore in subsiding settings provide a useful paleobathymetric marker for interpreting the history of sea level and to infer island subsidence. A series of submerged coral terraces surrounds the subsiding island of Hawaii. The model of terrace formation on Hawaii [1, 2] and more recent numerical modeling of reef development there [3, 4] predict that reef growth establishes itself during the sea-level falls preceding glacial periods. Ludwig et al. [5] published the first comprehensive study of uranium-series ages of six coral terraces from -10 m to -1336 to -1146 m of water depth of Hawaii, computing a long-term subsidence rate for Hawaii (-2.6 m/kyr) and supporting the Moore and Fornari model of terrace formation. Subsequently, Webster et al. [6] presented new ^{230}Th and radiocarbon ages for the -150 m reef, also supporting the model.

We report new ^{230}Th ages of samples from three locations in Hawaii (the –400 m reef at Mahukona and the –1000 m terrace at east and northwest Kohala, and new ^{14}C ages for five of the samples in the Webster et al. [6] study of the -150 m reef. In addition, we also measured one of the previously measured samples from the Ludwig et al. [5] study. We provide a quantitative analysis of the isotopic compositions of our samples, using an open-system model to explore the effects of diagenetic changes in submerged coral samples from Hawaii and to identify well-preserved samples. We use the ages of well-preserved samples that provide reliable ages from the -1000 m reef and previously published ages from the –150 m reef [2, 6] to constrain the rate of subsidence of the island of Hawaii to -2.3 ± 0.4 m/ka. With this subsidence rate and

data from the -400 m reef, we determine that sea level was at or below –56 m at 136.7 ± 0.1 ka, immediately preceding Termination II.

1.1 Geologic Setting:

Over the past 70 million years, continued northwest movement of the Pacific Plate over the stationary Hawaiian "hot-spot" has resulted in the long (~6000 km) trail of volcanoes known as the Hawaiian Ridge-Emperor Seamounts chain [7]. The Hawaiian Archipelago consists of nineteen islands and atolls, numerous smaller islets and seamounts trending northwest to southeast. Hawaii is the southernmost and youngest island in the Hawaiian Archipelago (Fig 1); it is a composite of at least five young volcanic mountains, two of which are currently active [8, 9]. Lithospheric loading associated with continued volcanism over the Hawaiian hotspot during the last 500 ky is thought to generate the subsidence that Hawaii is currently experiencing [8, 10].

The models of the formation of coral terraces surrounding Hawaii [1-3] suggest that the terraces form during periods of and dropping sea level. The models suggest the corals continue to grow so long as the rate of sea level change is similar to the rate of land subsidence. Corals ultimately drown during periods of rapid eustatic sea-level rise during the initial deglacial period when the rate of relative sea-level rise exceeds the coral's vertical growth rate. For instance, Webster et al. [6] correlated the drowning of the -150 m reef to Meltwater Pulse 1A. Following a drowning event, coral reestablishes itself landward of the drowned terrace while the original terrace continues to move to deeper water. Based on this model we assume that shallow water coral from the top of

each terrace has a unique age and represents just one sea-level rise event during which time relative sea-level rise (including both subsidence and eustatic sea level changes) outpaced vertical accretion of coral reefs.

Previous investigations of the drowned reefs off northwest Hawaii [1, 2, 5, 6, 11] indicate a mean, long-term subsidence rate of 2.5-2.6 m/kyr. Sharp and Renne [11] calculated a similar subsidence rate of 2.7 ± 0.7 m/kyr for Hilo, on the eastern side of Hawaii (from the subaerial/submarine transition in the volcanic rocks, now located at -1079 m. Moore et al. also calculated a subsidence rate of 2.5-2.6 m/ka for the last 500 ka based on ^{14}C ages of the upper part of the Hilo drill hole [12]. Webster et al. [3] also calculated maximum and minimum possible subsidence rate for Hawaii over the last 15,000 years of 3.2–2.6 m/ka, based on the original Webster et al. [6], paleowater depth estimates (0-10 m, for the corals and the algae) and the Barbados sea level curve.

Subsidence of Hawaii is directly linked to lithospheric loading. Since neither the size of the load (the volcanoes) nor the rheology of the lithosphere change on a timescale corresponding to a glacial cycle, it is reasonable to assume that the subsidence rate remains constant over thousands of years [10, 13]. As the Pacific Plate continues to migrate northwest, the location of the center of the load slowly shifts to the southeast, causing an associated post-drowning tipping of the reefs to the southeast (Clague et al., in prep).

1.2 Previous Work:

Moore and Fornari [2] suggested that the Hawaiian reefs began forming during sea-level falls preceding glacial maxima. The reefs continue to grow until drowning during

subsequent deglaciations due to the combined effects of rapid sea-level rise and continued subsidence [1, 2]. Estimates of the timing of glacial terminations (when the reefs drown) come from the marine oxygen isotope record: 18, 130, 245, 340 and 430 ka [14]. Several studies provide a quantitative test of the Hawaiian terrace formation model. Moore and Fornari [2] presented radiocarbon ages and Ludwig et al. [5] presented mass-spectrometric $^{234}U/^{238}U$ ages (which assume the marine $^{234}U/^{238}U$ ratio has been constant with time) and $^{230}Th/^{238}U$ isotopic data for six submerged coral reefs of northwestern Hawaii (-10 m, -150 m, -430 m, -693 m, -945 m, -1146 m). Although the uranium ages and thorium ages agree within error of each other, Ludwig et al. relied upon the uranium ages for interpretations due to the large errors associated with alpha-spectrometric thorium age measurements. The ranges of corresponding measured $^{234}U/^{238}U$ ages from the Ludwig et al. [5] study are (and their associated terrace depths are): 17-19 ka (-150 m reef); 133 ka (-430 m reef); 225-276 ka (-693 m reef); 287-314 ka (-945 m reef); and 360-475 ka (-1146 m reef). Ludwig et al. speculated that measured $^{234}U/^{238}U$ ages that are older than predicted drowning times of the reef are likely due to sampling interior materials on the reef while ages that are younger than predicted drowning times are likely due to open system diagenetic effects. These uranium ages on coral samples from the terraces suggest that: (a) the terraces are in stratigraphic order (i.e. the shallowest is the youngest and the deepest is the oldest); (b) each terrace drowned during a period generally associated with a sea-level rise; and (c) the northwestern side of the island of Hawaii has been subsiding at a roughly uniform rate of 2.6 ± 0.4 m/ka for the past 475 ka.

Webster et al. [6] present a paleoenvironmental reconstruction of the -150 m coral reef around Hawaii, incorporating all available radiometric dates, high-resolution bathymetry, dive observations, and coralgal paleobathymetry data. The coral reef ranges in age from 14.7–15.2 ka [6]. Webster et al. document a shift from the shallow reef-building *Porites* corals to deep-water coralline algal growth, preserved as a crust on the drowned reef crest, which shows a rise in paleowater depth. This study also confirms the Moore and Campbell model predictions [1].

Combining the absolute ages of corals [5, 6] and the theoretical models of reef formation [1, 2], Webster et al. [3] developed a quantitative test of Hawaii's submerged reef development, focused on the last two glacial cycles (~250 kyr). Using observations of the sedimentary environment and radiometric ages, their numerical model provides a quantitative predictive internal stratigraphy for the -150 m and -400 m reefs (in addition to drowning ages). They modeled the growth and development of both reefs with growth rates of 2.5–2.85 m/kyr for the main shallow reef-building facies and a subsidence rate of 2.5 m/kyr. The model suggests these two reefs initiated growth during stable eustatic sea level conditions during highstands circa 222 ka (MIS7) and circa 126 ka (MIS5e), respectively, and continued to grow episodically for 90 kyr until they finally drowned during the penultimate (~134 ka) and last deglaciation (14–12 ka). In this paper, we improve upon the measured ^{230}Th ages of the -400, and -1000 m reefs and report additional ^{14}C ages for the -150 m reef.

2.0 Sample Sites:

Twelve reefs have been mapped around Hawaii and eleven of those occur off the northwest coast [Clague et al., in prep; [2, 4-6] (Figure 1). The -150 m reef offshore Hawaii forms a consistent break in slope extending 150 km from the Kohala Peninsula in the north to Kealakekua Bay in the west [2]. Submersible dives and bathymetric surveys [2, 6] identified the -150 m reef off Ka Lae (South Point). There are few data indicating the presence of the -150 m reef off the eastern coast of Hawaii, although a survey by the MBARI Mapping Team [15] imaged a prominent reef-like structure off Hilo at -125 to -150 m that presumably extends northwest along the broad shelf for only a short distance north of Hilo. In 2001, ROV dives (*Tiburon*) were carried out off Kawaihae (T276) and Kealakekua Bay (T291). Samples from those dives and previous dives were dated and data presented in Webster et al. [6].

The –400 m terrace follows the contour of the paleoshoreline and tilts slightly to the SE due to lithospheric flexure [10]. In April 2001, seven dives with the ROV Tiburon were conducted from the *R/V Western Flyer* on the –400 m Mahukona terrace. A total of 86 carbonate samples were retrieved for analysis. In addition to coral and coralline algae, the carbonate samples contain a variety of fossilized encrusting, boring and infilling invertebrate fauna. Taxonomically identified coral and coralline algae species indicate a drowning reef environment for the corals [4].

Samples from the -1000 m reef were collected during a series of two dives with the ROV Tiburon that were conducted from the *R/V Western Flyer* on the –1000 m Kohala terrace northeast of the Kohala peninsula in April 2001. ROV observations

show a well-exposed 40 m thick stratigraphic section through the -1000 m reef. Nine coral samples were recovered from a insitu, massive coral reef facies growing directly on the basalt substrate at the base of this section. Sedimentary facies analysis of the corals (eg. *Porites sp. P. lobata?, and Leptastrea*) and thick coralline algae (eg. *Hydrolithon onkodes*) indicate a shallow, high energy paleoenvironment in < 10 m[4]. In addition, we measured three samples recovered via dredge during the TUIM01MV cruise on the R/V Melville in January 2005.

3.0 Methods and Results:

The coral samples were washed and crushed and then picked under a binocular microscope. The samples were then dried overnight before they were weighed. Typical sample amounts ranged from 100 to 300 mg. The chemical procedure used to separate the uranium and thorium is similar to that described in Edwards et al. [16]. The sample was dissolved with nitric acid, spiked with a mixed $^{229}Th/^{233}U/^{236}U$ tracer, and dried. After the addition of an iron chloride solution, NH_4OH was added dropwise to precipitate iron complexes. The sample was then centrifuged to separate the iron from the rest of the solution and the supernate removed. After loading the sample onto columns containing anion resin, HCl was added to elute the thorium and water was added to elute the uranium. With the uranium and thorium separated, each sample was then dried and dilute nitric acid was added for injection into the ICP-MS.

Analyses were conducted by means of inductively coupled plasma mass spectrometry (ICP-MS) on a Finnigan-MAT Element outfitted with a double focusing sector-field magnet in reversed Nier–Johnson geometry and a single MasCom

multiplier. The instrument was operated at low resolution and in electrostatic peak hopping mode. Combined ionization plus transmission efficiency is 0.1 to 0.2% for both uranium and thorium. Further details on instrumental procedures are explained by Shen et al.[17]. Several of the dredge samples were analyzed using similar techniques, but on the Thermo-Finnigan Neptune multi-collector inductively-coupled plasma mass spectrometer, which has ionization/transmission efficiency an order of magnitude higher (1 to 2%) for both uranium and thorium. Details of this method will be forthcoming.

We measured the U-series isotopic composition of 32 coral samples from the -1000 m Kohala and -400 m Mahukona terraces and one of the -400 m samples from the suite included in Ludwig et al. [5]. The sample context and dating results are listed in Table 1.

In studies of uplifted corals, the presence of calcite would deem the ages unreliable. In our study of the corals from Webster et al. [6] we were surprised to find five of the corals from -150 m reef contain between 2 and 14 percent calcite, yet have consistent ^{14}C (calibrated) and ^{230}Th ages (within error of each other and always within one percent of each other, see Table 1). For assessing the reliability of ages for the -400 and -1000 m corals, we used the following criteria: coral has < 20% calcite, a uranium concentration within range of modern corals (2-3 ppm) and a $\delta^{234}U_i$ values within error of modern seawater (145.8 ± 1.7 ‰) [18].

Of ten corals from the -400 m Mauhukona terrace, five meet the <20% calcite criterion, and three of the samples meet the $\delta^{234}U_i$ criterion. The samples we deem to

be the most reliable (with $\delta^{234}U_i$ close to that of modern sea water) are: the youngest sample, T277-R8b collected from –412 m (136.7 ± 0.9 ka; $\delta^{234}U_i$ = 149.5 ± 2.0; 7% calcite); a sample Ludwig had previously dated, P5-70-4a, from –525 m (145.4 ± 1.2 ka; $\delta^{234}U_i$ = 143.6 ± 3.3; 0% calcite) and the oldest sample collected from –562 m, T278-R3, (151.8 ± 1.7 ka; $\delta^{234}U_i$ = 148.5 ± 2.3; 15% calcite). Only the top sample is in place, the other two were collected from loose material.

We measured four samples from the top of the -1000 m terrace (all in situ) and thirteen from the base of the same terrace (five loose samples and eight in situ). All samples from the top of the terrace show evidence of alteration: one sample contains <2% calcite, the remainder of the samples contain >19% calcite. T301-R49, which has <2% calcite, has a ^{230}Th age of 481.1 +56.2/-35.3 ka with an elevated $\delta^{234}U_i$ of 200.8 +35.3/-22.6. All twelve samples from the base of the terrace appear to be less altered than those from the top and all twelve contain less calcite (<2%). Two in situ samples from the base of the -1000 m terrace meet the $\delta^{234}U_i$ criterion and their ages (and $\delta^{234}U_i$ values) are T301-R46: 377.2 +13.4/-12.2 ka ($\delta^{234}U_i$: 146.2 +7.2/-6.6) and T301-R39: 392.5 +20.5/-17.9 ka ($\delta^{234}U_i$: 153.4 +11.2/-10.0). In addition, we measured three samples collected via dredge from the -1000 m terrace. None of the three dredge samples meet the $\delta^{234}U_i$ criterion or the calcite criterion. Measured ages range from 286.5 to 342.8 ka.

Five calibrated radiocarbon ages from the -150 m reef range from 13.5 ka to 15.0 ka. For comparison with the ^{230}Th ages (ka), all radiocarbon ages (14-C ka) were

converted to calibrated ages (cal ka) using the Calib program and the Marine04 curve [19] and reported with 2σ errors. Marine data are normalized to the "global" ocean by subtracting ΔR, the regional difference from the model ocean reservoir age of 405 yr.

4.0 Discussion:

4.1 Diagenesis: Calcite Content

The validity of any radiogenic isotopic chronometer is based on the assumption that the system has remained closed for chemical species involved in the radiometric clock. Traditionally, we have expected submerged coral samples to be better preserved than their subaerially exposed counterparts because in some specific settings (such as Hawaii) it is likely that submerged coral samples collected from the top of the reef have remained within their environment of deposition and have not been exposed to meteoric waters. When meteoric water (which is undersaturated with respect to carbonate species) migrates through carbonate rocks it can cause extensive leaching and recrystallization. Our data suggests that the uranium-series isotopic compositions of submerged corals lying uncovered on the sea floor of Hawaii are not better preserved than subaerially exposed samples. Due to limitations of the submarine sample collection process, we suggest that it may be more challenging to find submerged corals that will provide reliable ages without drilling into the coral terraces.

Precipitation of carbonate material can only happen in environments where the water is supersaturated with respect to $CaCO_3$ and where some turbulence is present to flush volumes of water through the pore spaces. As such, in modern environments this process is limited to the shallow, near-surface waters of the tropics to sub-tropics [20].

Although seawater is not generally supersaturated with respect to $CaCO_3$, carbonate precipitation is especially favored where agitation and warming of waters triggers CO_2 degassing [21]. This carbonate precipitation can occur while the coral is still living: Potthast [22] documented development of aragonite syntaxial cements in the deeper parts of living coral.

The clearest indication of diagenesis in submerged Hawaiian corals is the frequent occurrence of calcite. Since corals are initially composed of aragonite, the presence of calcite is an indication of post-depositional changes in the skeletal material -- either via infilling by marine calcite cement or recyrstallization of primary or secondary aragonite. Aragonite is a less stable polymorph of calcite, having the same chemistry but different structure and a different uranium concentration (~0.1 ppm to as much as 1 ppm in calcite vs. 3 ppm in aragonite) [23, 24]. Coral skeletons that are primary aragonite can alter to high-magnesium calcite in marine settings and to low-magnesium calcite in subaerial, meteoric environments (e.g. [25]). Allison et al. [26] analyzed evaluated fossil corals samples from the submerged Hawaiian reefs for type of calcite present in the samples and found high-magnesium calcite – further support for marine diagenesis. Modern corals have typical uranium concentrations of 2.0–3.5 ppm [27]. Likewise, uranium concentration can vary in aragonite as well. Pristine primary skeletal parts average 2.8 ppm uranium vs. 4.1 ppm uranium in secondary aragonite.

A decrease in porosity by deposition of secondary aragonite during reef submergence also can produce small but measurable effects on uranium-series ages (after 1000 years of subsidence, Lazar et al. [28] identified samples with a 5 percent decrease in porosity that appeared 70 years younger). Enmar et al. [23] documented

fossil corals with secondary aragonite precipitation resulting in a decrease of porosity of 3-4% over a period of 40-1000 years of diagenesis. Rejuvenation effects, that is the appearance of being younger due to addition of younger material, of less than 1000 years are not within the analytical dating resolution for older corals.

Conversion to calcite is common in emergent corals. For instance, corals from the emergent terraces of east New Britain, Papua New Guinea show evidence of recyrstallization [29]; corals from the pre-Holocene terraces were greater than 90% calcite and all had low uranium concentrations (< 1 ppm), suggestive of uranium loss during or after recrystallization to calcite. Corals from the Barbados terraces are also converted to calcite: corals are generally older and increasingly altered to calcite with increasing elevation on the island (C. Gallup, unpublished data). Likewise, Esat et al. report that only about a third of analyses of corals from the Huon Peninsula's last interglacial terrace resulted in reliable ages [30]. Increase in calcite content in both Barbados and on the Huon Peninsula with increasing elevation suggests that calcification continues to occur in fossil corals with prolonged subaerial exposure.

We propose that, unlike emergent corals, submerged Hawaiian corals are altered to calcite early in their diagenetic history. We base this statement on ^{14}C and ^{230}Th ages of samples from Webster et al. [6] that agree to within one-percent of each other at roughly 15 ka, yet contain up to 14 percent calcite (Table 1). Traditionally we would consider these ages to be unreliable because of their high calcite content. Because the calibrated radiocarbon ages and ^{230}Th ages agree with each other, we hypothesize that recyrstallization to calcite occurred early in the sample's diagenetic history. To evaluate

this hypothesis, we tested the effects of a single replacement event occurring at 500 and 2000 years in a coral's history.

We modeled the theoretical impacts on the isotopic composition of the coral when 20 percent of the coral skeleton is replaced with calcite, assuming that the only uranium-series transformation that occurs with replacement of aragonite is a uranium loss. To do so we assumed the $^{230}Th/^{238}U$ ratio increased instantaneously due to the loss of ^{238}U upon introduction of calcite and that the $^{234}U/^{238}U$ ratio remained unchanged. We created two models: one with uranium concentration in calcite = 0.1 ppm and one with 1 ppm (in both models uranium concentration in aragonite = 3 ppm). We let our modeled system evolve as a closed system both before and after the introduction of calcite.

We anticipated the net effect would be to make the apparent age older than the closed-system age because the loss of ^{238}U increases the $^{230}Th/^{238}U$ ratio, which grows with age. Regardless of which concentration of uranium in calcite we choose, with a substitution at 500 years, the modeled open-system and closed-system values are within one percent of each other by 15 ka (see Fig. 3). Conversely, when we add the calcite at 2 ka, neither case is within one percent of the closed system by 15 ka (Fig. 3). This modeling result suggests that the calcite replacement in the -150 m reef corals of Webster et al. [6] either happened prior to 2 ka or that the replacement did not involve a significant gain or loss of uranium. The timescale of this modeled alteration is in agreement with those Potthast [22] and Enmar et al. [31] documented.

The model suggests that older Hawaiian samples with less than 20 percent calcite did not necessarily experience a shift in age. However older samples with greater

than 20 percent calcite and elevated $\delta^{234}U$ and high ^{232}Th concentration may have experienced both late addition of calcite and other types of alteration. In addition, not all corals in our sample set experienced increases in calcite content. Specifically ten samples from the -1000 m terrace contain no measurable calcite in the samples. In order to evaluate our samples from Hawaii, it is essential to look at overall trends in isotopic composition.

4.2 Trends in Isotopic Composition

Coral samples from both the -1000 m terrace and the -400 m terrace have elevated $^{234}U/^{238}U$ and $^{230Th}/^{238}U$ ratios (see Table 1), as can be seen on a $[^{234}U/^{238}U]$-$[^{230Th}/^{238}U]$ evolution diagram (see Fig. 2). We observe three main trends in the data:

1. Trend One: a correlated increase in $^{230}Th/^{238}U$ with $^{234}U/^{238}U$ (shown mainly in -400 m data);
2. Trend Two: an increase in $^{230}Th/^{238}U$ with little change in $^{234}U/^{238}U$ (as shown mainly in -1000 m data);
3. Trend Three: low $^{230}Th/^{238}U$ with both low and high $^{234}U/^{238}U$ ratios (illustrated by samples from both -400 m and -1000 m terraces).

Similar trends have been observed in coral data before. Trend one is similar to that produced by alpha recoil [32-34] and frequently observed in emergent corals. Trend two is similar to that produced by ^{230}Th addition [34]. We suggest that trend three is produced by ^{238}U addition.

4.2.1 Modeling Trends in Isotopic Composition

To explore the extent to which alpha-recoil and ^{230}Th addition explain the trends we observed in the submerged Hawaiian samples, we turn to analytical models. We use these models to generate model ages for the samples. We use these model ages to evaluate the success of the models in explaining the data, not to generate additional reliable ages. We concentrate on samples that meet the less than 20 percent calcite criterion.

Gallup et al. [32] were the first to include diagenetic addition terms in the differential equations describing U-series decay. Gallup et al. estimated the rate of addition of ^{234}U and ^{230}Th using the U/He age and U/Th isotopic composition of a coral with ^{234}U/^{238}U and ^{230}Th/^{238}U ratios that could not be explained by closed-system evolution. Henderson et al. [35, 36] showed that alpha-recoil had significant effects on the isotopic composition of marine carbonate sediments, and made the first attempt to quantify the physical process of alpha-recoil in U-series decay equations. Combining these two ideas, Thompson et al. [37] derived equations to account for the coupled addition of ^{234}U and ^{230}Th to fossil corals. The Thompson model uses the systematics of U-series decay with appropriate physical and geochemical constraints, not the empirical assessment of model parameters from selected data (which distinguishes their approach from Gallup et al.). Villement and Feuillet [34] proposed a similar, yet slightly different model of alpha recoil controlled diagenesis that accounts for continuous selective redistribution (gain or loss) of ^{234}U, ^{234}Th and ^{230}Th and also can include excess initial ^{230}Th. Both the Thompson et al. and Villement and Feuillet models show that recoil processes tend to increase ^{234}U/^{238}U and ^{230}Th/^{234}U ratios with time, leading

to an overestimation of the apparent age of the sample. These models present an alternative way to date old reef terraces with systematic alteration. However, Andersen et al. [38] provide evidence to suggest that both the Villemant and Feuillet model and the Thompson model are limited for older samples, indicating additional diagenetic mechanisms at work beyond alpha recoil.

To characterize the extent to which our samples have been affected by alpha recoil processes and ^{230}Th addition, we evaluate the samples using the equations developed by Villemant and Feuillet [34] to model open system behavior. Their model accounts for the two main sources of disturbance to the closed system model: recoil controlled continuous selective redistribution of isotopes (specifically gain or loss of ^{234}U, ^{234}Th and ^{230}Th) and presence of initial or added thorium. Villemant and Feuillet define the relationship between two parameters (f_{234} and f_{230}) that describe the fractions of ^{234}U and ^{230}Th lost ($f<1$) or gained ($f>1$) by the system as a simple function of the associated alpha-recoil energies. More specifically, the f_{234}/f_{230} ratio is fixed by the ratio of the isotopes' respective alpha-recoil energies.

The energy involved in the alpha decay of some nuclides within the ^{238}U decay chain leads to the largely physical fractionation process of alpha-recoil. During the decay, a particle is ejected from the nucleus, causing the daughter nuclide to recoil in the opposite direction. This recoil causes a fraction of the daughter nuclide produced during a decay to be ejected from the host mineral into the surrounding medium. An additional fraction of the daughter is left residing in damaged crystallographic sites within the mineral, from where it can be more readily mobilized. Alpha recoil therefore induces higher selective mobilities of ^{238}U daughter isotopes and hence greater

likelihood of redistribution throughout the system [39].

For each sample's isotopic composition, it is possible to describe the diagenetic pathway by considering two end-member scenarios and the possible combination of the two: all open-system behavior is the result of alpha recoil (selective redistribution of ^{234}U and the shorter-lived ^{234}Th) or all observed open-system behavior is the result of variation in thorium (i.e. $^{234}U/^{238}U$ age is valid and $^{230}Th/^{238}U$ age is altered due to open-system processes adding or subtracting ^{230}Th). These two scenarios can be visualized on a [$^{234}U/^{238}U$]-[$^{230}Th/^{238}U$] diagram. Addition and/or subtraction of thorium results in a shift in the horizontal direction [$^{230}Th/^{238}U$] of the decay curve for a closed system. Alpha recoil (or selective redistribution of specific isotopes) results in a shift to higher $^{230}Th/^{238}U$ and $^{234}U/^{238}U$.

Villemant and Feuillet [34] suggest a simplified inversion method for calculating the model age of a series of cogenetic sub-samples that were initially isotopically homogeneous that have evolved through time. Because of the geomorphology of our sampling locations, we do not consider all samples from one reef to represent the same age. Instead, we use the equations developed by Villemant and Feuillet to forward calculate the age of a sample. For each sample there is a non-unique set of f_{234} and f_{230} parameters (which correspond to addition or loss of ^{234}U and ^{230}Th, respectively) and initial $^{230}Th/^{238}U$ ratios that can evolve to the measured isotopic composition. The f-parameters dictate how far from a closed system the isotopic composition moves along the alpha-recoil trend. In modeling the data, we seek the unique combination of f value and initial $^{230}Th/^{238}U$ ratio that requires the least amount of ^{230}Th addition and gives a minimum model age. By comparing the minimum model ages from each terrace, we

can evaluate how much the model reduces the scatter in the ages; thereby, we gauge how much of a role alpha-recoil and ^{230}Th addition played in the diagenesis of the submerged Hawaii samples.

The minimum model ages for our samples are shown in Table 2. The modeled ages of the -400 m terrace range from 135 ka to 153 ka, representing a difference less than 2 kyr from the measured ages of 136.7-153.9 ka. These model ages cluster in two groups: one with average age 136.3 ka and one with an average age of 150.0 ka. Our best-fit f_{234} values are also shown in Table 2. We were able to model all -400 m samples without adding thorium to the system. Our f_{234} values ranged from 0.995 to 1.019, very close to the closed system value of 1.0. The modeled age of 133-153 ka supports the measured age of 136.7 ka and suggests alpha recoil affected the isotopic composition of most of the -400 m samples.

Results from the -1000 m terrace indicate that the isotopic compositions of the samples are more varied than for the -400 m terrace. For the -1000 m samples most, but not all, of the variation in the coral isotopic composition can be explained using just alpha recoil (see table 2). We model addition of thorium by creating initial ^{230}Th/^{238}U ratios not equal to zero for some samples and assume that additional ^{230}Th is added initially (although we suspect thorium is added to the system over time either episodically or continuously following the coral's death). The requirement of additional thorium for modeling the oldest samples, sometimes requiring substantial additions is not surprising given that these corals are older than the -400 m samples and that the corals have been submerged and exposed to sources of additional thorium such as from terrigenous material of from radioactive decay of uranium in the overlying water

column. The resulting modeled ages (and modeling parameters) are shown in table 2.

Modeled ages of coral samples from the bottom of the -1000 m terrace range from 340 to 455 ka (vs. measured ages of 337 ka to infinite age). Modeled ages from the top of the coral terrace range from 375 to 425 ka (vs. measured ages of 365-413 ka). Although modeling the effects of open-system behavior does reduce the scatter in age, there is the possibility of a stratigraphic reversal -- i.e. the top of the -1000 m reef is older than the bottom.

Modeling the isotopic trends in the samples with alpha recoil and, in select cases, addition of thorium reduces the scatter in ages. We conclude therefore that most of the drowned Hawaii corals have been altered by alpha recoil and in some cases ^{230}Th addition. The modeled minimum ages are also useful in evaluating the quality of our criteria in identifying reliable ages. Taken individually, most of our measured ages do not meet the criteria for being considered "reliable." Two samples from the base of the -1000 m terrace meet the narrow definition of a reliable age (both the $\delta^{234}U_i$ criterion and the more traditional < 2% calcite criterion); their ages are 377.2 ka and 392.5 ka, which are within error of the average modeled age (average = 394). One sample from the -400 m terrace meets the strictly reliable test, with < 2% calcite; its measured age is 156.9 ± 2.0 ka and its corresponding modeled age is 153 ka (± 2.0 if we include the error on the measured age). This comparison shows that although the isotopic measurements are highly scattered, modeling the effects of alpha recoil/thorium addition produces model ages that are in agreement with the ages of the samples that meet our reliability criteria (< 20 % calcite). This agreement in ages adds confidence to our ability to identify well-preserved samples.

4.3 Discussion: Timing of Reef Drowning

The drowning times of the -150 m, -400 m, and -1000 m terraces are consistent with the idea that final terrace drowning occurs during periods of rapid sea-level rise. Our understanding of terrace formation is that reef growth begins during stable eustatic sea-level conditions and continues episodically through the regression until sea-level rise is too rapid for coral to keep up during the major deglaciations. The material at the tops of the terraces represents that which was growing immediately preceding the ultimate drowning of the terrace. Our results indicate that the -150 m terrace drowned after 14.7 ka [5], the -400 m terrace drowned after 136.7 ± 0.1 ka and the -1000 m terrace drowned after 377.2 +13.4/-12.2 ka. These dates are consistent with the -150 m terrace drowning during Termination I [5], the -400 m terrace drowning during an orbitally predicted Termination II (half-peak in insolation at 65 north occurs at 134 ± 3 ka), and the -1000 m samples growing during a long Stage 11 (see Fig. 4).

Using the Siddall et al.[40] sea-level curve, each reliable age from the -1000 m terrace (377.2 and 392.5 ka) may correlate with an individual sea-level rise event (Fig. 4), however the data are not of sufficient resolution to make such correlations. Since the material at the very top of the -1000 m terrace was not as well preserved as these two samples, it is possible that we only document one of the intermediate periods of growth and not the ultimate drowning event for the -1000 m terrace.

4.4 Discussion: Subsidence:

The present depth (meters below sea level) of a submerged coral is a function of its age, the subsidence rate, the eustatic sea level at which the terrace grew and the depth at which the coral grew (given in meters relative to sea level): depth =

(subsidence rate x age) +(eustatic sea level + growth depth). For the -150 m terrace, sample number T291-r16 (Porites), was collected from -149 m water depth and has an age of 14.7 ± 0.1 ka. The ^{230}Th ages and the new ^{14}C ages for the same -150 m reef samples suggest the MWP-1A occurred around 14.7 ka.

If we assume the coral grew at sea level and use a eustatic sea level of -98 m [14], then we compute a rate of subsidence of -3.5 m/ka. However, if the coral grew at 14 m water depth, then the subsidence rate would be -2.5 m/ka. The relatively shallow depth of the -150 m reef makes the calculation of subsidence rate very sensitive to the initial growth depth. Sedimentological evidence from the -150 m reef argues that the corals grew in less than 10 m of water depth [3]. For the -400 meter terrace, there is no good eustatic sea level curve available. For the -1000 m reef, however, the eustatic sea level is a small component of the present depth below sea level. A typical glacial-interglacial sea-level cycle consists of ~120 m of sea-level change or roughly 10 percent of the water depth for the -1000 m reefs. For a coral that grew at sea level, we disregard eustatic sea-level change; we use the modern depth of the sample and the age of the sample to compute a rough estimate of subsidence rate (subsidence rate = depth/age).

If we use the top of the terrace (-935 m) as the water depth and the reliable age from the -1000 m terrace (ave: 384.9 ka, collected from -968 m), we compute a subsidence rate of -2.4 m/ka. However, a closer look at this calculation suggests a broader range of values for the subsidence rate. An error analysis shows that the error in the ages represents ~5 % relative error in the age. In addition, there are three asymmetric sources of error: the samples could have grown at a lower sea level (up to 120 m lower if we include the full eustatic range); the samples could have come from

their collection depths instead of the terrace crest (~30-35 m lower); and although not ideal growth conditions, the corals could have grown up to 20 m below the sea surface as shallow water corals. Given these sources of error, the range in the current elevation of the sea level mark associated with these samples is -935 m to -795 m. Using the full age range (including error) produces a range in subsidence rate of -1.9 to -2.6 m/ka. As the model of reef formation suggests that the samples likely grew during a period of intermediate sea level, a value of -2.3 ± 0.4 m/ka well represents our data. Our rate is in agreement with the long-term published rate from Ludwig et al. [5] (2.6 ± 0.4 m/ka) from a linear regression of the $^{234}U/^{238}U$ ages vs. the average terrace depths and that from the modeling of Webster et al. [3] of the last 250 ka, which suggests 2.5 m/ka as an ideal modeled subsidence rate.

4.5 Discussion: Magnitudes of Sea Level

With a rate of subsidence, the depth at which the sample was recovered and the age of the sample, it is possible to compute a paleo sea level. Using a subsidence rate of –2.3 ± 0.4 m/ka, the age, and the modern depth of the uppermost sample (collected *in situ* at -412 m), we compute a paleo sea level of –97 +55/-60 m at 136.7 ± 1.0 ka. Our result suggests that sea level had not yet risen much more than 50% from its glacial low stand of –120 m (see Fig. 4) [40]. Our calculation indicates, when error is included, that sea level was at or below -56 m at 136.7 ± 1.0 ka. This result is consistent with orbital forcing, which would place the termination (50% of post-glacial sea-level rise) at or after the high-latitude boreal summer insolation half-peak (at 134 ± 3 ka, see Figure 3). It is also consistent with the two-phase termination of Cheng et al. [41], where early sea

level rise occurs prior to the boreal insolation half-peak due to a) high austral summer-low boreal summer insolation causing reduced Northern Hemisphere moisture and b) to melting associated with glacial isostatic lithospheric depression following full glacial conditions.

5.0 Conclusions

We report new ^{230}Th ages of samples from three locations in Hawaii: the –400 m reef at Mahukona (136.7 ± 0.9 ka to 151.8 ± 1.7 ka), the –1000 m terrace off eastern Kohala (377.2 +13.4/-12.2 ka and 392.5 +20.5/-17.9 ka) and the -1000 m reef off northwestern Kohala (286.5 ± 1.4 ka to 342.8 ± 1.4 ka)) and new calibrated ^{14}C ages (13.5 to 15.1 ka) for some of the samples in the Webster et al. [6] study of the -150 m reef. None of the three dredge samples meet the $\delta^{234}U_i$ criterion or the calcite criterion. We also measured one of the previously measured samples from the Ludwig et al. [5] study (145.4 ± 1.2 ka).

Uranium-series isotopic compositions of Hawaiian submerged corals resting on the sea bottom are not better preserved than subaerially exposed samples, although their diagenetic signatures differ. From these samples we identify three main trends in isotopic composition of submerged coral samples from Hawaii:

1. An increase in both ^{230}Th/^{238}U and ^{234}U/^{238}U
2. An increase in ^{230}Th/^{238}U with little change in ^{234}U/^{238}U
3. Low ^{230}Th/^{238}U with both low and high ^{234}U/^{238}U

We provide a quantitative analysis, using an open-system model [34] to help

explain these isotopic trends in submerged coral samples from Hawaii. We use the ages from the -1000 m reef and previously published ages from the –150 m reef [2, 6] to constrain the rate of subsidence of the island of Hawaii to -2.3 ± 0.4 m/ka. With this subsidence rate and data from the -400 m reef, we identify sea level at or below -56 m at 136.7 ± 1.0 ka, in agreement with orbital forcing and Cheng et al.'s [41] two-phase termination model.

6.0 Acknowledgements

We thank P. Morton for help with XRD analyses. Financial support for isotopic analytical work on this project came from the National Science Foundation (Grant OCE-9907869) and from the University of Minnesota Duluth. Most samples were collected using The Monterey Bay Aquarium Research Institute's ROV Tiburon funded by a grant from the David and Lucile Packard Foundation to MBARI. The TUIM01MV dredging was completed during a cruise funded by NSF Grant OCE-00-02470 to Gabi Laske for the PLUME project. The Pisces sample was provided by Jim Moore.

7.0 References

[1] J. Moore, J.F. Campbell, Age of tilted reefs, Hawaii, Journal of Geophysical Research 92(1987) 2641-2646.

[2] J. Moore, D.J. Fornari, Drowned reefs as indicators of the rate of subsidence of the island of Hawaii, Journal of Geology 92(1984) 753-759.

[3] J.M. Webster, L.M. Wallace, D.A. Clague, J.C. Braga, Numerical modeling of the growth and drowning of Hawaiian coral reefs during the last two glacial cycles (0–250 kyr), Geochemistry, Geophysics, Geosystems 8(2007) Q03011.

[4] J.M. Webster, J.C. Braga, D.A. Clague, C.D. Gallup, J.R. hein, D.C. Potts, W. Renema, R. Riding, K. Riker-Coleman, E. Silver, L.M. Wallace, Coral Reef Evolution on Rapidly Subsiding Margins, Global and Planetary Change, Special Issue(accepted, in revision).

[5] K.R. Ludwig, B.J. Szabo, J.G. Moore, K.R. Simmons, Crustal subsidence rate off Hawaii determined from 234U/238U ages of drowned coral reefs, Geology 19(1991) 171-174.

[6] J.M. Webster, D.A. Clague, K. Riker-Coleman, C. Gallup, J.C. Braga, D. Potts, J.G. Moore, E.L. Winterer, C.K. Paull, Drowning of the -150 m reef off Hawaii: A casualty of global meltwater pulse 1A?, Geology 32(2004) 249-252.
[7] J.T. Wilson, A possible origin of the Hawaiian Islands, Canadian Journal of Physics 41(1963) 863-870.
[8] J.F. Campbell, D.L. Erlandson, Geology of the Kohala submarine terrace, Hawaii, Marine Geology 41(1981) 63-72.
[9] P.R. Moore, Ages of the raised beaches of Turakirae Head, New Zealand: A reassement based on radiocarbon dates., Royal Society of New Zealand Bulletin. 74(1987) 357-375.
[10] J.G. Moore, Subsidence of the Hawaiian Ridge, in: R.W. Decker, T.L. Wright, P.H. Staufer, (Eds), Volcanism in Hawaii U.S. Geological Survey Professional Paper, Washington DC, 1987, pp. 85-100.
[11] W.D. Sharp, R.P. Renne, The 40Ar/39Ar dating of core recovered by the Hawaii Scientific Drilling Project (Phase 2), Hilo, Hawaii, Geochemistry, Geophysics, Geosystems 6(2006).
[12] J.G. Moore, B.L. Ingram, K.R. Ludwig, D.A. Clague, Coral ages and island subsidence, Hilo drill hole, Journal of Geophysical Research 101(1996) 11599-11606.
[13] J.G. Moore, D.A. Clague, Coastal laval flows from Mauna Loa and Hualalai volcanoes, Bulletin of Volcanology 49(1987) 752-764.
[14] N.J. Shackleton, N.D. Opdyke, Oxygen isotope and palaeomagnetic stratigraphy of equatorial Pacific core V28-238: Oxygen isotope temperatures and ice volumes on a 10^6 year scale, Quat. Res. 3(1973) 39-55.
[15] M.M. Team", Hawaii Multibeam Survey No. 2, Monterey Bay Aquarium Research Institute Digital Data Series, 1998.
[16] R.L. Edwards, J.H. Chen, G.J. Wasserburg, U-238-U-234-Th-230-Th-232 systematics and the precise measurement of time over the past 500,000 years., Earth and Planetary Science Letters(1987).
[17] C.-C. Shen, L.R. Edwards, H. Cheng, J.A. Dorale, R.B. Thomas, M.S. Bradley, S.E. Weinstein, H.N. Edmonds, Uranium and thorium isotopic and concentration measurements by magnetic sector inductively coupled plasma mass spectrometry, Chemical Geology 185(2002) 165-178.
[18] H. Cheng, R.L. Edwards, J. Hoff, C.D. Gallup, D.A. Richards, Y. Asmerom, The half-lives of uranium-234 and thorium-230, Chemical Geology 169(2000) 17-33.
[19] K. Hughen, M. Baillie, E. Bard, A. Bayliss, J. Beck, C. Bertrand, P. Blackwell, C. Buck, G. Burr, K. Cutler, P. Damon, R. Edwards, R. Fairbanks, M. Friedrich, T. Guilderson, B. Kromer, F. McCormac, S. Manning, C.B. Ramsey, P. Reimer, R. Reimer, S. Remmele, J. Southon, M. Stuiver, S. Talamo, F. Taylor, J.v.d. Plicht, C. Weyhenmeyer, MARINE04 Marine radiocarbon age calibration, 0–26 cal kyr BP, Radiocarbon 46(2004) 1059-1086.
[20] R.G.C. Bathurst, Early diagenesis of carbonate sediments, in: A. Parker, B.W. Sellwood, (Eds), Sediment Diagenesis, D. Reidel Publishing Company, 1983, pp. 349-377.

[21] B.W. Sellwood, Principles of Carbonate Diagenesis in: A. Parker, B.W. Sellwood, (Eds), Quantitative Diagenesis: Recent Developments and Applications to Reservoir Geology, Kluwer Academic Publishers, Netherlands, 1994, pp. 1-32.
[22] I. Potthast, Short-term progressive early diagenesis in density bands of recent corals:Porites Colonies, Mauritius Island, Indian Ocean, Facies 27(1992) 105-111.
[23] A.J. Amiel, D.S. Miller, G.M. Friedman, Incorporation of uranium in modern corals, Sedimentology 20(1973) 523-528.
[24] R.J. Reeder, M. Nugent, C. D. Tait, D. E. Morris, S. M., K.M.B. Heald, W. P. Hess, and A. Lanzirotti, Coprecipitation of uranium (VI) with calcite: XAFS, micro-XAS, and luminescence characterization, Geochim. Cosmochim. Acta 65(2001) 3491-3503.
[25] C.E. Sherman, C.H. Fletcher, K.H. Rubin, Marine and meteoric diagenesis of Pleistocene carbonates from a nearshore submarine terrace, Oahu, Hawaii, J. Sed. Res. 69(1999) 1083-1097.
[26] N. Allison, A.A. Finch, J.M. Webster, D.A. Clague, Palaeoenvironmental records from fossil corals: The effects of submarine diagenesis on temperature and climate estimates, Geochim. Cosmochim. Acta 71(2007) 4693-4703.
[27] G.T. Shen, and R. B. Dunbar Environmental controls on uranium in reef corals, Geochim. Cosmochim. Acta 59(1995) 2009-2024.
[28] B. Lazar, R. Enmar, M. Schossberger, M. Bar-Matthews, L. Halicz, M. Stein, Diagenetic effects on the distribution of uranium in live and Holocene corals from the Gulf of Aqaba, Geochimica et Cosmochimica Acta 68(2004) 4583-4593.
[29] K.E. Riker-Coleman, C.D. Gallup, L.M. Wallace, J.M. Webster, H. Cheng, R.L. Edwards, Evidence of Holocene uplift in east New Britain, Papua New Guinea, Geophys. Res. Letters 33(2006) L18612
[30] T.M. Esat, M.T. McCulloch, J. Chappell, B. Pillans, A. Omura, Rapid fluctuations in sea level recorded at Huon Peninsua during the penultimate deglaciation, Science 283(1999) 197-201.
[31] R. Enmar, M. Stein, M. Bar-Matthews, E. Sass, A. Katz, B. Lazar, Diagenesis in live corals from the Gulf of Aqaba I: The effect on paleo-oceanography tracers, Geochim. Cosmochim. Acta 64(2000) 3123-3132.
[32] C.D. Gallup, R.L. edwards, R.G. Johnson, The timing high sea level over the past 200,000 years, Science 263(1994) 796-800.
[33] W.G. Thompson, S.L. Goldstein, Open-system coral ages reveal persistent suborbital sea-level cycles, Science 308(2005) 401-404.
[34] B. Villemant, N. Feuillet, Dating open systems by the 238U-234U-230Th method: application to Quaternary reef terraces, Earth and Planetary Science Letters 210(2003) 105-118.
[35] G.M. Henderson, Seawater (234U/238U) during the last 800 thousand years., Earth and Planetary Science Letters 199(2002) 97-110.

[36] G.M. Henderson, N.C. Slowey, M.Q. Fleisher, U–Th dating of carbonate platform and slope sediments. , Geochim. Cosmochim. Acta 65(2001) 2757-2770.
[37] W.G. Thompson, M.W. Spiegelman, S.L. Goldstein, R.C. Speed, An open-system model for U-series age determinations of fossil corals, Earth and Planetary Science Letter 210(2003) 365-381.
[38] M.B. Andersen, C.H. Stirling, E.-K. Potter, A.N. Halliday, S.G. Blake, M.T. McCulloch, B.F. Aylin, M. O'Leary, High-precision U-series measurements of more than 500,000 year old fossil corals, Earth and Planetary Science Letters 265(2008) 229-245.
[39] G. Henderson, N. Slowey, Evidence from U-Th dating against Northern Hemisphere forcing of the penultimate deglaciation, Nature 404(2000) 61-66.
[40] M. Siddall, E.J. Rohling, A. Almogi-Labin, C. Hemleben, D. Meischner, I. Schmelzer, D.A. Smeed, Sea-level fluctuations during the last glacial cycle, Nature 423(2003) 853-859.
[41] H. Cheng, R.L. Edwards, Y. Wang, X. Kong, Y. Ming, M.J. Kelly, X. Wang, C.D. Gallup, W. Liu, A penultimate glacial monsoon record from Hulu Cave and two-phase glacial terminations, Geology 34(2006) 217-220.
[42] J.R. Smith, Satake, K., and Suyehiro, K., Deepwater multibeam sonar surveys along the southeastern Hawaiian Ridge: Guide to the CD-ROM in: E. Takahashi, et al., (Ed), Hawaiian volcanoes: Deep underwater perspectives, 2002, pp. p. 3–9.
[43] D.A. Clague, J.R. Reynolds, N. Maher, G. Hatcher, W. Danforth, J.V. Gardner, High-resolution Simrad EM300 Multibeam surveys near the Hawaiian Islands: Canyons, reefs, and landslides, Eos (Transactions, American Geophysical Union) 79(1998) F826.
[44] A. Berger, M.F. Loutre, Insolation values for the climate of the last 10 million years, Quaternary Science Reviews 10(1991) 297-318.

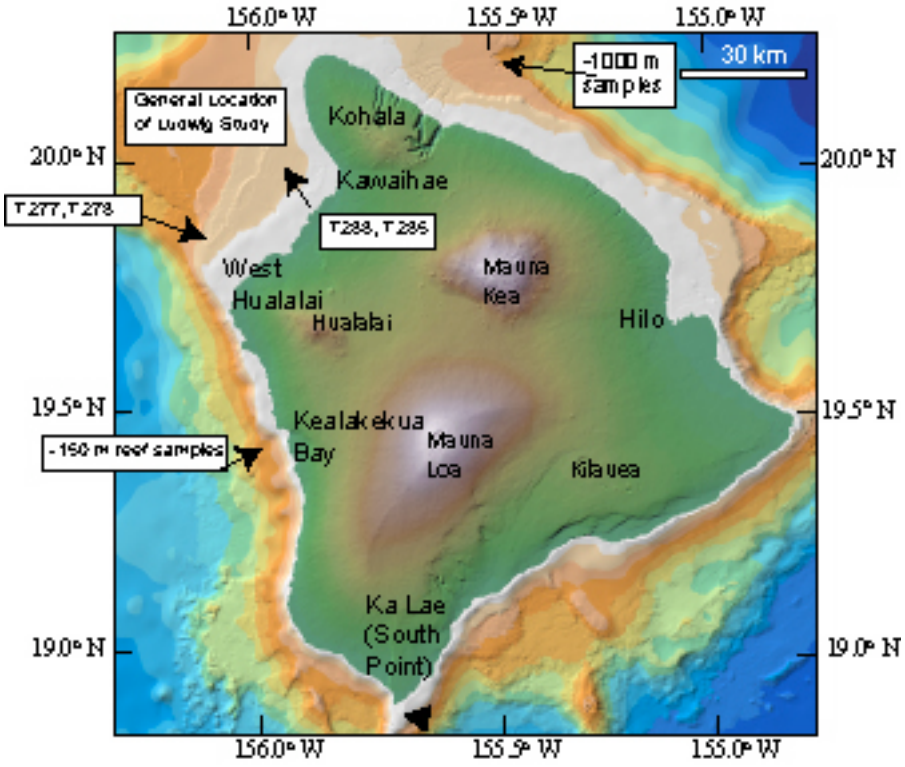

Figure 1: Hawaii and offshore bathymetry, showing sample locations [Based upon Webster et al. 2004 (Fig. 1)]. Bathymetry data are after [42, 43].

Figure 2: Plot of $^{234}U/^{238}U$ activity vs. $^{230}Th/^{238}U$ activity for Hawaiian corals from this study. Data are plotted including 2σ errors. The closed system (bold contour) corresponds to the evolution of a coral that starts with the modern marine $^{234}U/^{238}U$ value of 1.146 per mil value ($\delta^{234}U = 146$). Dashed lines represent lines of equal age and are labeled in ka, solid lines represent evolution of samples with different initial uranium isotopic compositions. Open triangles represent dredge samples. (A). Data from the -150 m terrace, -400 m terrace and -1000 m terraces, excluding data from suspect mass spectrometer runs (noted in data table). (B) A subset of the -1000 m terrace data.

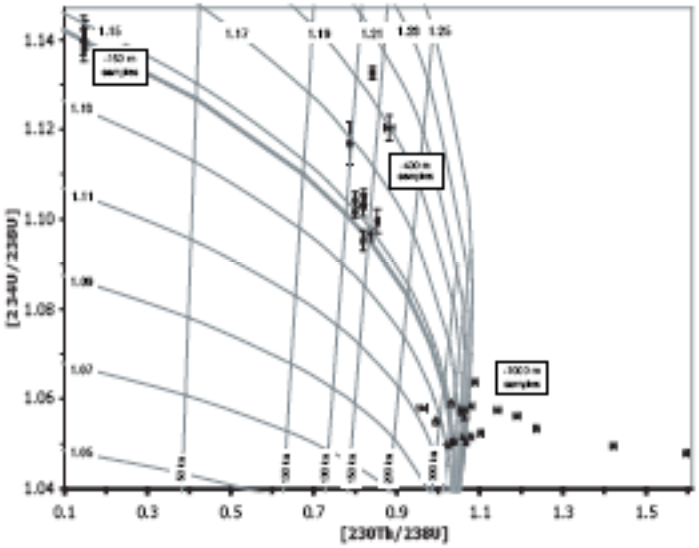
[234U/238U]
[230Th/238U]

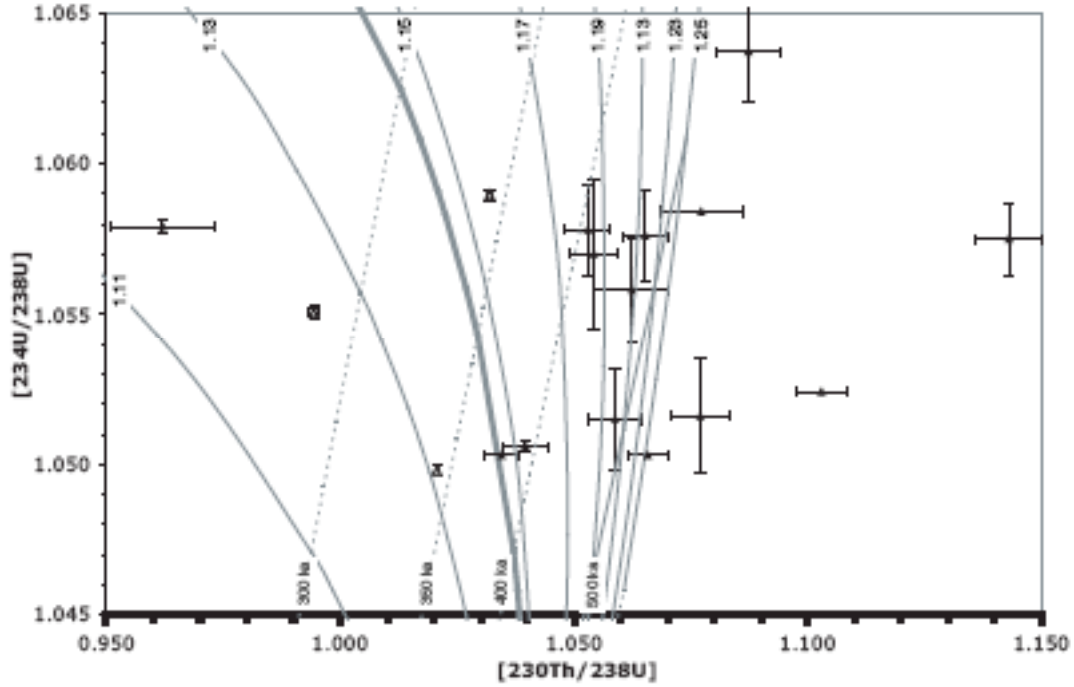
1.065
1.060
1.055
1.050
1.045
[234U/238U]
0.950
1.000
1.050
1.100
1.150
[230Th/238U]
1.13
1.15
1.17
1.19
1.13
1.23
1.25
1.11
300 ka
350 ka
400 ka
500 ka

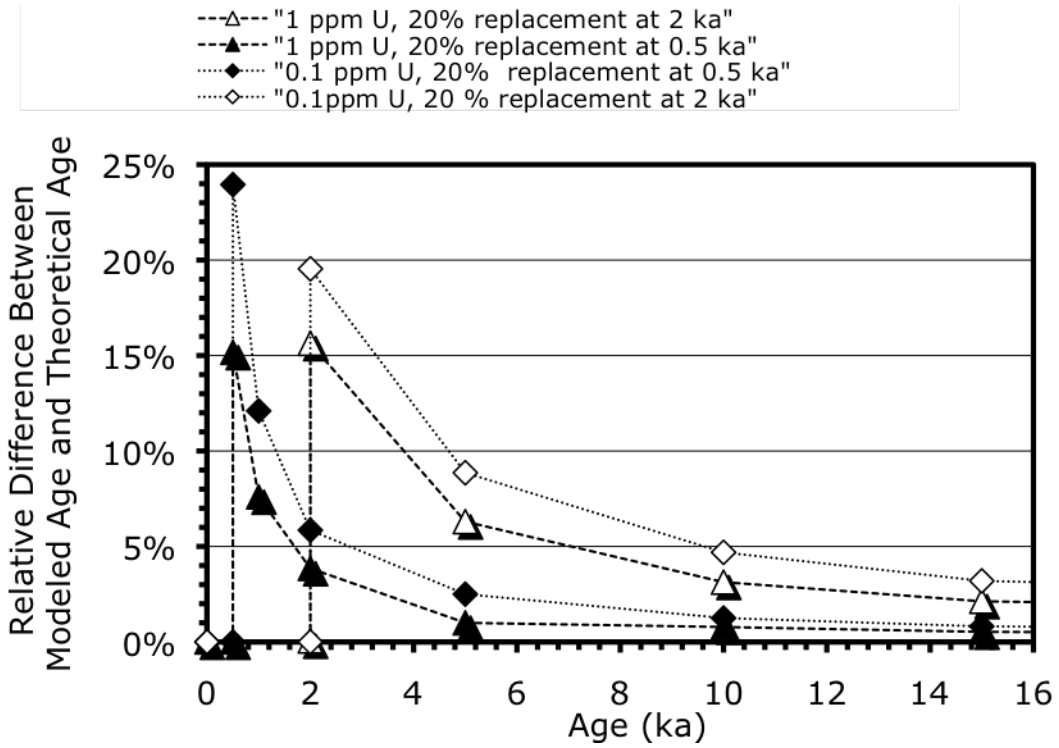

Figure 3. Plot of age vs. relative age difference between modeled age and theoretical age for calcite-replacement model described in text. Diamonds represent 20 percent replacement with 0.1 ppm U; triangles represent 20 percent replacement with 1 ppm U. Closed symbols indicate modeled calcite replacement at 0.5 ka, open symbols indicate modeled calcite replacement at 2 ka.

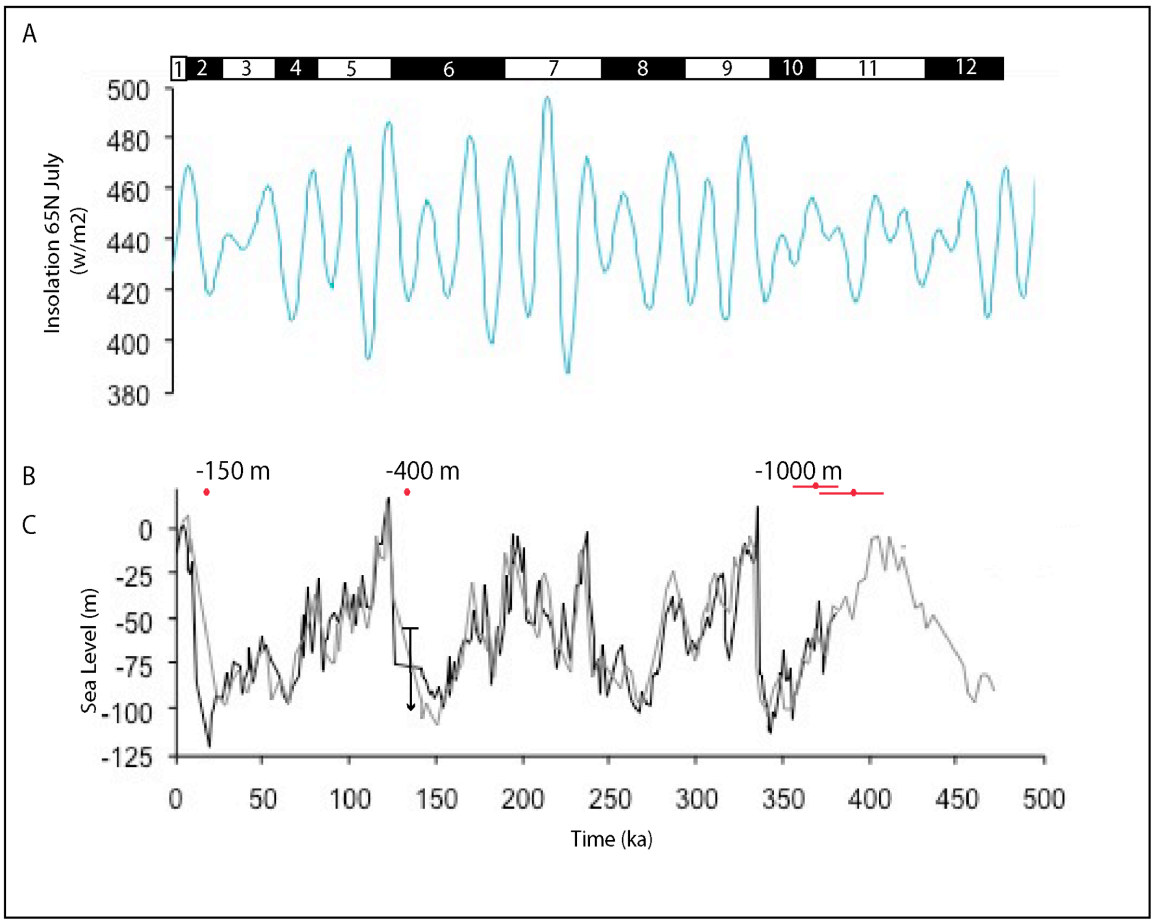

Figure 4: A). July insolation at 65˚N [44]. B). Our reliable ages and their errors, except where error is smaller than the symbol. C). Siddall et al. sea level record based on a Red Sea salinity record of $\delta^{18}O$ [40].

Table 1. ^{230}Th and ^{14}C dating results. The error is 2σ.

Data from the -1000 m reef -- dredge samples

Sample Number	^{238}U (ppb)	^{232}Th (ppt)	^{230}Th / ^{232}Th (atomic x10^{-6})	δ^{234}U (measured)*	^{230}Th / ^{238}U (activity)**	δ^{234}U$_{Initial}$ (corrected)*,***	^{230}Th Age (kv BP) (corrected)$	Depth (m)	Percent Calcite#
mvd3-r-12	4280 ±0	829 ±2	86890 ±190	49.8 ±0.2	1.0207 ±0.0004	131.0 ±0.6	**342.8 ±1.1**	-930	22
mvd3-r11-4	2578 ±0	508 ±1	83300 ±190	55.1 ±0.2	0.9944 ±0.0010	123.6 ±0.7	**286.5 ±1.4**	-930	23
mvd3-r11-7	2789 ±0	267 ±1	178000 ±580	59.0 ±0.2	1.0319 ±0.0006	154.7 ±0.8	**341.8 ±1.4**	-930	33

Data from the -1000 m reef at Kohala

Sample Number	^{238}U (ppb)	^{232}Th (ppt)	^{230}Th / ^{232}Th (atomic x10^{-6})	δ^{234}U (measured)*	^{230}Th / ^{238}U (activity)**	δ^{234}U$_{Initial}$ (corrected)*,***	^{230}Th Age (kv BP) (corrected)$	Depth (m)	Percent Calcite#
t301-r39	2067 ±2	33 ±32	1070000 ±1060000	50.6 ±2.2	1.0396 ±0.0047	153.4 +11.2/-10	**392.5 +20.4/-17.9**	-968	< 2
t301-r40	2929 ±6	975 ±10	478000 ±7000	57.9 ±1.7	0.9620 ±0.0109	116.4 ±5.0	**247.0 +10.8/9.9**	-968	< 2
t301-r42	2557 ±3	102 ±11	424000 ±46000	55.1 ±0.2	0.9944 ±0.0010	135.6 ±6.0	**337.8 +11.0/-10.2**	-967	< 2
t301-r43	9321 ±11	1603 ±39	27000 ±700	36.0 ±1.2	0.2778 ±0.0009	39.7 ±1.3	**34.0 ±0.1**	-967	< 2
t301-r45	1051 ±1	115 ±4	1612000 ±5000	50.3 ±1.2	1.0658 ±0.0044	257.0 +110.5/-42.8	**577.1 +126.4/-63.4**	-967	< 2
t301-r46	1239 ±2	184 ±6	1148000 ±4000	50.3 ±1.5	1.0345 ±0.0037	146.2 +7.2/-6.6	**377.2 +13.4/-12.2**	-967	< 2
t301-r47	2780 ±4	15604 ±71	3240 ±20	52.4 ±1.5	1.1030 ±0.0055	52.4 ±1.5	** **	-936	19
t301-r48	1957 ±4	23526 ±138	1630 ±10	56.2 ±2.6	1.1889 ±0.0078	** **	** **	-935	54
t301-r49	3050 ±6	2899 ±16	18390 ±140	51.5 ±1.9	1.0588 ±0.0056	200.7 +35.3/-22.5	**481.1 +56.1/-39.8**	-936	< 2
t301-r51	4945 ±9	657 ±8	64000 ±800	146.6 ±1.9	0.5111 ±0.0021	175.5 ±2.3	**63.5 ±0.4**	-936	20
t302-r27	868 ±2	246 ±8	66670 ±2200	57.5 ±3.0	1.1430 ±0.0071	** **	** **	-989	57
t302-r28	2955 ±4	4556 ±32	11400 ±94	57.6 ±1.7	1.0653 ±0.0050	216.3 27.8/-19.8	**468.4 +41.7/32.1**	-989	45
t302-r28	4732 ±10	516 ±27	159500 ±8300	57.8 ±2.9	1.0529 ±0.0047	182.1 ±16.3	**406.1 +25.3/-21.7**	-989	45
t302-r30	2584 ±6	5485 ±27	8200 ±50	57.0 ±3.2	1.0542 ±0.0051	184.4 +19.6/-16.5	**415.3 +30.4/-25.3**	-989	17
t302-r32**	2349 ±3	4087 ±14	15150 ±70	47.9 ±1.6	1.5964 ±0.0057	** **	** **	-989	34
t302-r32	4601 ±6	9841 ±37	10970 ±60	49.5 ±1.6	1.4211 ±0.0059	** **	** **	-989	34
t302-r36	3209 ±5	1344 ±14	424610 ±50	51.6 ±1.7	1.0770 ±0.0065	** **	** **	-1022	< 2
t302-r40	2802 ±4	128 ±10	3931000 ±31900	63.7 ±1.5	1.0873 ±0.0068	** **	** **	-1020	< 2
t302-r41	2807 ±6	251 ±20	196400 ±16000	55.8 ±2.9	1.0624 ±0.0079	208.1 +49.3/-28.7	**465.7 +73.5/-48.1**	-1020	< 2

Data from the -400 m reef

Sample Number	^{238}U (ppb)	^{232}Th (ppt)	^{230}Th / ^{232}Th (atomic x10^{-6})	δ^{234}U (measured)*	^{230}Th / ^{238}U (activity)**	δ^{234}U$_{Initial}$ (corrected)*,***	^{230}Th Age (kv BP) (corrected)$	Depth (m)	Percent Calcite#
P5-66-1A	16193 ±37	145278 ±618	1450 ±10	116.9 ±4.7	0.7870 ±0.0045	168.1 ±6.8	**128.6 ±1.8**	-410	22
P5-70-4A	2951 ±6	495 ±6	80500 ±900	95.2 ±2.2	0.8187 ±0.0027	143.6 ±3.3	**145.4 ±1.2**	-525	< 2
T277-R20	1553 ±2	10210 ±53	2100 ±20	132.6 ±1.4	0.8412 ±0.0049	198.1 ±2.3	**141.8 ±1.6**	-510	24
T277-R8B	2910 ±3	2249 ±14	17000 ±120	101.6 ±1.2	0.7991 ±0.0023	149.5 ±1.9	**136.7 ±0.9**	-412	8
T278-R10	2567 ±3	712 ±18	47500 ±1190	104.2 ±1.9	0.7992 ±0.0033	153 ±2.8	**136.0 ±12.1**	-499	< 2
T278-R12	2535 ±8	3692 ±22	9290 ±80	103.0 ±2.5	0.8196 ±0.0056	154.4 ±3.9	**143.3 ±2.1**	-538	20
T278-R14	3106 ±10	4527 ±20	9664 ±60	99.5 ±2.7	0.8531 ±0.0044	155 ±4.2	**156.9 ±2.0**	-538	2
T278-R17	2118 ±5	31582 ±27	909 ±3	104.9 ±1.7	0.8205 ±0.0034	157.2 ±2.6	**142.6 ±1.3**	-448	10
T278-R3	2730 ±3	8438 ±38	4475 ±30	96.7 ±1.4	0.8375 ±0.0041	148.5 ±2.3	**151.8 ±1.6**	-562	16
T285-R1**	4614 ±16	6465 ±36	3920 ±30	81.0 ±3.1	0.3326 ±0.0023	90.7 ±3.5	**39.9 ±0.4**	-436	3
T288-R1	1187 ±3	31295 ±368	550 ±10	120.3 ±2.8	0.8813 ±0.0114	189.1 ±5.1	**159.9 ±4.7**	-472	21

Data from the -150 m reef (Webster et al., 2004)

Sample Number	^{238}U (ppb)	^{232}Th (ppt)	^{230}Th / ^{232}Th (atomic x10^{-6})	δ^{234}U (measured)*	^{230}Th / ^{238}U (activity)**	δ^{234}U$_{Initial}$ (corrected)*,***	^{230}Th Age (kv BP) (corrected)$	Depth (m)	Percent Calcite#	14C calibrated age (ka)@
T291-R16	3477 ±9	44 ±16	187000 ±69000	139.4 ±2.8	0.1443 ±0.0008	145.3 2.8	**14.7 ±0.1**	-149	2	**15.0 ±0.4**
T291-R17A	3049 ±7	688 ±20	10800 ±300	137.6 ±2.4	0.1470 ±0.0013	143.5 ±2.5	**15.1 ±0.1**	-150	7	**14.6 ±0.5**
T291-R4	3092 ±6	1001 ±25	7600 ±200	140.2 ±2.4	0.1489 ±0.0009	146.4 ±2.5	**15.2 ±0.1**	-149	12	**13.5 ±0.4**
T291-R7A	2739 ±9	470 ±12	14400 ±400	141.4 ±2.8	0.1492 ±0.0012	147.6 ±2.9	**15.3 ±0.1**	-153	14	**15.1 ±0.4**
T291-R9	2828 ±8	518 ±14	13300 ±380	142.4 ±2.8	0.1457 ±0.0010	148.6 ±2.8	**15.1 ±0.1**	-153	5	**14.9 ±0.5**

* δ^{234}U = ([^{234}U/^{238}U]activity – 1)x1000.

** Activities and ages were calculated using λ_{230} = 9.1577 x 10^{-6} year^{-1}, λ_{234} = 2.8263 x 10^{-6} year^{-1}, λ_{238} = 1.55125 x 10^{-10} year^{-1} and λ_{235} = 9.8485 x 10-10 year^{-1} (age equations and references for λs are from [17,38]).

*** δ^{234}U$_{initial}$ was calculated based on ^{230}Th age (T), i.e., δ^{234}U$_{initial}$ = d^{234}U$_{measured}$ x e^{l234xT}.

$ Corrected ^{230}Th ages assume the initial ^{230}Th/^{232}Th atomic ratio of 4.4 ±2.2 x10^{-6} (The errors are arbitrarily assumed to be 50%).
Those are the values for a material at secular equilibrium, with the bulk earth ^{232}Th/^{238}U value of 3.8.
B.P. stands for "Before Present" where the "Present" is defined as the year 1950 A.D.

Calcite contents below the limit of detection (we consider to be less than two percent)is indicated as < 2.
** after the sample number indicates data included with a suspect uranium run.

@ 14C calibrated ages were converted using the Calib program and the Marine04 curve [18].

Recoil Modeling results - Results shown are minimum model ages (see text).

Data from the -1000 m reef -- dredge samples

Sample Number	f_{234}	initial 230Th/238U	Modeled ^{230}Th Age	Measured ^{230}Th Age (kv BP)*** (corrected)	
mvd3-r-12	0.994	-	355	**342.8**	±1.1
mvd3-r11-4	0.995	-	325	**286.5**	±1.4
mvd3-r11-7	1.000	0.20	325	**341.8**	±1.4

Data from the -1000 m reef at Kohala

Sample Number	f_{234}	initial 230Th/238U	Modeled ^{230}Th Age	Measured ^{230}Th Age (kv BP)*** (corrected)	
t301-r39	1.001	0.12	**378**	**392.5**	+20.4/-17.9
t301-r42	0.989	-	**340**	**337.8**	+11.0/-10.2
t301-r45	1.014	0.05	**455**	**577.1**	+126.4/-63.4
t301-r46	1.000	0.02	**375**	**377.2**	+13.4/-12.2
t301-r49	1.010	0.04	**425**	**481.1**	+56.1/-39.8
t301-r51	1.120	0.26	**30**	**63.5**	±0.4
t302-r27	1.013	3.10	**395**	**infinite**	infinite
t302-r28	1.015	-	**405**	**468.4**	+41.7/32.1
t302-r28	1.010	0.06	**375**	**406.1**	+25.3/-21.7
t302-r30	1.010	0.15	**380**	**415.3**	+30.4/-25.3
t302-r36	1.002	1.20	**375**	**infinite**	infinite
t302-r40	1.027	0.04	**415**	**630.3**	infinite
t302-r41	1.014	-	**410**	**465.7**	+73.5/-48.1
t302-r42	1.014	-	**410**	**infinite**	infinite

Data from the -400 m reef

Sample Number	f_{234}	initial 230Th/238U	Modeled ^{230}Th Age	Measured ^{230}Th Age (kv BP)*** (corrected)	
P5-70-4A	0.995	-	**145**	**145.4**	±1.2
T277-R8B	1.007	-	**135**	**136.7**	±0.9
T278-R10	1.012	-	**133**	**136.0**	±12.1
T278-R12	1.015	-	**139**	**143.3**	±2.1
T278-R14	1.013	-	**153**	**156.9**	±2.0
T278-R17	1.019	-	**138**	**142.6**	±1.3
T278-R3	1.000	-	**152**	**151.8**	±1.6

*$d^{234}U = ([^{234}U/^{238}U]_{activity} - 1)x1000$. ** $d^{234}U_{initial}$ was calculated based on ^{230}Th age (T), i.e., $d^{234}U_{initial} = d^{234}U_{measured} \times e^{l234xT}$. Corrected ^{230}Th ages assume the initial $^{230}Th/^{232}Th$ atomic ratio of 4.4 ±2.2 $x10^{-6}$. Those are the values for a material at secular equilibrium, with the bulk earth $^{232}Th/^{238}U$ value of 3.8. The errors are arbitrarily assumed to be 50%.

***B.P. stands for "Before Present" where the "Present" is defined as the year 1950 A.D.

Table 2

Chapter 4: A riddle wrapped up in an enigma: uranium series data (and a few) ^{230}Th ages of corals from the Huon Gulf, PNG

1.0 Introduction

The Huon Gulf, Papua New Guinea contains a series of submerged fossil coral reefs, which are thought to be mainly glacial reefs that developed in response to rapid subsidence (~2-6 m/kyr). Modeling results suggest that similar to the Hawaiian reefs, the tops of the Huon terraces may represent reef material that was growing during or just immediately prior to a glacial termination (e.g. Galewsky, 1996; Ludwig et al., 1991; Wallace, 2002; Webster et al., accepted, in revision). Reefs are most likely to drown during periods of rapid eustatic sea-level change, such as during a glacial termination. Thus ages of fossil corals from the submerged Huon Gulf reefs could provide a chronometer linked to global ice volume that is precise enough to test the Milankovitch Theory's predictions of the timing of ice-sheet demise.

My initial hypothesis at the conception of this project was that submerged corals would be more likely to have remained closed systems with respect to the uranium-series isotopes than emergent corals because they would have remained in contact with marine water. Here I present a suite of uranium-series isotopic measurements (and a handful of ^{230}Th ages) from the Huon Gulf and calculate a long-range subsidence rate of -2.6 m/ka for the gulf. I also describe lab methods applied to the corals in an effort to produce ^{230}Th ages.

2. Setting of the Huon Gulf

2.1 Tectonic Setting of the Huon Gulf

Papua New Guinea occupies the eastern half of the larger island of New Guinea. Much of the island sits on the northern margin of the Australian plate, which is actively colliding with the Huon-Finisterre Terrane (Abbott et al., 1994) (Figure 1). Onshore this collision manifests itself in the Ramu-Markham fault and offshore collision is a subduction zone, located in the Huon Gulf. The modern tip of collision lies in the western Solomon Sea at about 147°E (Crook, 1989; Davies et al., 1987; Silver, 1991)**.** West of 147°E (the western portion of the country of PNG) consists of an actively growing mountain system where the Bismarck forearc has thrust over the Australian continental margin (Abbott et al., 1994). The Huon-Finisterre Mountains, with present elevations of 4 km, and the Huon Peninsula, the location of a series of highly studied fossil reefs (e.g.Chappell, 1974; Esat et al., 1999), are direct products of this collision. Gravity observations by Abers and Mccaffrey (1994) suggest that subsidence in the Huon Gulf is likely the expression of regional compensation of the load of the Finisterre Mountains and related subsurface loads.

2.2 Models of reef development

Galewsky et al. (1996) modeled the flexural subsidence of the Australian (down-going) plate and its effects on carbonate platform development. Inputs to their model were eustatic sea level, tectonic rates, flexural characteristics of the Australian plate, and coral platform growth rates. The tectonic subsidence of the model was constrained

with a ^{230}Th date (348 ± 10 ka) from a coral sample dredged from -1950 meters, yielding a subsidence rate of -5.7 m/ka.

Coral growth rates vary as a function of water depth, due largely to the limit of the ability of sunlight to pass through the water column (Bosscher and Schlaer, 1992; Chalker, 1981). Under conditions of slowly varying eustatic sea level, the growth rate of corals on the subsiding Australian plate can match the rise in relative sea level and generate a large carbonate platform. The corals drown when relative sea-level rise becomes too rapid for skeletal growth to keep up, such as during a glacial termination. Following sea-level rise, subsidence continues, moving the coral platform still further from the photic zone. A new platform establishes itself in the new photic zone window of depth and the material at the top of each platform represents material that formed immediately before or during the introduction of a pulse of meltwater (i.e. during a termination). The original analytical model (Galewsky, 1996) produced four large carbonate platforms that initiate growth during major interglacial periods and continue to accumulate during subsequent interstadial and glacial periods; a new platform is built during each 100 ka glacial-cycle.

Wallace (2002) expanded the numerical model of the bathymetry of the Huon Gulf to include additional (observed) terraces. Her numerical modeling is constrained by the dredge sample (Galewsky, 1996) and sample #89 (data presented in this chapter), from -240 m water depth. The Wallace model incorporates flexural subsidence of the Huon Gulf due to the load from subduction; coral growth on the subsiding plate; and changing eustatic sea levels (Imbrie, 1984; Lambeck, 2001). Vertical reef growth rates were calculated as a function of water depth from the equations of Bosscher and

Schlager (1992). Wallace (2002) found that variable plate thickness, with significant thinning toward the trench (from 16 to 10 km effective elastic thickness) provides the best fit between the observed and modeled data.

Webster et al. (2004a; 2004b) examined the sedimentological setting of the platforms during development, combining observational data (from the 2001 cruise) and numerical modeling. The Webster et al. (2004a) model adds in complexity to the basic understanding of platform development in the Huon Gulf. Like Galewsky et al. (1996) and Wallace (2002), the Webster et al. (2004a) model predicts that platforms generally initiate growth following the end of a sustained period of high sea level, either a major highstand or a smaller interstadial. Platform growth continues with periods of falling sea levels (toward the major lowstands or stadials), with sometimes complex growth histories characterized by alternating periods of abrupt drowning and subaerial exposure controlled by millennial-scale sea-level oscillations. Final platform drowning occurs during both the initial stages of both major deglaciations and smaller amplitude interstadial events.

3. Sample Collection and Methods

3.1 Samples

In August and September 2001, we collected reef material, including many fossil corals from a series of submerged coral platforms in the Huon Gulf, PNG. These corals are the submerged counterparts to the well-studied corals on the Huon Peninsula (e.g. Chappell, 1974; Esat et al., 1999). Using the remote controlled submersible, Jason, we collected over two tons of samples from the tops of nine carbonate platforms

between 300 and 2600 meters of water depth. The sedimentology of the samples is summarized by Webster et al. (2004a).

We collected samples from the tops of nine fossil coral reefs. Their depths (and estimated ages based on the models of Galewsky et al. (1996), Wallace (2002), and Webster et al. (2004a) are as follows): -250 m (60 ka), -625 m (112 ka), -830 m (145 ka), -1130 m (200 ka), -1280 m (230 ka), -1650 m (295 ka), -1950 m (348 ka), -2120 m (375 ka), -2390 m (410 ka). Because our model suggests that the top of the coral terraces was the last material growing before the corals ultimately drown, I set out to identify (visually) the best sample from the top of each terrace. Preliminary ages of the terraces would enable the rest of the collaboration (Laura Wallace (UCSC), Jody Webster (UCSC), Eli Silver (UCSC), Don Potts (UCSC) and Bruce Applegate (U of Hawaii)) to use the ages to constrain the tectonic model, characterize the geomorphology and sedimentology of the reefs, and to set the context in which these reefs developed. In addition, Leah Gruhn from the University of Minnesota Duluth needed the ages of some of the reefs for a stable isotope/trace element paleoclimate study.

3.2 Methods

I subsampled the most promising samples from the tops of each terrace for initial measurement, based upon gross observations of hand samples. I then washed, crushed and picked samples under a binocular microscope and dried them overnight before weighing them. Typical sample amounts ranged from 200 to 300 mg. The chemical procedure I used to separate the uranium and thorium from the coral skeleton

is similar to that described in Edwards et al. (1987). Samples were dissolved with nitric acid, a mixed $^{229}Th/^{233}U/^{236}U$ tracer added to them, and then dried down. After the addition of an iron chloride solution, NH_4OH was added drop-wise to precipitate the iron complexes. The sample was then centrifuged to separate the iron from the rest of the solution and the supernate removed. After loading the sample onto columns containing anion exchange resin, HCl was added to elute the thorium and water was added to elute the uranium. With the uranium and thorium separated, each sample was then dried down again and finally dilute nitric acid was added for injection into the ICP-MS.

Analyses were conducted by means of inductively coupled plasma mass spectrometry (ICP-MS) on a Finnigan-MAT Element outfitted with a double focusing sector-field magnet in reversed Nier–Johnson geometry and a single MasCom multiplier. The instrument was operated at low resolution and in electrostatic peak hopping mode. Combined ionization plus transmission efficiency of 2.5 to 3x has been measured for uranium and 1.5 to 2x has been measured for thorium. Further details on instrumental procedures are explained in Shen et al. (2002).

To analyze coral samples for assessment of their carbonate mineralogy, I took the subsample (generally ~0.2 grams) and crushed the coral with a clean, quartz glass mortar and pestle, reducing the mean particle diameter to ~5 μm. I then loaded the sample onto a glass slide utilizing a thin layer of petroleum jelly for the smear mount. The mounted sample was then inserted into the x-ray diffractometer and a scan run from a 2 theta start angle of 25.005º to an end angle of 34.995º, with a 0.01º step size and 1.50 seconds per step.

Calcite-to-aragonite composition ratios were determined using a standard curve generated from the peak area ratios, using the 2-theta peaks of 26.219 for aragonite and 29.404 for calcite, of known mixtures of aragonite and calcite. From triplicate measurements of 10 different known standards, the relationship between the peak area ratio and percent calcite was computed. For each sample I then took the peak area ratio and compared to the standard curve to derive percent calcite.

4. Results

4.1 Hand sample/subsampling observations:

Without exception, corals in hand sample do not look pristine. The outsides of coral samples were encrusted with iron-manganese oxides and some interior sections of coral skeletons were discolored orange or brown (vs. a white to cream as an unaltered color). Coral samples from the -250 m terrace were not massive head corals; rather they were fragments of coral, packed into mud and other reef debris in bindstones. Massive coral samples from every other terrace (except -2200 m) show evidence of sponge boring into the samples, presumeably post-depositionally. In addition, the pores of some of the corals contain loose sediment – red to brown mud. In some instances the mud is pervasive into the interior of the coral samples. While subsampling, I took care to select sections of corals that appeared the least diagenetically altered for isotopic measurements: no visible calcite recrystallization, no clear evidence of discoloration of coral skeleton, and minimal sediment preservation within pores of the corals. After subsampling, the corals were examined again under a microscope in an attempt to further reduce the amount of discoloration and alteration contained within the sample

for isotopic measurements and to ascertain that no visible sediments were present in the pores. Even with elimination of obvious secondary material and/or discoloration in the subsample, when I dissolved the subsamples, the resultant solute was discolored (usually a shade of orange, vs. an expected clear to yellow color.

4.2 Uranium-series measurements:

I measured the U-Th isotopic composition and calcite/aragonite composition of 41 coral samples. I initially limited measurements to samples with minimal visible alteration in hand sample, but then expanded to include a variety of other samples. In addition, Dr. Hai Cheng measured the U-Th-Pa isotopic composition of 6 samples. In the following section I will describe the best data from each terrace, but the complete results of these measurements are contained within Table 1. Including samples from all terraces, samples contained from 10^3 to 10^5 ppb uranium and from 100 to 260,000 parts per trillion thorium (ppt). The full range of $\delta^{234}U_i$ measured in my samples ranged from 30 to over 200.

From the -250 m terrace, I measured the isotopic composition of seven coral samples; four of these samples meet the traditionally reliable criteria (see introduction to thesis). The reliable measured ages of samples from this terrace range from 57.7 ± 1.5 ka ($\delta^{234}U_i = 143.5 \pm 2.5$) to 107.3 ± 0.9 ka ($\delta^{234}U_i = 150.3 \pm 2.5$). Sample #89 contained three isolated fragments of corals (that could have grown at different times) that I measured: 89-A is 60.3 ± 0.5 ka ($\delta^{234}U_i = 143.5 \pm 2.5$); 89-B is 57.7 ± 1.5 ka ($\delta^{234}U_i = 149.9 \pm 2.0$); and 89-C is 64.0 ± 0.5 ka ($\delta^{234}U_i = 141.0 \pm 3.6$). The reliable ages (and $\delta^{234}U_i$ values) of the other corals from this terrace are: # 108: 61.8 ± 0.9 ka

($\delta^{234}U_i$ = 145.6 ± 4.4), #77a: 67.4 ± 0.8 ka ($\delta^{234}U_i$ = 142.8 ± 2.7), and #77b: 59.1 ± 0.9 ka ($\delta^{234}U_i$ = 144.2 ± 3.4).

From the -250 m terrace I also measured the isotopic composition of two isolated coral fragments from sample #57 and infilling of the pore spaces of the same coral fragments composed of material that looked like carbonate. To subsample #57, I used a microdrill to drill out subsamples of the coral and infilling. Sample size was limited, with just enough material for isotopic measurement (and not enough to measure the calcite content of the samples). The coral fragments had ages of 103.1 ± 1.0 ka ($\delta^{234}U_i$ = 147.2 ± 3.1) and 107.3 ± 0.9 ka ($\delta^{234}U_i$ = 150.4 ± 2.5); the infillings had ages of 110.3 ± 1.2 ka ($\delta^{234}U_i$ = 142.6 ± 3.8) and 103.6 ± 0.7 ka ($\delta^{234}U_i$ = 140.8 ± 2.8).

I measured the isotopic composition of eight corals collected from between -645 and -853 m of water depth. Of these corals, one meets the criteria for traditionally reliable ages. Two corals have $\delta^{234}U_i$ values within error of modern seawater (#3 and #18), but #18 has a low uranium concentration. #3 (from -853 m water depth) contains <2% calcite and has a uranium concentration that is between 2-3 ppm, with an age of 430 +25/-21 ka ($\delta^{234}U_i$ = 143.7 ± 14.0). Sample #18 (-726 m collection depth) has a low uranium concentration (1168 ± 2 ppb), a high ^{232}Th concentration (11,024 ± 36 ppt), and is 23 percent calcite. Its $\delta^{234}U_i$ is 151.5 ± 11.5 and its ^{230}Th measured age is 248.6 ± 25.1 ka.

Of four measured samples from the -1200 m terrace, one meets the criteria for traditionally reliable ages: #197. Sample #197's age is 377.5 +22.4/-19.5 ka (<1% calcite; $\delta^{234}U_i$ = 149.4 +20.4/-18.6). Of the other three samples from the -1200 m terrace, one has less than 2 percent calcite: #166 computes an age of 413.0 +15/-14 ka

(<1% calcite; $\delta^{234}U_i$ = 159.0 +9/-8). The remaining two have greater than two percent calcite – one with a low $\delta^{234}U_i$ value (>90% calcite) and one with a high $\delta^{234}U_i$ value (8% calcite).

None of the five samples measured from the -1650 m terrace meet all of the criteria for traditionally reliable ages. All of the samples from this terrace have low $\delta^{234}U_i$ values, with the exception of sample #244 ($\delta^{234}U_i$ > 193). Three samples from the -1650 m terrace contain more than 2 percent calcite (#232 = 10%; #225 = 35%; #228 >19%). Similarly, of six measured samples from the -1950 m terrace, none meet the reliability criteria. Samples from this terrace have low $\delta^{234}U_i$ values, yet with the exceptions of sample # 199 and 142 (almost 20% calcite), the samples do not show evidence of calcite. The submerged samples from -1950 m terrace contain at least 10 times more ^{232}Th than the original dredge samples (Galewsky, 1996). The submerged samples have a ^{238}U content (range: 2272-5283 ppb, average 3097 ppb) that is similar to that of the dredge samples. The calcite content of the submerged samples ranges from <2% to 19%, a range larger than that of the dredge samples (which were all <2%) (Galewsky, 1996). All samples measured from >2200 m contain more than 2% calcite and have either low $\delta^{234}U_i$ values (range: 45-133) or high $\delta^{234}U_i$ values – i.e. $\delta^{234}U_i$ is infinite.

The results of the protactinium dating are shown in Table 2. The results represent a total of 11 samples -- 6 samples (#89a, #3, #166, #226, #135, #298) and the EDTA cleaning of 5 of those samples. The protactinium age from sample #89a (59.5 ± 1.1 ka) is concordant with the measured ^{230}Th age (60.3 ± 0.5 ka). With the exception of sample #89a (from -250 m reef), all of the samples are at secular equilibrium (and thus

their computed ages are infinite). If the samples are older than ~200 ka, the [^{231}Pa /^{235}U] ratio must equal one (be at secular equilibrium), if the sample has behaved as a closed-system (Cheng et al., 1998). However since the ^{230}Th ages of the samples are older than ~200 ka, secular equilibrium is not a completely diagnostic check on closed-system behavior as one would expect the sample to have been at secular equilibrium for some time (perhaps almost 300 ka).

5. Discussion of Initial Results

The expected ages of samples we collected ranged from 60 – 410 ka (all less than 650 ka) (Galewsky, 1996; Wallace, 2002), yet a large number of samples measured had infinite ages (>650 ka) and/or high or infinite $\delta^{234}U_i$ values. The best available ages for each terrace are summarized in Table 3. The terrace formation model predicts that the terraces should be preserved in stratigraphic order: deeper terraces should be older, shallower terraces should be younger. Samples from the -250, -1200, -1600, -1950 and -2200^{+} m terraces appear to increase in age with an increase in depth. These terraces follow the pattern of shallowest terraces being youngest and deepest terraces being oldest. However # 3 from the -830 m terrace presents an exception to stratigraphic order: # 3 from -853 m depth is 430 +25/-21 ka, older than (or the same age as) the -1200 m terrace (#197b from the -1200 m terrace is 367.9 +22/-19 ka).

My measurements of Huon Gulf samples do not match the expected (modeled) ages and the $\delta^{234}U_i$ values of the measured samples were (for the most part) not within error of seawater. The measured ^{230}Th age of dredge samples from the -1950 m terrace is 348 ± 10 ka (Galewsky, 1996). These samples were collected in 1991 and measured

in 1993 in the Minnesota Isotope Lab by Dr. Christina Gallup. The age of the dredge samples does not match the age from the submerged samples we collected from the Huon Gulf in 2001. As the samples from 1991 were obtained via dredging, it is possible that they are actually from a different depth and/or sampled material in the interior of the reef that we were unable to sample with the remote controlled submersible in 2001.

My initial measurements suggested evidence of corals growing in MIS 3-6 (57-110 ka) from the shallower terraces and MIS 10-14+ (older than 367 ka) from deeper terraces, but limited evidence of corals growing between 60 ka and 367 ka (with the exception of two coral fragments at ~100 ka). The modeling work suggested that corals should be growing in the HG more or less continuously from the present to the oldest corals. This unconformity represents a significant amount of time—almost 300 ka, during which corals theoretically could have been growing on the subsiding plate.

Not only were the geochemistry results less than pristine, some of the coral samples were discolored (either totally or partially) in hand-sample. Even though I minimized the amount of secondary material and discoloration in the subsample via visual inspection and physically selecting non-altered material, the corals obviously contained material (organic perhaps?) that led to a discolored solute and eventually chemistry results indicative of some kind of alteration. I did not expect the corals to be more altered than their emergent counterparts.

6.1 Experimenting With Chemical Cleaning Protocols

My project was initially conceived to be the quantitative link between tectonics and climate – I was to provide the ages and in turn my collaborators could refine the

tectonics model. I attempted a number of quick experiments that were designed to provide a preliminary evaluation of whether a specific method would be helpful in quickly getting to an age. After each of these experiments I decided (with the help of Dr. Christina Gallup), whether to proceed with that line of thinking or to discard it and attempt another method. In hindsight, this method of testing protocols left a number of incomplete data sets and did not provide for a full evaluation of each method.

I sought an identifiable contaminant component that would add detrital thorium to my samples, making them appear older. If each component had a characteristic chemical signal, then it would be possible to remove this contaminant "signal" from the bulk value and thereby calculate a model age for samples that are otherwise undateable. I set out to see if I could remove these fractions from the bulk coral without altering the age. Secondarily, I wanted to identify a sampling/separating protocol that would minimize the amount of coral contaminant and maximize the amount of primary skeletal material I analyzed. For instance, if I could identify a coating on the samples that had a characteristic ^{232}Th concentration when I removed it (via physical or chemical cleaning) from multiple samples, then I would be able to subtract the detrital ^{232}Th (and more importantly, the associated ^{230}Th) from the total measured concentration.

I tried a total of four different pre-cleaning protocols in an attempt to isolate a specific contaminant and identify the best cleaning procedure. Two of these methods, which attempted to use a dissolution step to dissolve surface contaminants and a chelation step to prevent readsorption onto the carbonate skeleton, were based on techniques developed for deep-sea corals (Lomitschka and Mangini, 1999) and forams (Martin and Lea, 2002). The third method attempted to dissolve the outermost portions

of the coral, leaving behind the internal, presumeably less-altered material. Finally, the last method involved crushing the coral skeleton and measuring specific size-fractions of the crushed skeleton, again attempting to isolate less-altered material. The details of these methods are described below.

6.1.1 EDTA Pre-cleaning

Lomitschka and Mangini (1999) developed and tested a cleaning procedure to reduce contamination when preparing deep-sea coral samples for ^{230}Th dating that uses ascorbic acid to dissolve surficial manganese and iron oxides. Ascorbic acid (Vitamin C) is a strongly reducing acid that reduces and dissolves manganese and iron oxides on the sample surface of the coral; when these oxides dissolve, they release associated authigenic thorium into solution. To prevent the thorium from readsorbing onto the carbonate after the sample was immersed in ascorbic acid, the samples were treated with Na_2EDTA (sodium-ethylene diamine tetra acetic acid), a chelating substance that forms a strong complex with thorium (and with manganese, copper, iron, lead, cobalt and calcium, which it is often used to remove from solution).

Dr. Christina Gallup performed the cleaning step and Dr. Hai Cheng separated the uranium and thorium from the coral skeletons to perform an initial test of this protocol on six samples (3, 89, 135, 166, 226, 292). Each ~400 mg sample was ultrasonically cleaned in water and then dried overnight in an oven to eliminate any sediment that might have been contained within the coral skeleton. The dried samples were then immersed for 10 minutes in solution containing 0.134 mol/l Na_2EDTA and 0.250 mol/l ascorbic acid. The liquid solution was removed from the beaker via pipette

and the samples rinsed twice with water. The samples were dried overnight in the oven and reweighed in order to obtain a sample weight and processed following the steps outlined in Section 3.2 of this chapter.

The results of this experiment are included in table 1 and are plotted in figure 2. All samples included in this study have ^{238}U concentrations between ~2300 and 3300 ppb. Samples #226 and #298 had a higher ^{238}U concentration in the control (untreated) sample, samples #166 and #306 had a higher ^{238}U concentration in the treated sample, and sample #3's ^{238}U concentration did not change significantly between the control and the treatment sample. The ^{232}Th of samples #3 and #166 did not appear to change from control to treated sample, the ^{232}Th of samples #226 and #135 was slightly lower in the control than the treated sample, and the ^{232}Th of sample #306 was slightly lower in the treated sample. The [230/238] of samples #3 and #226 was lower in the treatment samples and the [230/238] of samples #166, #135, #306 and #298 were higher in the treatment samples. I considered this preliminary experiment of the EDTA cleaning method to be reasonably successful because the $\delta^{234}U_i$ value of samples #3 and 226 were reduced in the treatment samples, but the treatment was not good enough to give actual ^{230}Th dates.

Because this preliminary test looked promising, I repeated the steps with samples #197 and #306, lengthening the leach time to 20 minutes (to allow it to go to the full reaction). Although our results show that ^{232}Th concentration was significantly reduced (7439 ppm in control for sample 306 and 4025 ppm in treated sample 306), I identified a problem with using this method in the Huon Gulf samples: it was difficult to remove the cleaning agents from my samples. Despite several rinsing steps, the

darker color (presumeably the Na_2EDTA) persisted, posing problems for interference during measurement and in running the ICP-MS in general. Because of the porous nature of the surface of coral skeletons, I suspect that the compound actually bonded with the carbonate and remained in my sample. I ultimately moved on to a slightly more complicated procedure (with the hope of removing more of the cleaning agents from the sample prior to measurement).

6.1.2 **Foram cleaning protocol/Deep Sea Coral Protocol:**

Mg/Ca ratios from shells of foraminifera are used to reconstruct deep-water temperature changes during the Quaternary (e.g. Lea et al., 2002). These benthic foram shells often contain remnant organic matter and adsorbed phases, similar to my submerged corals and as such, require a careful sample preparation. Martin and Lea (2002) evaluated cleaning procedures used to remove adsorbed phases from benthic forams. I traveled to the University of Chicago to assess the use of a modification of the foram cleaning method on corals with Dr. Pam Martin.

For this procedure I selected a handful of previously measured samples from the Huon Gulf (#89, #166 and #244), two samples from Barbados as a second set of controls (SL3-3 and SL3-5), and four additional samples from the Huon Gulf (#171, #193, #185, #225). I intended to use the two sets of controls to characterize what the cleaning protocol did and then to use the protocol to provide initial measurements for the third, previously unmeasured, set. If this protocol proved promising, then I planned to repeat it in Duluth. Each individual sample was divided into two fractions: one received the chelation steps and the second fraction did not.

Each sample received a pre-cleaning to remove loose material, the cleaning to remove adsorbed material, and then was dissolved and measured (as described in section 3.2). The pre-cleaning step was based upon previous work by Lomitschka and Mangini (1999) and Cheng et al. (2000). Each sample was pre-cleaned to remove pieces of mud by rinsing with MilliQ water while being ultrasonicated. As the water became cloudy, the water and fines were siphoned off and replaced. The process was repeated for a total duration of 15 minutes. This step was followed with a weak leach in 0.075 N superclean HNO_3 while ultrasonicating for five minutes. Following this leach step, (and following every step hereafter), I rinsed with clean water and siphoned off the water. The pre-cleaning oxidizing step entailed adding 5 mL (or enough to cover the sample) of a 1:1 solution of 30% H_2O_2: 0.2 N NaOH. I capped the vials and immersed in a hot water bath for fifteen minutes, replacing the solution when it was no longer visibly oxidizing the sample. Following the oxidizing step, I rinsed with 0.02 N NaOH (a weak base) and then with two clean water rinses. The samples were then dried at 70 degrees C, crushed and picked, concluding the pre-cleaning methods.

The process of the actual cleaning steps began with a 10 minute rinse (cover sample with water/ultrasonicate/siphon off the liquid), followed by a 2 minute-long weak leach in 0.15 N HNO_3 (leach, rinse, ultrasonicate, siphon off the liquid). For the oxidizing step, samples spent 20 minutes in 1:1 solution of 30% H_2O_2: 0.2 N NaOH in a hot water bath, replacing solution as it was spent. The samples were then rinsed with a weak base (0.2 N NaOH) and rinsed twice with superclean water. The oxidation step is balanced with a reducing step of 30 minutes in a 1:5:5: solution of hydrazine (H_2NHH_2):NH_4O_4:buffered citrate solution, ultrasonicating every five minutes. I rinsed

twice with superclean water. I then performed a chelation step with half of the samples, consisting of 20 minutes in DTPA (Diethylene triamine pentaacetic acid), a weak base rinse and water rinse and then 2 minutes in a weak leach of 0.15 N HNO_3 (leach, rinse, ultrasonicate, siphon off the liquid). Finally, I repeated the oxidation step, transferred samples to clean Teflon beakers, and returned the samples to the lab in Duluth for the chemical separation of uranium and thorium from the coral skeleton (see Section 3.2). See Table 4 for a complete summary of data, including samples from Barbados. Samples are noted in the data table as (sample# -c for foram cleaning protocol, e.g. 166c, or sample#-c1 for foram cleaning protocol with chelation).

While the ^{232}Th and presumeably the associated detrital ^{230}Th concentration of the samples decreased with this cleaning procedure (see Table 3), the processing of samples with this cleaning protocol unfortunately increased the uranium concentration of the samples. Sample SL3-5 gained almost 1000 ppb of ^{238}U with the full processing, 500 ppb ^{238}U without the chelation step. The uranium run on the mass spectrometer had very low intensity while running the partial cleaning of sample SL3-3b, but SL3-3b also gained uranium with cleaning, almost 450 ppb with the full cleaning. Likewise, 89 gained uranium with the cleaning (control = 3508 ppb, 89c = 3744, 89c-1 = 4161).

I sent a second set of two samples from the Huon Gulf (3 and 197) to Kevin Canariato (at the University of California at Santa Barbara) to run through the same foram cleaning process. Both samples experienced a significant loss of uranium –almost 70 percent (sample #3 308 ppb vs. 93 ppb after cleaning and sample #197 2581 ppb and 709 ppb after cleaning).

These preliminary results of testing both the foram-cleaning method (Martin and

Lea, 2002) and the Lomitschka and Mangini (1999) methods suggest that they are not appropriate for precleaning corals for ^{230}Th dating of Huon Gulf samples. The foram cleaning protocol followed in Chicago may have introduced uranium into the sample via contamination from the lab, however its possible the cleaning protocol just mobilized uranium. The weak leach steps could dissolve some sample and also detrital material (containing uranium), which may then readsorb onto the remaining solid, similar to results of selective dissolution experiments on carbonate bank sediments by Gallup (1997). Extra ^{238}U in the sample from this readsorption process violates the closed system assumption: that all ^{238}U in the coral is incorporated at the time of deposition. Additional ^{238}U acquired sometime after deposition both changes the amount of parent isotope in the sample and could potentially add more daughter isotope (^{234}U and/or ^{230}Th) as the uranium decays. There is a small possibility that the increased uranium concentration came from detrital material (such as carbonate sediments), not visible on observation in hand sample or under the microscope.

6.1.3 Selective Dissolution

Corals are highly porous rocks. The porosity of coral skeletons is interconnected, meaning that all the pores are in communication with one another. For example, two genera of coral, *Acropora* and *Porities*, differ significantly in the architecture of their exoskeletons. *Porities* exhibit a porosity of almost 50% with have a mean pore diameter of 250 micrometers, whereas *Acropora* porosity is about 12%, but

the mean pore diameter is 500 micrometers, twice that of *Porities* (Guillemin et al., 1989). Furthermore, submerged fossil coral samples are constantly in contact with seawater, allowing the possibility of sorption of materials to the edge of the coral and/or ion exchange with the seawater. Thus the edges of a coral skeleton could be more altered than the interior because they remain in contact with seawater. If it were possible to selectively remove (possibly via dissolution) this outer portion, then it would be possible to measure only unaltered fossil coral.

I used three favid corals (# 197, 227, 228) to attempt to remove the outer, presumeably more altered portion of the skeleton via dissolution. All corals were favids because the favids contained in the Duluth collection have the largest pore size (and the most solid wall structure), representing the least amount of surface area for exchange with the seawater. For each dissolution step I used 15mL of 0.1 Nitric acid in a 30 mL Teflon beaker. The sample was swirled approximately every 30 seconds for 15 minutes. The liquid solute was pipetted into a new, clean 30 mL Teflon beaker, and capped. The remaining coral was dried overnight in a 90°C oven and reweighed. The process was then repeated three times, allowing the final dissolution to go to completion (for a total of four dissolutions per sample). Each subsample was then taken through the thorium and uranium separation chemistry (described in section 3.2 of this chapter). Samples #197 and #227 contain less than 2 percent calcite while sample #228 contains almost 20 percent calcite. The bulk sample I numbered with the sample number (ex: #227) and then used -2 to indicate the first dissolution step (#227-2), -3 the second (#227-3), and so on.

The results of this experiment are summarized in Figure 4 and contained within Table 1. The behavior of uranium in these experiments was unpredictable. The ^{238}U concentration in sample #227 was the highest overall to begin with and increased with some of the dissolution steps. Uranium in sample #227 was more moderate initially, but the last two dissolution steps contained nearly no uranium. Finally uranium in #197 was highly variable with each dissolution step.

Likewise, the behavior of thorium during this experiment was unpredictable. The $^{230}Th/^{232}Th$ ratio of #197 decreased then increased with progressing dissolution and that of #227 and #228 increased with progressing dissolution. An increasing $^{230}Th/^{232}Th$ ratio indicates either increasing ^{230}Th is increasing and/or decreasing ^{232}Th throughout the experiment. Focusing on just ^{232}Th concentrations, #228 increased with progressing dissolution and the ^{232}Th concentration of #227 and #197 varied with progressing dissolution. I ultimately decided against selective dissolution as a precleaning protocol because both uranium and thorium appeared to behave unpredicatably and thus I was unable to use this method to pretreat samples, correct for removed uranium and/or thorium, and ultimately produce ^{230}Th ages.

Gallup performed similar experiments on Nicaragua Rise marine sediments and on coral HOB-EE-3 from the Huon Peninsula in Papua New Guinea (Gallup, 1997) and interpreted an increase in uranium throughout the experiment as the result of readsorption of uranium on the solute on the residual sediment. Gallup used the uranium concentration and the gradually decreasing $\delta^{234}U$ values throughout her dissolution steps to ultimately model $\delta^{234}U$ of the sediment. She performed multiple dissolution

steps (10+) and calculated a predicted uranium concentration in each step – controlling the dissolution by theoretical uranium concentration.

In order to circumvent readsorption of uranium during selective dissolution, Gallup experimented with adding acetyl acetone to the nitric acid she used in the dissolution and found that 92% of uranium in the solute partitioned into the acetyl acetone, successfully preventing the readsorption. However, since acetyl acetone is a toxic substance, I attempted to minimize the readsorption by keeping the solution acidic. If I were to revisit selective dissolution, Gallup's method of dissolution may be worth reevaluating. In order to do so it would be essential to begin with crushed samples to increase the effective surface area and to manually eliminate small, discolored bits of corals and sediment that can be present in the submerged corals. I would also divide each coral's dissolution into more steps (i.e. to take more subsamples), allowing a more precise evaluation of the method. In addition I would evaluate adding acetyl acetone to the nitric acid solution in order to prevent readsorption of uranium.

6.1.4 Grain Size Experiment.

Observation of corals in hand-sample and under the microscope revealed that the thickness of the coral skeleton is not uniform. When the coral is still alive, the individual coral polyp secretes a skeleton and produces a cup in which the polyp sits. The walls surrounding the cup, the theca, and the floor (the basal plate) are thinner than the septa that arise from the basal plate and provide the polyp with increased, structural integrity of the skeleton. The thicker pieces of coral skeleton have a lower surface area

to volume ratio; any alteration of the coral via exchange with seawater would be minimized. Thus if the sample measured for ^{230}Th dating consisted of pieces of the theca and basal plate and did not include the septa, the samples measured may have exchanged less with the seawater.

I tested this protocol on two previously measured samples: #197 and 226. Both samples were favid corals and both contain less than 2 percent calcite. Sample #197's ^{230}Th age (and corresponding $\delta^{234}U_i$) is #197: 387.1 +22.4/-19.5 ka (151.0 +12.6/-11.6) and sample #226 has infinite age and $\delta^{234}U_i$. I selected these samples because their morphology contained both thin and thick pieces of skeleton and because they came from two terraces that are in the middle of the suite of depths represented (-1200 m and -1600 m).

I washed, rinsed and dried samples of ~5 g and then crushed those samples using a mortar and pestle. At this point I segregated a bulk sample from each coral's crushed material (which I called 197B and 226B) and sieved the rest of the material into three size fractions: large -- >1mm; medium -- 1-0.5 mm; and fine -- 0.5-0.25 mm. I labeled these fractions 197L, 197M, 197F and 226 L, 226M and 226F. Sample #197 had a remaining fraction of powder smaller than 0.25mm diameter; I collected that powder and included it as a fourth size fraction (called 197vf – very fine). Samples were weighed and run through the standard coral-separation and measurement protocol (see methods section of this chapter, section 3.2).

The results from this experiment are included in Table #1 and shown in Figure 5.

Sample 197M I have no measurement for. With the exception of 197L the ^{230}Th ages of all subsamples were within error of each other. Their ages (and corresponding

$\delta^{234}U_i$ values) are 197B: 367.9 +22.3/-19.3 ka (147.7 +16.1/-15); 197L: infinite age (infinite); 197F: 338.4 +10.1/-9.4 ka (138.5 +5.4/-5.1); 197VF: 344/6 +21.9/-18.7 ka (131.9 +10.7/-.95). The ^{230}Th ages of samples (corresponding $\delta^{234}U_i$ values) from 226 are: 226B: infinite age; 226L: 70.9 ± 2.0 ka (37.8 ± 1.9); 226M: infinite age; 226F: infinite age.

For both 197 and 226, the sample with the highest ^{238}U concentration was also the smallest grain size. For sample 197 the pattern is pretty clear: smaller grain sizes equate with increased ^{238}U, decreased $^{230}Th/^{238}U$ activity and higher measured $^{234}U/^{238}U$ ratios. Sample 226 follows the same basic pattern, with the exception of the medium size fraction. The 226M (compared to the other 226 size fractions) is the lowest in ^{238}U and has the highest $^{234}U/^{238}U$ measured ratio; however its $^{230}Th/^{238}U$ activity is intermediate. Uranium does not vary nearly as much among the size fractions as thorium does. In both sets of size of samples, ^{232}Th concentration increased with decreasing grain size and the calculated $^{230}Th/^{232}Th$ ratio decreased with decreasing grain size. However the results from this experiment were not consistent enough to allow me correct for excess thorium and to actually compute ^{230}Th ages.

Overall the results from this method are mixed. It does appear that the bulk fractions of each coral may be the best fractions. Lessons learned from this experiment: it is reasonably time-effective to wash/dry/crush coral and pick out the bits that are discolored before measurement.

6.1.5 Final Sampling Protocol

The final cleaning protocol I decided upon was to wash each subsample in MilliQ water and dry overnight in an oven. Then I crushed the bulk samples (ranging

from > 1 kg in size to ~ 5 g in size) with a clean, quartz mortar and pestle and picked the samples under a binocular microscope, aiming for about 0.5 g of sample that was internally consistent in color (and not discolored) and contained pieces of the coral skeleton without extra sediment and/or secondary minerals. Coral fragments were typically 0.1 to 0.5 cm in diameter. I washed the samples with MilliQ water in an ultrasonication bath and siphoned off the water and fines, repeating the process until the water was clear, or 30 minutes. Samples were then dried overnight in the oven and examined again under a binocular microscope for signs of discoloration. Any pieces that were discolored were eliminated. After this exam, coral fragments were weighed and taken through the standard coral protocol (as described in Section 3.2 of this chapter, the methods section), reserving enough of the sample to perform XRD-analysis. The reasons I picked this protocol were because nothing else conclusively proved to be better and it did eliminate much of the discoloring during the dissolution phase.

7 Discussion

7.1 Discussion: Geochemistry

Although submerged fossil coral samples from the Huon Gulf, PNG appear to be significantly older and significantly more altered than I initially anticipated, I can identify a handful of trends in the chemical diagenesis of these samples. These trends are not as robust as the trends identified in the Hawaiian corals. Submerged samples from HG are high in ^{232}Th, and presumably contain associated ^{230}Th, that is, not from *in situ* radioactive decay of ^{238}U. Nearly 75% of measured Huon Gulf coral samples

contain more than 2 percent calcite. Open system behavior in the Huon Gulf samples may be difficult to model.

7.1.1 Thorium Content

Accurate ^{230}Th dating requires that a sample's ^{230}Th content is limited to that produced *in situ* by the decay of ^{238}U. In limited cases, it is possible to characterize a sample's extra ^{230}Th – that derived from the surrounding environment rather than that produced *in situ* – and to make corrections to the age calculations. Most corals have low thorium/uranium ratios (and low to negligible levels of non-radiogenic ^{230}Th and ^{232}Th). Because corals have low thorium concentrations, making corrections for extra ^{230}Th is negligible for corals older than a few thousand years or that contain less than ~100 pg/g ^{232}Th (Edwards, 1988; Edwards et al., 1987; Edwards et al., 1997). The corals from the Huon Gulf do not fall into this category: all measured coral samples from the Huon Gulf contain more than 100 pg/g ^{232}Th (up to 3 x 10^5 pg/g). Of 41 samples measured, 26 contained ^{232}Th concentrations greater than 5000 pg/g (or 5 ppm).

Correcting for additional ^{230}Th is not trivial and can introduce a large uncertainty in ^{230}Th ages. In order to appropriately correct for excess thorium, it is essential to consider the source of the thorium and the timing of the thorium introduction. A coral can incorporate some excess thorium into its skeleton as it is forming – this thorium would come from thorium present in the seawater in a higher-than expected amount. Correcting for excess thorium, present from the birth of the coral skeleton involves combining sample ^{232}Th concentrations with estimates of the ^{230}Th/^{232}Th ratio of the non-radiogenic thorium. Most young corals with low levels of ^{232}Th have insignificant levels of excess ^{230}Th (Edwards, 1988; Edwards et al., 1987),

but their thorium isotopic ratios reflect the seawater from which they form (Robinson et al., 2004). For instance, there is evidence from Sumatra that modern corals can contain high ^{232}Th and associated non-radiogenic ^{230}Th (e.g. Zachariansen (Zachariasen, 1998) -- a PhD thesis I have on request from the UMD library and the library has been unable to supply so far -- as noted in (Cobb et al., 2003)). Sumatra is close to continentally derived sources of thorium and analogous in plate tectonic setting to the Huon Gulf, Papua New Guinea. Robinson et al. (2004) measured the $^{230}Th/^{232}Th$ ratio of a variety of carbonate sediments (and the seawater in which they were forming) and suggested using local seawater values to correct for initial thorium.

Other sources of excess thorium in submerged samples could include wind-blown dust or sediment from onshore (the $^{230}Th/^{232}Th$ ratio of the sediment or dust is likely close to that of the bulk Earth at secular equilibrium is ~4×10^{-6} e.g. (Kaufman, 1993; Taylor and McLennan, 1985)), seawater ($^{230}Th/^{232}Th$ ratio of seawater varies geographically and with depth), and from erosion of the coral reefs and carbonate sediments in the area (the $^{230}Th/^{232}Th$ ratio of this sediment would depend on that in the original sediment). A third source category of excess thorium in the samples comes from the redistribution of thorium due to alpha-recoil processes both within the same coral skeleton and in other corals (see chapter 3 on Hawaii). To correct for this source of thorium it is necessary to use one of the alpha-recoil models (Thompson et al., 2003; Villemant and Feuillet, 2003).

In the case of the Huon Gulf, corrections for multiple sources of thorium may be necessary. Due to the proximity to the New Guinea Highlands (see Fig. 1 for a tectonic map), the Huon Gulf corals are constantly exposed to an influx of clastic sediments into

the Gulf. These sediments come from an area rich in volcanic rocks, which may be rich in thorium. As a result, the seawater from which the corals formed may have initially had a non-zero amount of ^{230Th}. Thorium may be added to the corals since their death via adsorption to the surfaces. Additionally, fossil coral skeletons from the Huon Gulf may also contain carbonate sediments (with a non-zero amount of thorium in them). In short: corals from the Huon Gulf have more ^{232}Th than we expect and likely have associated ^{230}Th, but I am unable to correct for it. Experiments of various precleaning treatments on the samples do not suggest excess ^{230}Th is easily identified or removed from samples.

7.1.2 Calcite Content

I measured the mineralogy of 79 of 87 coral samples in the Duluth collection of Huon Gulf corals via x-ray diffraction. Corals are initially aragonite in composition, yet 60 of the measured Huon samples contain 2% or more calcite. Corals samples from -250 m and -830 m were largely fragments encased in coral-algal bindstones) with limited sample size. Only one fragment from the -250 m terrace (a piece from sample #89) is <2% calcite and none of the samples from the -830 m terrace (of 18 measured samples from these depths) are <2% calcite. From the -1200 m terrace, five samples (of 25 measured) contain <2% calcite. From the -1650 m terrace 10 of 17 samples and from the -1950 m terrace nine of 14 measured samples contain <2% calcite. Deeper samples are presumably older and have had more time to experience alteration. From -2055 m none of 4 samples measured is <2% calcite; from -2100 m and deeper only one of 13 measured samples is <2% calcite.

The simplest way to explain calcite in a fossil coral would be subaerial exposure and subsequent percolation of meteoric waters leading to dissolution of aragonite and reprecipitation of calcite. Emergent corals from New Britain, Papua New Guinea that are Holocene in age (see chapter 2) and have been subaerially exposed contain large amounts of sparry calcite. Although sparry calcite is present in a few of the Huon Gulf hand samples, corals from the Huon Gulf generally do not contain large crystals of sparry calcite. Lack of sparry calcite suggests that the calcite formed in a submarine setting.

Coral skeletons that are primary aragonite can alter to high-magnesium calcite in marine settings and to low-magnesium calcite in subaerial, meteoric environments (e.g. Sherman et al., 1999). Allison et al. (2007) analyzed samples from the submerged fossil reefs of Hawaii for type of calcite present in the samples and found high-magnesium calcite – evidence of marine diagenesis. In Hawaii (see chapter 3) I identify early onsite of calcite alteration, suggesting marine diagenesis can have an early onset.

To evaluate exactly which fraction of the fossil coral skeleton is calcite, it is useful to examine samples in thin section under a microscope. In order to distinguish high-mg calcite from low-mg calcite on a fine-scale, it would be necessary to evaluate for each quantitatively via XRD. As a preliminary step, I examined approximately 30 of the Huon Gulf rock samples in thin section (due to the nature of the collection process via submersible, we collected many rock samples that included coral skeletons, but not necessarily every sample we collected included coral). A handful of these rock samples (~2-3) contained evidence of what might be marine high-magnesium calcite cement.

In reefs, depositional and diagenetic processes operate in tandem: reefs grow, are cemented, attacked by waves, and bioeroded, all contemporaneously (Tucker and Wright, 1990). Post-depositionally, increased fluid flow in the reefs can increase the degree to which the samples are cemented and/or altered from aragonite to calcite. With an idea of whether the samples contain high-mg or low-mg calcite, and where the calcite is, it would be possible to understand the circumstances under which calcification occurred. 60 of 79 (76%) measured Huon samples contain 2% or more calcite. This high number of submerged fossil samples containing calcite was unexpected at best: my initial hypothesis was that the coral samples would be better preserved than their emergent counterparts. The presence of so much calcite in the samples suggests a high amount of fluid circulation in the fossil reefs – flushing fluid through the samples would increase the amount of cementation and/or recrystallization.

7.1.3 Other Trends in U-Series Data – Lack of trends in U-Series Data

The model of terrace formation suggests that samples from the same terrace are broadly the same age. Given such a model, each terrace should plot in a distinct cluster in $[^{234}U/^{238}U]$–$[^{230}Th/^{238}U]$ space. Figure 7 is an image of all data (not including experiments) plotted in $[^{234}U/^{238}U]$–$[^{230}Th/^{238}U]$ space. With the exception of samples from the -250 m terrace plot, samples from the Huon Gulf are scattered throughout the graph space, mostly located in the regions associated with very old samples. Unlike their submerged counterparts from Hawaii, when Huon Gulf samples are identified according to their terrace location, no trend appears. For the Hawaiian corals, I call upon two processes to explain deviance from closed system behavior: alpha recoil and

thorium addition (see Chapter 3). Other potential open system processes in submerged fossil corals could include uranium addition and/or loss. In the Huon Gulf it is likely that both the alpha recoil processes and thorium addition are both going on within the Huon Samples, but it is difficult to distinguish what role each plays in the process. Data from the cleaning experiments also show no trends observable in [$^{234}U/^{238}U$]–[$^{230}Th/^{238}U$] space, indicating possible heterogeneity within each sample in addition to among samples.

7.2 Discussion: Resolving the Age of the Samples

The preliminary model of terrace formation in the Huon Gulf (Galewsky, 1996; Wallace, 2002; Webster et al., accepted, in revision; Webster et al., 2004a) suggests that for each terrace there should be one age of drowning and a corresponding major rise in sea level. My dating results from the Huon Gulf samples suggest that the terrace formation/drowning may have been more complex. The best estimates of ages for each terrace depth are contained in Table 3. These ages were selected based upon the reliability criteria (see section in Introductory Chapter) for defining a traditionally reliable/unreliable sample. The best ages from each of the terraces represent the samples for which most of the criteria were met. I discuss the ages in more detail in section 4 of this chapter, but the ages in Table 3 are not all traditionally reliable ages. I include samples for which the errors in $\delta^{234}U_i$ value are quite large and are barely overlapping. For instance, the -830 m terrace "best" age comes from the foram cleaning protocol, where it is not entirely clear what the process does to the uranium in the sample. The -

1650 terrace age (414 ka), from sample #232, and the -1950 m terrace age (437.3 ka), from #142, have low $\delta^{234}U_i$ values.

Sample #89 (and other corals from -250 m) suggests that corals were growing at 60 ka and sample #57 provides evidence of corals growing at 110 ka. From -1140 m there are no decent ages upon which to place estimates of terrace age. With two exceptions (#3 from -830 m and the dredge sample from -1950 m), samples from -1280 m, -1650 m, -1950 m, and -2100+ m broadly follow the pattern of increasing age with increasing depth (375-400ka, 400ka, 425-450 ka, and 500 ka, respectively). These age results place the development of four terraces during the time in between Termination V (367 ka) and Termination VI (~500 ka) (see Figure 8, age vs. depth). With more precise ages, it might be possible to more precisely constrain the age of individual terraces.

There is no evidence of corals growing from ~350 ka to ~110 ka. One might call upon several explanations to explain this missing gap in time. First, the age gap could simply mean that we missed collecting corals representing this time period. We collected samples in a systematic fashion, collecting samples from different stratigraphic layers within each distinct terrace beyond 200 m of water depth, with sampling locations guided by bathymetric imaging and sidescan sonar results. It is highly unlikely that the time gap is the result of sampling issues. Secondly, it is possible that no coral was growing in the Huon Gulf (350 - 110 ka), consequently there was no coral (of this age) from which to sample. However this explanation seems implausible because nearby on the Huon Peninsula, multiple corals have been identified including this time period (e.g. (Cutler, 2003) and (Esat et al., 1999). A third possibility for the time gap is that corals grew and were buried by younger material. Material between 60

and 110 ka in age is located today at -250 m, in order for that older material to have been buried by younger material on top subsidence would have had to be significantly faster during the period 350-110 ka, allowing for rapid burial and buildup of the -250 m (60 ka) reef.

In addition to no samples from 350-110 ka, I identify two potential age reversals (sample #3 (from the -830 m reef) is older than samples from deeper reefs, and the dredge samples (from -1950 m reef) are younger than samples from shallower reefs). This result could serve as evidence for faulting – older material emplaced upon the younger material. When I plot the sample locations on a bathymetric map, a linear feature in the stands out (figure 9). Material to the northwest of this lineament is generally younger than material to the east, suggesting maybe this age difference is structurally controlled.

Tectonic motion is not a linear process. The "missing" age span could potentially be explained with a variable subsidence rate. For instance, on the Huon Peninula, north of the Huon Gulf there is documented evidence of seismic uplift of up to 14 cm from a single seismic event in a region that experiences and average uplift rate of 2-4 mm/yr (Pandolfi et al., 1994). The Huon Gulf's subsidence rate may be similarly variable in time and space. While subduction in the Gulf has been ongoing, the material subducted could vary in thickness. Wallace calls upon a varying plate thickness in her model to explain the subsidence rate required to match one terrace to each sea level rise (Wallace, 2002). Instead of varying the plate thickness to maintain a constant subsidence rate, it may be necessary to vary the subsidence rate and/or the plate thickness to refine the tectonic model to match the coral ages.

In addition to the missing time period, there is the problem identifying a distinct drowning age for each reef. I have evidence of three terraces (-1280 m, -1650 m, and -1950 m) growing during Stage 11. Although there is evidence that Stage 11 represents the warmest and longest interglacial interval of the past 500 ka (Howard, 1997), our model of terrace formation in the Huon Gulf suggests that each terrace should be progressively older than the last and that for each major rise in sea level (e.g each termination) there should be one and only one terrace (Galewsky, 1996; Wallace, 2002; Webster et al., 2004a). Perhaps the -1280 m, -1650 m and -1950 m terraces are all a part of the same large platform, which may have been forming during Stage 11, providing evidence for long periods of accumulation and growth of coral terraces, with perhaps multiple short subaerial exposures (see section 7.4 for a further discussion of Stage 11).

7.3 Discussion: Subsidence

Modeling in the Huon Gulf suggests that corals should begin drowning during the glacial or late phases of the previous interglacial. The corals should be able to continue to grow with falling eustatic sea level. If global sea level falls more rapidly than subsidence, then the accommodation space for the development of new reef material goes to zero depth and a period of subaerial exposure is possible (during which the corals would die and possibly erode). In a subsiding environment, when sea level begins to rise, then the coral can continue to grow provided the relative rate of sea-level change is less than the maximum growth rate of the coral. This project began as an incredible way to constrain both subsidence and paleo-sea level with samples from an area of tectonic interest and paleoclimate interest. It is only possible to determine subsidence if

paleosea level is known *a priori*, or conversely, to determine paleosea level with a pre-existing estimate of subsidence. In the absence of either, it is possible to use the best ages from the deepest terraces to get an estimate of subsidence.

Using the most reliable age from each of the deeper terraces and assuming constant subsidence, the calculations of subsidence become simply a linear regression (see chapter on Hawaii for a discussion of errors). To compute a subsidence rate for each sample, I took the depth of sample collection and divided by the coral's age. The results of this calculation are shown in Table 3. This technique of computing a subsidence rate assumes that the coral grew at sea level and disregards the eustatic sea level. The average computed subsidence rate for the Huon Gulf, including all terraces is ~ 4 m/ka, less than Galewsky et al. (1996) suggested of 5.7 m/ka, but still almost an order of magnitude higher than other subsidence rates from other, similar settings (Homewood, 1986; Jordan, 1981; Pigram, 1991). The one exception is in the Timor trough (Audley-Charles, 1986; Pigram, 1991) subsidence rates are ~ 1 m/ka.

A subsidence rate of 4.0 m/ka, coupled with superimposed eustatic sea-level changes would likely drown corals during periods of rapid-sea level rise (such as glacial terminations). 4.0 m/ka is less than half the maximum upward growth rate for platform building reefs (Davies and Hopley, 1983), yet faster than the vertical accumulation rate of reefs observed in a muddy environment in South Thailand (2.0-3.0 m/ka, (Tudhope and Scoffin, 1994)). Given the proximity to the nearby highlands, the Huon Gulf is not likely to enable growth at the maximum upward growth rate due to influx of sediment via rivers flowing into the Gulf, making it cloudy.

7.4 Discussion: Documentation of Stage 11

The Stage 11 interglacial is centered at 400 ka. The Earth's orbital configuration during stage 11 is similar to today's: eccentricity is at its minimum and the amplitude of precession is damped (Droxler et al., 2003). Yet researchers have characterized Stage 11 as a prolonged period (30 ka) of intense warmth, with sea level 13-20 meters above the present level (Droxler et al., 2003; Hearty et al., 1999; Howard, 1997), suggesting that insolation should be at a maximum not a minimum. This contradiction is what is known as the Stage 11 problem.

Corals from the tops of three Huon Gulf terraces (-1280 m, -1650 m, and -1950 m) were growing during Stage 11. Measured ages of the tops of these terraces are 367.9 +22/-19 ka (from -1280 m), 414 +43/-35 ka (from -1650 m) and 437.3 ± 1.3 ka (from -1950). It is tempting to consider these individual ages as representing three distinct drowning events, especially since these ages come from three distinct depths, but that interpretation is not appropriate. The errors in ages of two of these samples are quite large and overlap one another. It is more appropriate to consider the full range in age (349 to 457 ka). One of these samples, from -1950 m, has a small error on the age, but has a low $\delta^{234}U_i$ value so would not be considered reliable. With more precise ages, a more complete picture of the timing of drowning of reefs is possible.

The model of Huon terrace development (Galewsky, 1996; Wallace, 2002; Webster et al., 2004a) suggests that the submerged reefs of the Huon Gulf are mainly glacial reefs that developed in response to rapid subsidence. The models of these reefs suggest that the reefs drown during periods of rapid sea level rise. Considering the full age range 349 to 457 ka of the potential Stage 11 materials from the Huon Gulf suggest

that the corals were growing during the warm period of high sea level associated with Stage 11.

8.0 Conclusions

We sampled fossil corals from the submerged coral reefs of the Huon Gulf, Papua New Guinea to evaluate both a subsidence rate for the Huon Gulf and to look at the timing of reef drowning. The model ages of the corals ranged from 60-410 ka based upon a preliminary age of a dredge sample. This location was predicted to provide a well-preserved archive of the last five glacial terminations.

The measured ^{230}Th ages of coral samples are older than we expected. Measured ^{230}Th ages of coral samples from the Huon Gulf range from 60 ka to infinite age (>600 ka); however none of the measured corals were between 130 ka and 350 ka in age. Additionally, I identify two potential age reversals (sample #3 (from the -830 m reef) is older than samples from deeper reefs and the dredge samples (from -1950 m reef) are younger than samples from shallower reefs). Corals from three terraces (-1280 m, -1650 m, and -1950 m) represent material from Stage 11, suggesting that the model of terrace development is likely more complex than the original idea of a distinct sea-level rise event per terrace.

The subsidence rate (m/ka) computed from the most reliable ages of the deepest terraces suggests that the subsidence in the Huon Gulf averages 4 m/ka, slower than that predicted by Galewsky et al. (1996), but still higher than other subsidence rates from other, similar settings. For instance, in the Timor trough (Audley-Charles, 1986)

subsidence rates are thought to be at least 1 m/ka. Three terraces (-1280 m, -1650 m, and -1950 m) have corals with ages broadly associated with Stage 11, indicating that preliminary modeling of the region was incomplete.

9.0 References

Abbott, L.D., Silver, E.A., and Galewsky, J., Silver, E.A., Gallup, C.D., Edwards, R.L., and Potts, D.C., 1994, Structural evolution of a modern arc-continent collision in Papua New Guinea: Tectonics, v. 13, p. 1007-1034.

Abers, G.A., and Mcaffrey, R., 1994, Active arc-continent collision: earthquakes, gravity anomalies and fault kinematics in the Huon-Finisterre collision zone, Papua New Guinea: Tectonics, v. 13, p. 227-245.

Allison, N., Finch, A.A., Webster, J.M., and Clague, D.A., 2007, Palaeoenvironmental records from fossil corals: The effects of submarine diagenesis on temperature and climate estimates: Geochim. Cosmochim. Acta, v. 71, p. 4693-4703.

Audley-Charles, M.G., 1986, Timor-Tamimbar Trough: The foreland basin of the evolving Banda orogen: International Association of Sedimentologists Special Publication 8, p. 91–102.

Bosscher, H., and Schlaer, W., 1992, Computer simulation of reef growth: Sedimentology, v. 39, p. 503-512.

Chalker, B.E., 1981, Simulating light-saturation curves for photosynthesis and calcification by reef-building corals: Marine Biology, v. 63, p. 135-141.

Chappell, J., 1974, Geology of coral terraces, Huon Peninsula, New Guinea: A study of Quaternary tectonic movements and sea-level changes: Geological Society of American Bulletin, v. 85, p. 553-570.

Cheng, H., Adkins, J., Edwards, R.L., and Boyle, E.A., 2000, U-Th dating of deep-sea corals: Geochim. Cosmochim. Acta, v. 64, p. 2401-2416.

Cheng, H., Edwards, R.L., Murrell, M.T., and Benjamin, T.M., 1998, Uranium-thorium-protactinium dating systematics: Geochim. Cosmochim. Acta, v. 62, p. 3437-3452.

Cobb, K.M., Charles, C.D., Cheng, H., Kastnera, M., and Edwards, R.L., 2003, U/Th-dating living and young fossil corals from the central tropical Pacific: Earth and Planetary Science Letters, v. 210, p. 91-103.

Crook, K., 1989, Suturing history of an allochthonous terrane at a modern plate boundary traced by flysch-to-molasse facies transitions: Sedimentary Geology, v. 61, p. 49-79.

Cutler, K., 2003, Rapid sea-level fall and deep-ocean temperature change since the last interglacial period Earth and Planetary Science Letters, v. 206, p. 253-271.

Davies, H., honza, e., Tiffin, D., Lock, J., Okuda, Y., Keene, J., Murakami, F., and Kishimoto, K., 1987, Regional setting and structure of the western Solomon Sea: Geo-marine letters, v. 6, p. 181-191.

Davies, P.J., and Hopley, D., 1983, Growth fabrics and growth rates of Holocene reefs in the Great Barrier Reef: BMR Journal of Australia Geology and Geophysics, v. 8, p. 237-251.

Droxler, A.W., Alley, R.B., Howard, W.R., Poore, R.Z., and Burckle, L.H., 2003, Unique and Exceptionally Long Interglacial Marine Isotope Stage 11: Window into Earth Warm Future Climate, *in* Droxler, A.W., Poore, R.Z., and Burckle, L.H., eds., Earth's Climate and Orbital Eccentricity: The Marine Isotope Stage 11 Question, Volume 137, Geophysical Monograph Series.

Edwards, R.L., 1988.

Edwards, R.L., Chen, J.H., and Wasserburg, G.J., 1987, U-238-U-234-Th-230-Th-232 systematics and the precise measurement of time over the past 500,000 years.: Earth and Planetary Science Letters.

Edwards, R.L., Cheng, H., Murrell, M.T., and Goldstein, S.j., 1997, Protactinium-231 Dating of Carbonates by thermal ionization mass spectrometery: Implications for Quaternary climate change: Science, v. 276, p. 782-786.

Esat, T.M., McCulloch, M.T., Chappell, J., Pillans, B., and Omura, A., 1999, Rapid fluctuations in sea level recorded at Huon Peninsua during the penultimate deglaciation: Science, v. 283, p. 197-201.

Galewsky, J., Silver, E.A., Gallup, C.D., Edwards, R.L., and Potts, D.C. , 1996, Foredeep tectonics and carbonate platform dynamics in the Huon Gulf, Papua New Guinea: Geology, v. 24, p. 819-822.

Gallup, C.D., 1997, High-precision uranium-series analyses of fossil corals and Nicaragua Rise sediments: The timing of high sea levels and the marine delta U-234 Value, University of Minnesota.

Guillemin, G., Meunier, A., Dallant, P., Christel, P., Puliquen, J., and Sedel, L., 1989, Comparison of coral resorption and bone apposition with 2 natural corals of different porosities. : J Biomed Mater Res, v. 23.

Hearty, P.J., Kindler, P., Cheng, H., and Edwards, R.L., 1999, A +20 m middle Pleistocene sea-level highstand (Bermuda and the Bahamas) due to partial collapse of Antarctic ice: Geology, v. 27, p. 375-378.

Homewood, P., Allen, P. A., and Williams, G. D., 1986, Dynamics of the Molasse Basin of western Switzerland: International Association of Sedimentologists Special Publication, p. 199–217.

Howard, W., 1997, A warm future in the past: Nature, v. 388, p. 418-419.

Imbrie, J., J. D. Hays, D. G. Martinson, A. McIntyre, A. C. Mix, J. J. Morley, N. G. Pisias, W. L. Prell, and N. J. Shackleton, 1984, The orbital theory of Pleistocene climate: Support from a revised chronology of the marine d18O record, in Milankovitch and Climate, Part 1, *in* al, A.L.B.e., ed., Milankovitch and Climate, Part I: Norwell, Mass., D. Reidel, p. 269-305.

Jordan, T.E., 1981, Thrust loads and foreland basin evolution, Cretaceous, west-
ern United States: American Association of Petroleum Geologists Bulletin, v. 65, p. 2506–2520.

Kaufman, A., 1993, An evaluation of several methods for determining th-230/U ages in inpure carbonates: Geochim. Cosmochim. Acta, p. 2303-2317.
Lambeck, K., and J. Chappell 2001, Sea level change through the last glacial cycle: Science, v. 292, p. 679-686.
Lea, D.W., Martin, P.A., Pak, D.K., and Spero, H.J., 2002, Reconstructing a 350 ky history of sea level using planktonic Mg/Ca and oxygen isotope records from a Cocos Ridge core: Quaternary Science Reviews, v. 21, p. 283-293.
Lomitschka, M., and Mangini, A., 1999, Precise Th/U-dating of small and heavily coated samples of deep sea corals: Earth and Planetary Science Letter, v. 170, p. 391-401.
Ludwig, K.R., Szabo, B.J., Moore, J.G., and Simmons, K.R., 1991, Crustal subsidence rate off Hawaii determined from 234U/238U ages of drowned coral reefs: Geology, v. 19, p. 171-174.
Martin, P.A., and Lea, D.W., 2002, A simple evaluation of cleaning procedures on fossil benthic foraminiferal Mg/Ca: Geochem. Geophys. Geosyst., v. 3, p. 8401.
Pandolfi, J., M., Best, M.M.R., and Murray, S.P., 1994, Coseismic event of May 15, 1992, Huon Peninsula, Papua New Guinea: Comparison with Quaternary tectonic history: Geology, v. 22, p. 239-242.
Pigram, C.J., and Symonds, P. A. , 1991, A review of the timing of the major tectonic events in the New Guinea orogen: Journal of Southeast Asian Earth Sciences, v. 6, p. 307-318.
Robinson, L.F., Belshaw, N.S., and Henderson, G.M., 2004, U and Th concentrations and isotope ratios in modern carbonates and waters from the Bahamas: Geochim. Cosmochim. Acta, v. 68, p. 1777-1789.
Shen, C.-C., Edwards, L.R., Cheng, H., Dorale, J.A., Thomas, R.B., Bradley, M.S., Weinstein, S.E., and Edmonds, H.N., 2002, Uranium and thorium isotopic and concentration measurements by magnetic sector inductively coupled plasma mass spectrometry: Chemical Geology, v. 185, p. 165-178.
Sherman, C.E., Fletcher, C.H., and Rubin, K.H., 1999, Marine and meteoric diagenesis of Pleistocene carbonates from a nearshore submarine terrace, Oahu, Hawaii: J. Sed. Res., v. 69, p. 1083-1097.
Silver, E.A., Abbott, L.D., Kirchoff-Stein, K.S., Reed, D.L., Bernstein-Taylor, B., and Hilyard, D. , 1991, Collision propagation in Papua New Guinea and the Solomon Sea: Tectonics, v. 10, p. 863-874.
Taylor, S.R., and McLennan, S.M., 1985, The Continental Crust: Its Composition and Evolution: Oxford, Blackwell Scientific.
Thompson, W.G., Spiegelman, M.W., Goldstein, S.L., and Speed, R.C., 2003, An open-system model for U-series age determinations of fossil corals: Earth and Planetary Science Letter, v. 210, p. 365-381.
Tucker, M., E., and Wright, V.P., 1990, Carbonate Sedimentology: Oxford, Blackwell Science, 482 p.
Tudhope, A.W., and Scoffin, T.P., 1994, Growth and structure of fringing reefs in a muddy environment, South Thailand: Journal of Sedimentary Research, v. A64, p. 752-764.

Villemant, B., and Feuillet, N., 2003, Dating open systems by the 238U-234U-230Th method: application to Quaternary reef terraces: Earth and Planetary Science Letter, v. 210, p. 105-118.

Wallace, L.M., 2002, Tectonics and arc-continent collision in Papua New Guinea: Insights from geodetic, geophysical and geologic data: Santa Cruz, California, University of California.

Webster, J.M., Braga, J.C., Clague, D.A., Gallup, C.D., hein, J.R., Potts, D.C., Renema, W., Riding, R., Riker-Coleman, K., Silver, E., and Wallace, L.M., accepted, in revision, Coral Reef Evolution on Rapidly Subsiding Margins: Global and Planetary Change, Special Issue.

Webster, J.M., Wallace, L., Silver, E., Applegate, B., Potts, D., Braga, J.C., Riker-Coleman, K., and Gallup, C., 2004a, Drowned carbonate platforms in the Huon Gulf, Papua New Guinea: Geochemistry, Geophysics, Geosystems, v. Volume 5.

Webster, J.M., Wallace, L., Silver, E., Potts, D., Braga, J.C., Renema, W., Riker-Coleman, K., and Gallup, C., 2004b, Coralgal composition of drowned carbonate platforms in the Huon Gulf, Papua New Guinea ; implications for lowstand reef development and drowning Marine Geology, v. 204, p. 59-89.

Zachariasen, J., 1998, Paleoseimology and paleogeodesy of the Sumatran subduction zone: a study of the vertical deformation using coral microatolls, Caltech.

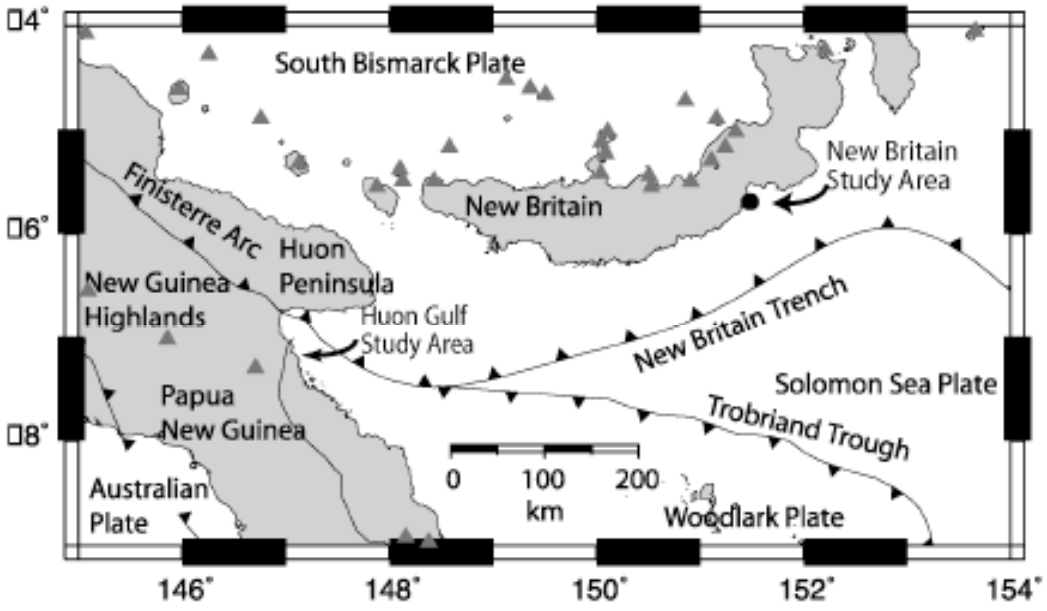

Figure 1. Tectonic setting of Huon Gulf. Grey triangles show location of active volcanic arc. Study location is shown with arrows.

Figure 2. Measured 230Th Ages (A), 238U and 232Th concentrations (B), 230/232 ratio and 232Th concentrations (C), δ234U values (open sysmbol = measured, closed symbol = initial) (D), 230/238 ratios (E) and percent calcite (F) of corals from the Chicago cleaning protocol. (F) Plot of [234U/238U] vs. [230Th/238U], including the same data set. Errors are not included.

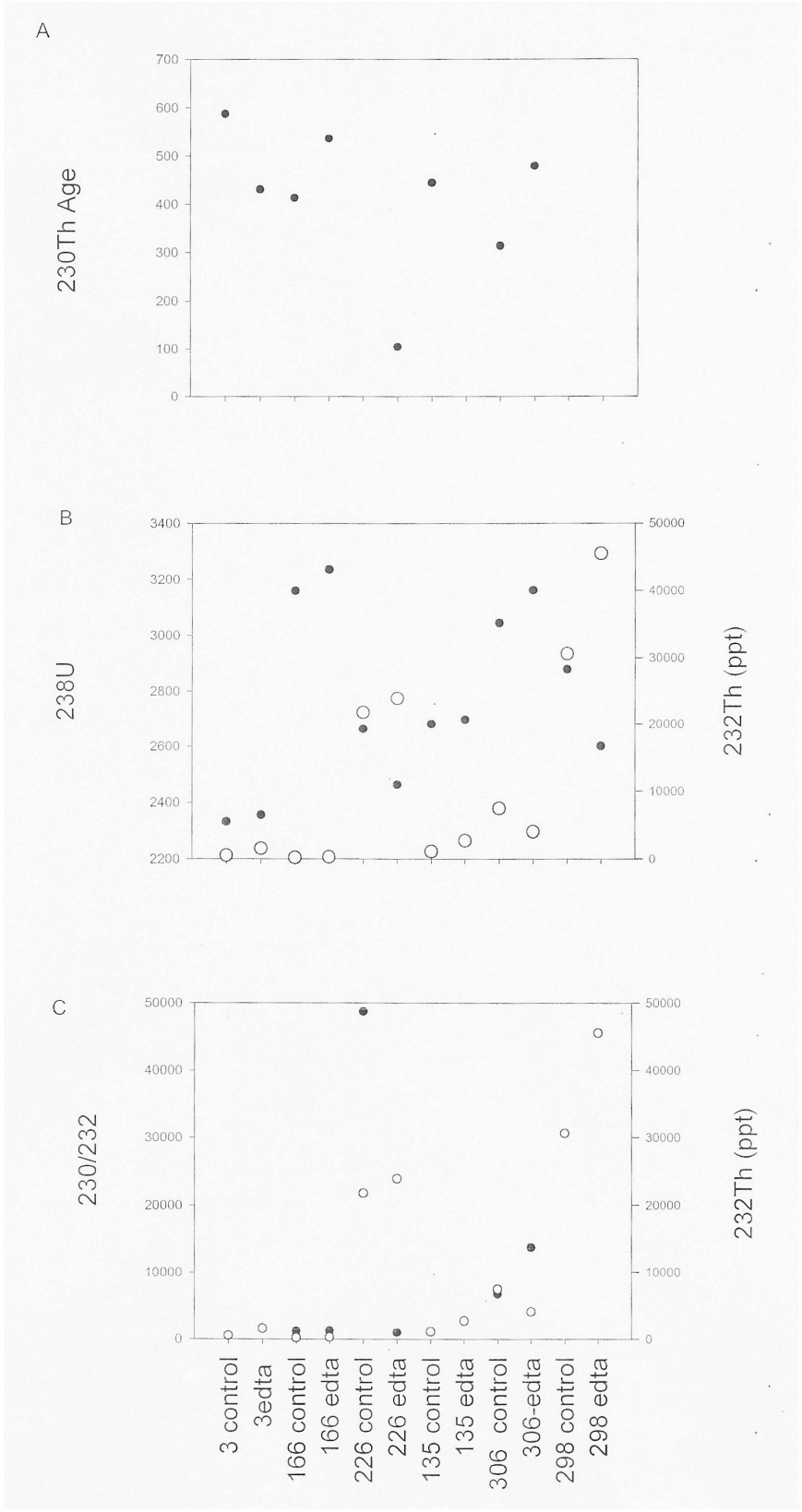
A
230Th Age
700
600
500
400
300
200
100
0
B
238U
3400
3200
3000
2800
2600
2400
2200
232Th (ppt)
50000
40000
30000
20000
10000
0
C
230/232
50000
40000
30000
20000
10000
0
232Th (ppt)
50000
40000
30000
20000
10000
0
3 control
3edta
166 control
166 edta
226 control
226 edta
135 control
135 edta
306 control
306-edta
298 control
298 edta

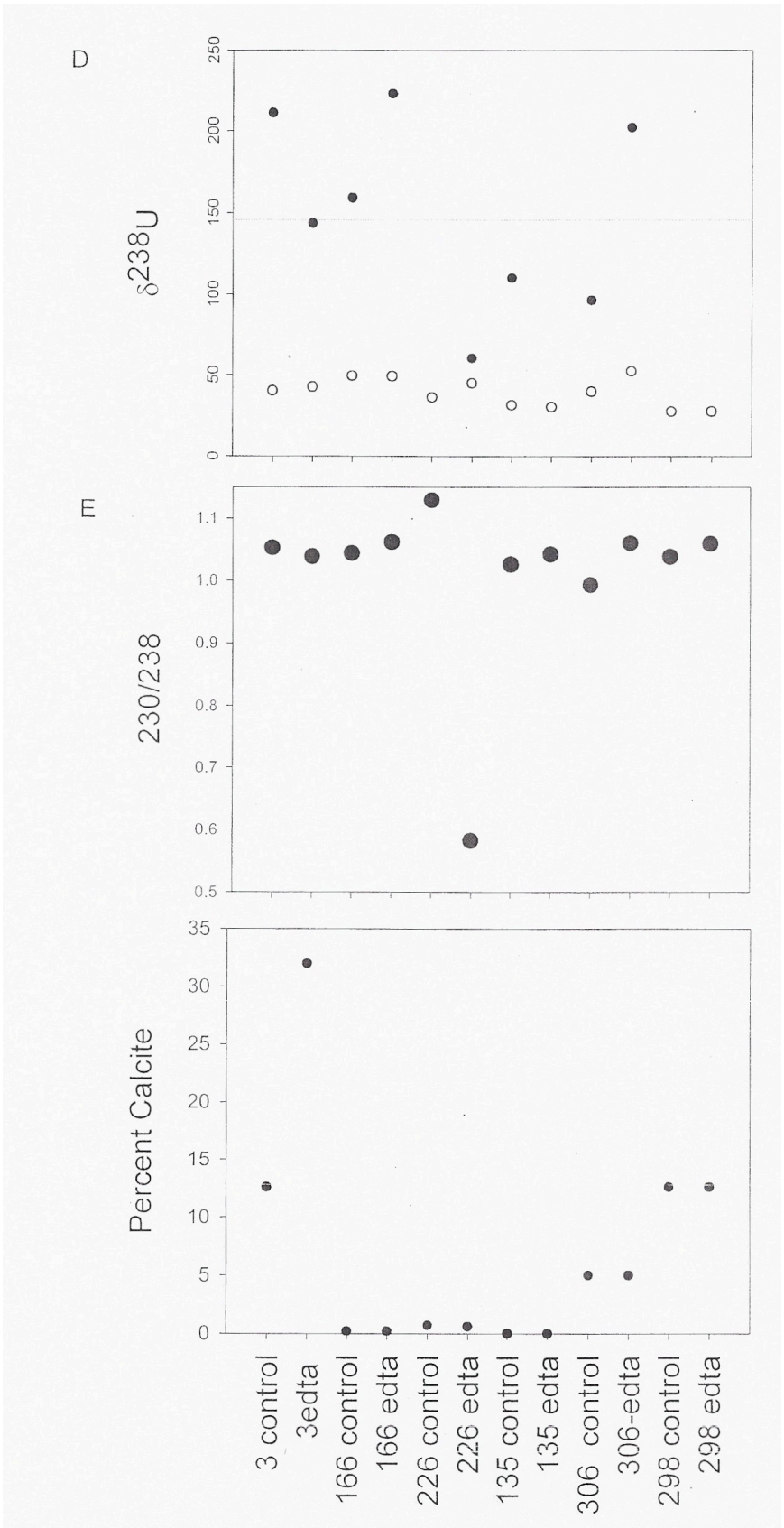
D
δ238U
0
50
100
150
200
250
E
230/238
0.5
0.6
0.7
0.8
0.9
1.0
1.1
Percent Calcite
0
5
10
15
20
25
30
35
3 control
3edta
166 control
166 edta
226 control
226 edta
135 control
135 edta
306 control
306-edta
298 control
298 edta

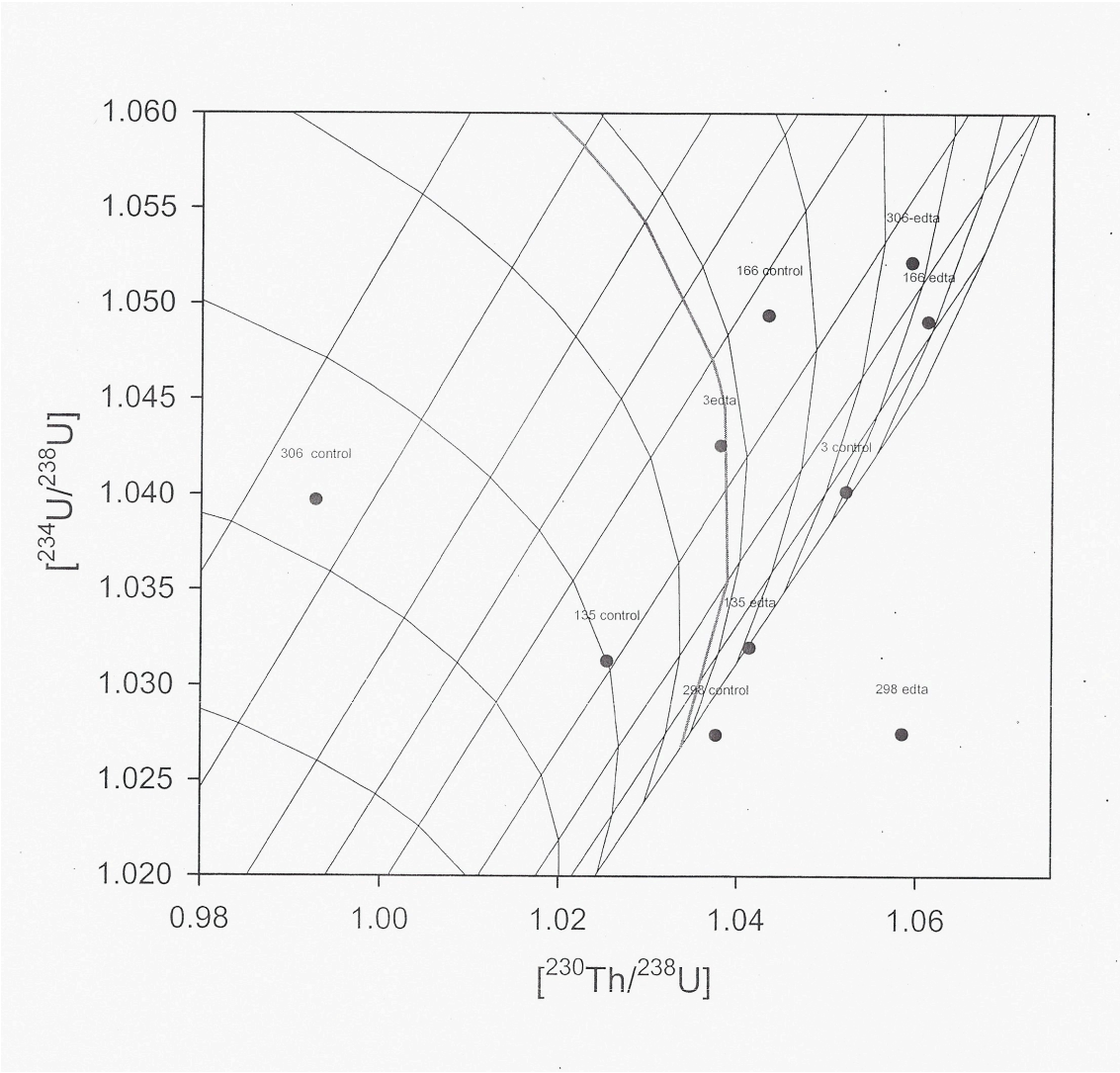
1.060
1.055
1.050
1.045
1.040
1.035
1.030
1.025
1.020
0.98
1.00
1.02
1.04
1.06
[234U/238U]
[230Th/238U]
306 control
306-edta
166 control
166 edta
3edta
3 control
135 control
135 edta
298 control
298 edta

Figure 3. Measured ^{230}Th Ages (A), 238U and 232Th concentrations (B), 230/232 ratio and 232Th concentrations (C), δ234U values (open sysmbol = measured, closed symbol = initial) (D), 230/238 ratios (E) and percent calcite (F) of corals from the grainsize experiments on samples 197 and 226.

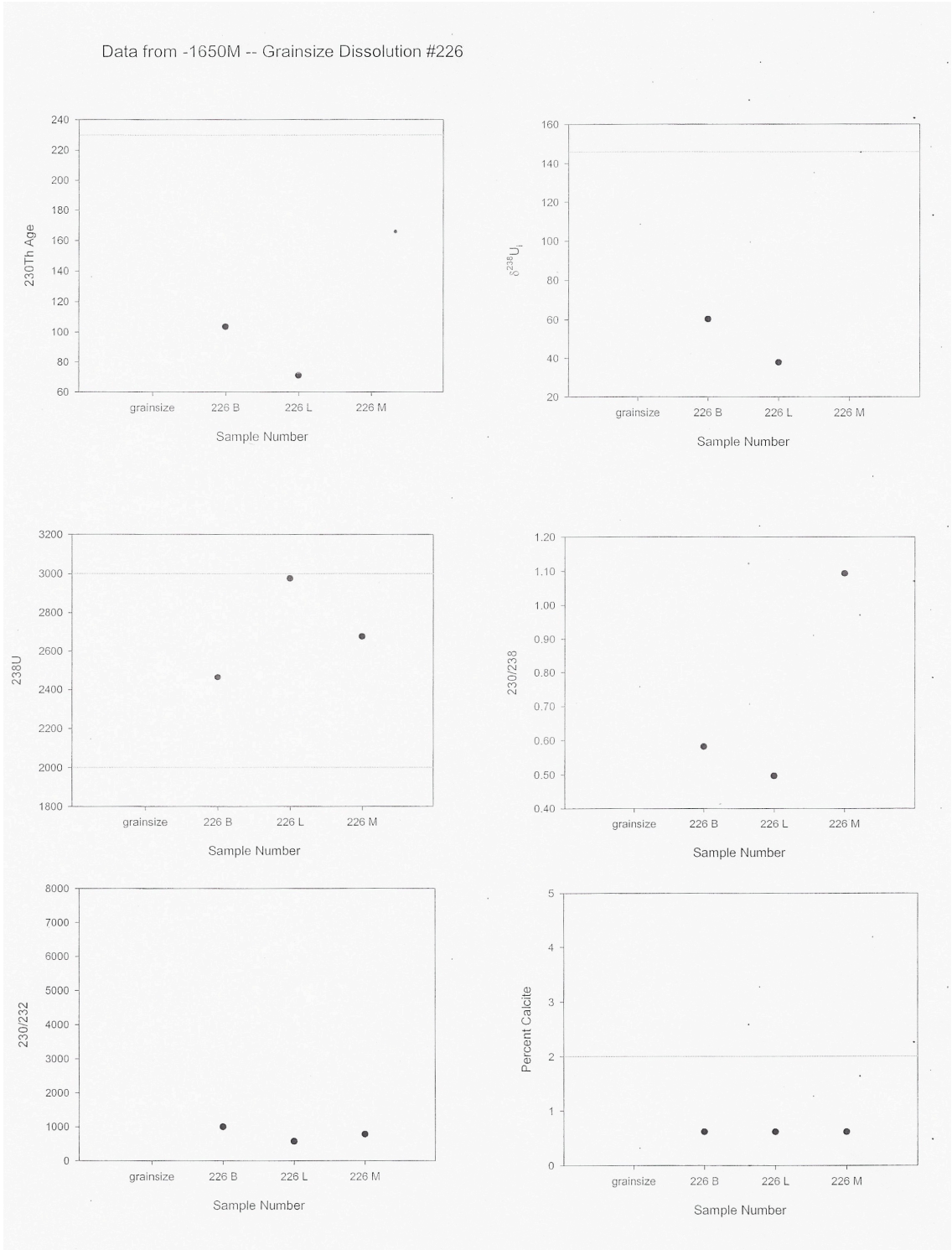
Data from -1650M -- Grainsize Dissolution #226
230Th Age
240
220
200
180
160
140
120
100
80
60
grainsize
226 B
226 L
226 M
Sample Number
δ234U
160
140
120
100
80
60
40
20
grainsize
226 B
226 L
226 M
Sample Number
238U
3200
3000
2800
2600
2400
2200
2000
1800
grainsize
226 B
226 L
226 M
Sample Number
230/238
1.20
1.10
1.00
0.90
0.80
0.70
0.60
0.50
0.40
grainsize
226 B
226 L
226 M
Sample Number
230/232
8000
7000
6000
5000
4000
3000
2000
1000
0
grainsize
226 B
226 L
226 M
Sample Number
Percent Calcite
5
4
3
2
1
0
grainsize
226 B
226 L
226 M
Sample Number

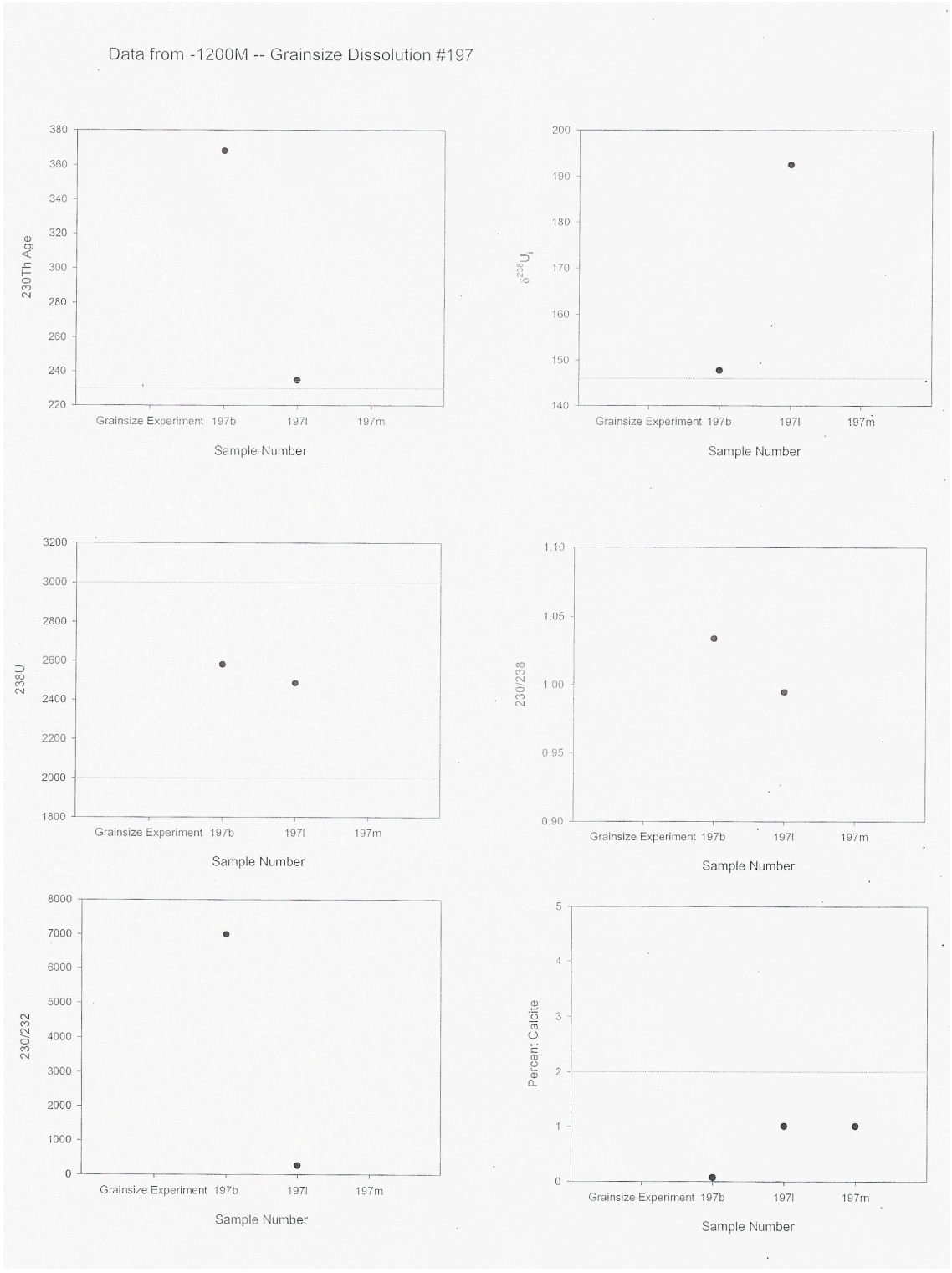
Data from -1200M -- Grainsize Dissolution #197
230Th Age
380
360
340
320
300
280
260
240
220
Grainsize Experiment 197b 197l 197m
Sample Number
δ234U
200
190
180
170
160
150
140
Grainsize Experiment 197b 197l 197m
Sample Number
238U
3200
3000
2800
2600
2400
2200
2000
1800
Grainsize Experiment 197b 197l 197m
Sample Number
230/238
1.10
1.05
1.00
0.95
0.90
Grainsize Experiment 197b 197l 197m
Sample Number
230/232
8000
7000
6000
5000
4000
3000
2000
1000
0
Grainsize Experiment 197b 197l 197m
Sample Number
Percent Calcite
5
4
3
2
1
0
Grainsize Experiment 197b 197l 197m
Sample Number

Figure 4. Measured 230^{Th} Ages (A), 238U and 232Th concentrations (B), 230/232 ratio and 232Th concentrations (C), d234U values (open symbol = measured, closed symbol = intial) (D), 230/238 ratios (E) and percent calcite (F) of corals from the selective dissolution experiments for samples #197, #227 and #228.

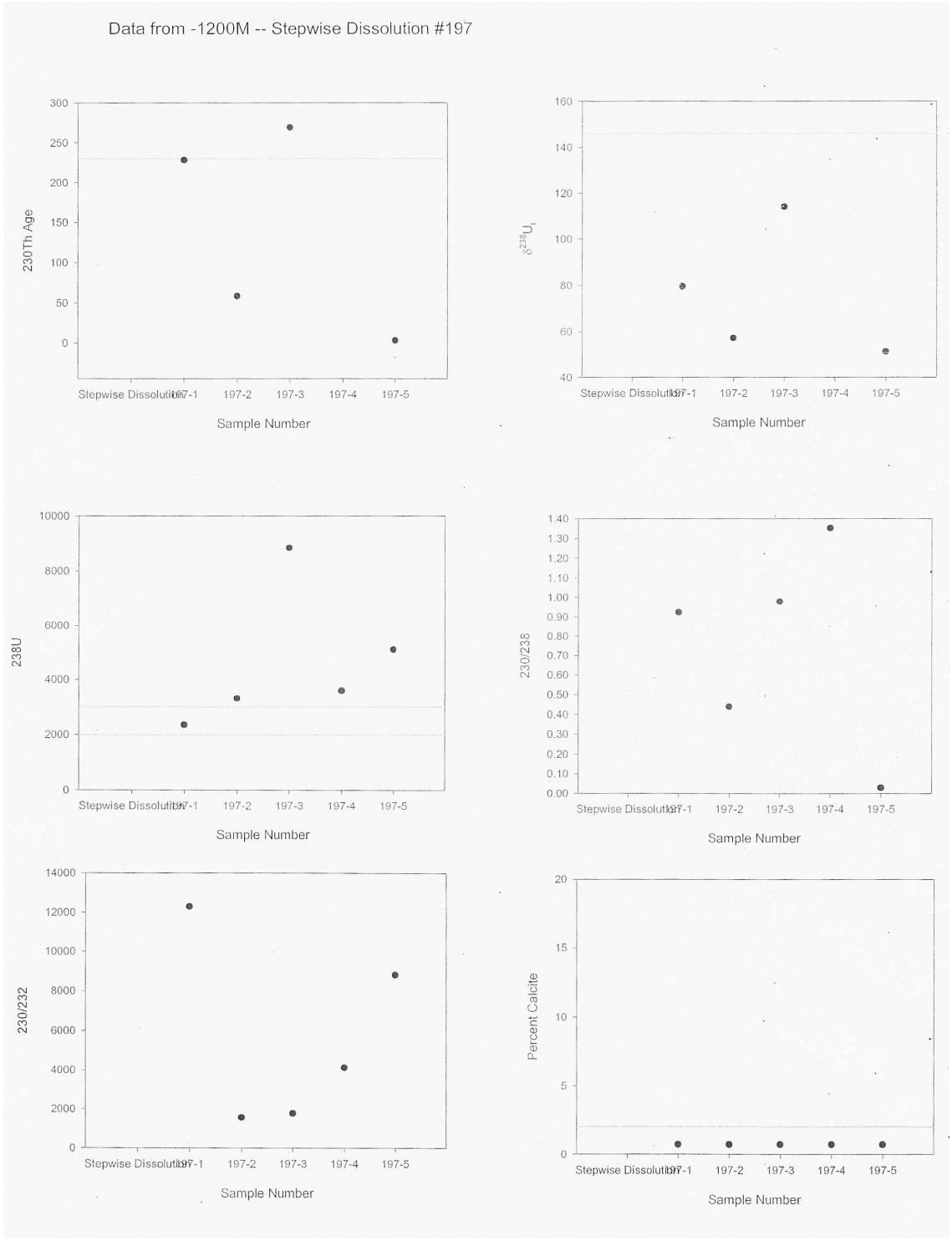
Data from -1200M -- Stepwise Dissolution #197
230Th Age
Sample Number
δ238U
Sample Number
238U
Sample Number
230/238
Sample Number
230/232
Sample Number
Percent Calcite
Sample Number
Stepwise Dissolution
197-1
197-2
197-3
197-4
197-5

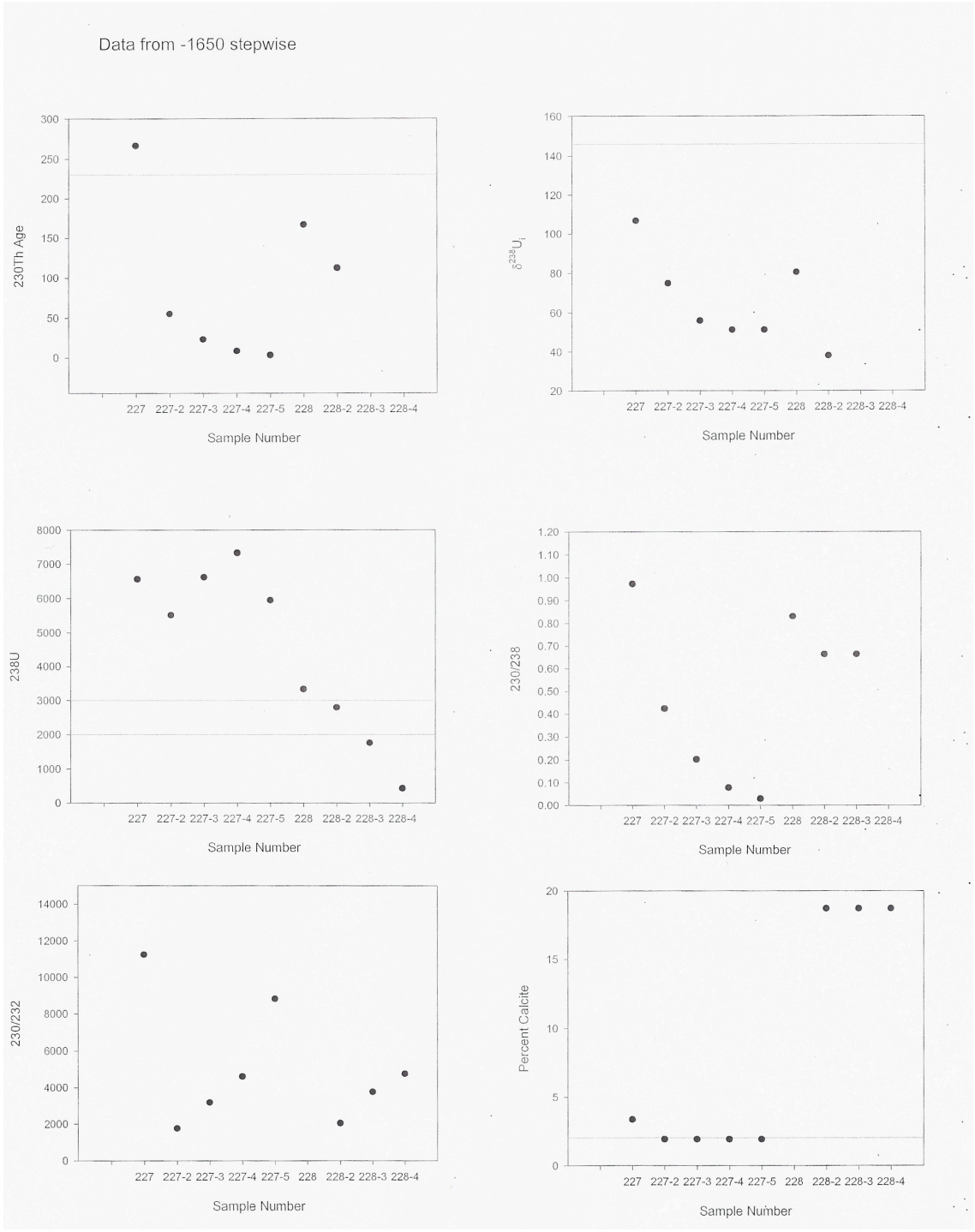
Data from -1650 stepwise
230Th Age
Sample Number
$\delta^{238}U_i$
Sample Number
238U
Sample Number
230/238
Sample Number
230/232
Sample Number
Percent Calcite
Sample Number
227 227-2 227-3 227-4 227-5 228 228-2 228-3 228-4

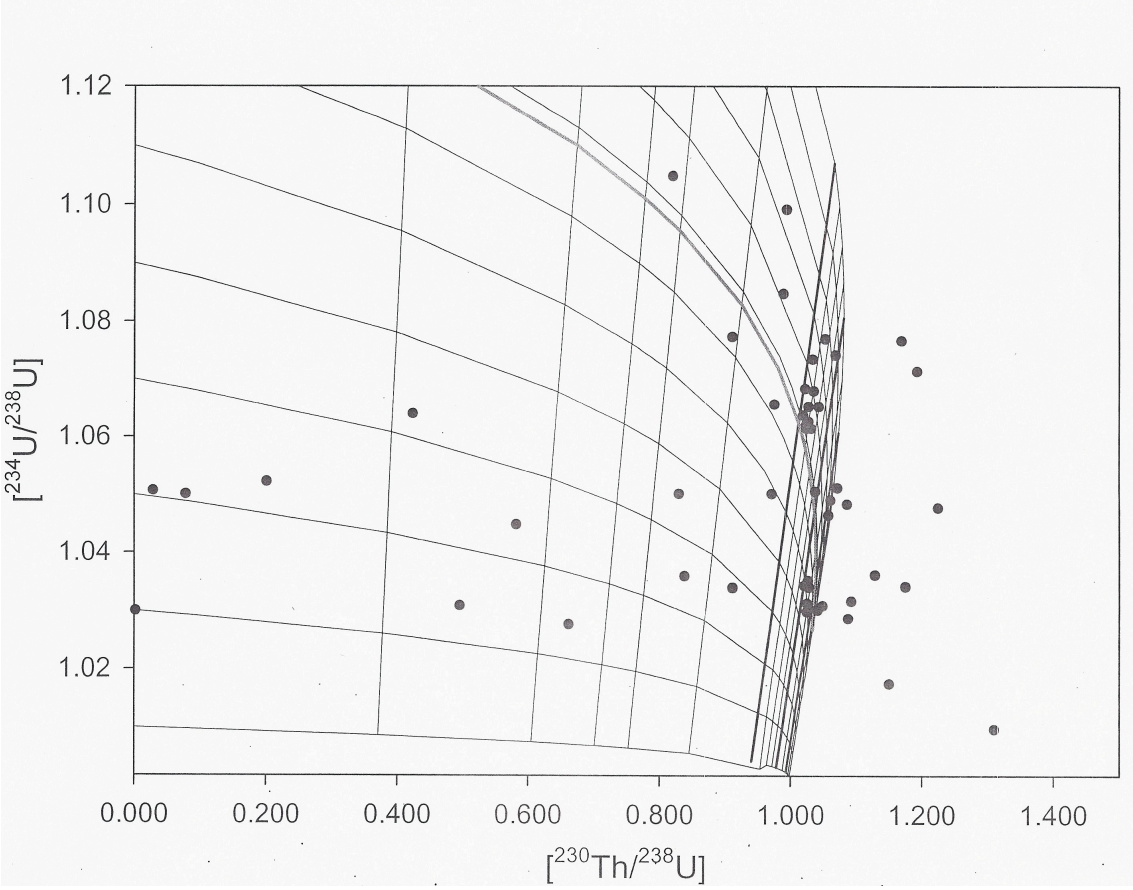

Figure 5: Plot of [234U/238U] vs. [230Th/238U] for all samples measured from the Huon Gulf (not including experiments). Errors are not included.

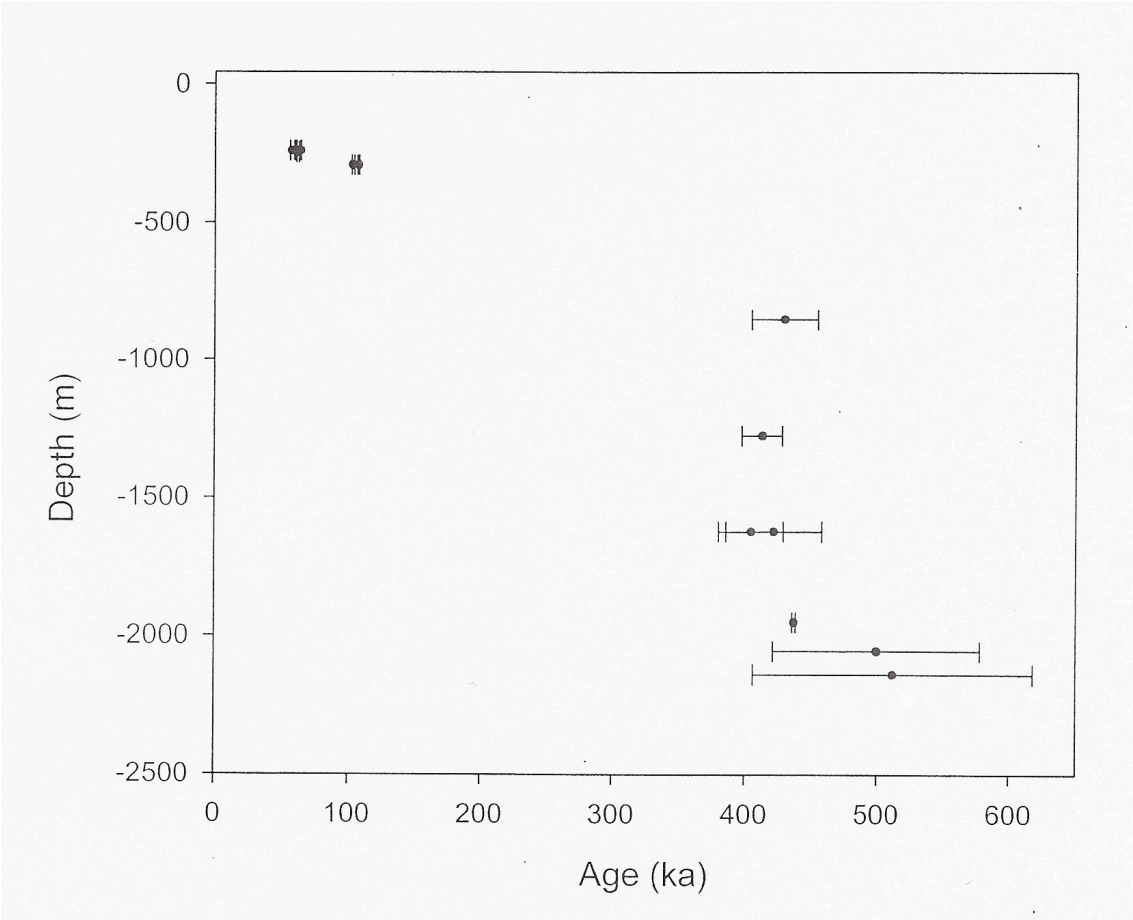

Figure 6: Depth (m) vs. 230^{Th} age for samples from the Huon Gulf. Includes all samples from -250 M and best data for deeper terraces. Errors in ages are 2 theta. Errors in depth are assumed to be 1-2 m and are not plotted.

Figure 7. Modified from Webster et al., 2004a, Figure 1. Map of bathymetry for the Huon Gulf sampling area. Black dots represent estimated sample locations and are numbered with ^{230}Th age (error), d234Ui (error); and percent calcite. Line indicates possible linear structural feature.

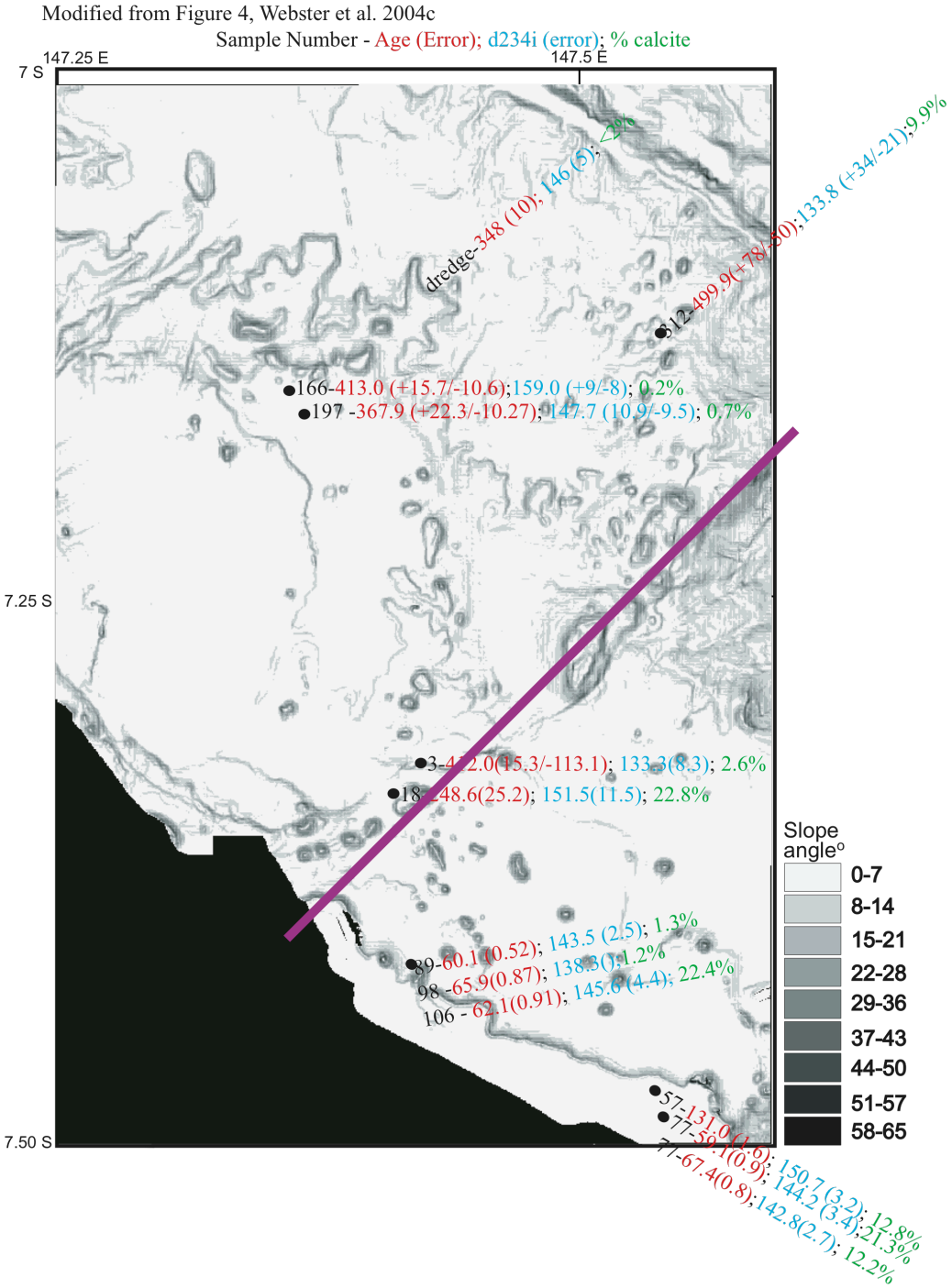

Data from the -250 m reef

Sample Number	^{238}U (ppb)	^{232}Th (ppt)	^{230}Th / ^{232}Th (atomic x10^{-6})	$\delta^{234}U$* (measured)	^{230}Th / ^{238}U (activity)	$\delta^{234}U$ ** (corrected)	^{230}Th Age (kv BP)*** (corrected)	Depth (m)	Percent Calcite	Species	
94	186 ±1	2334 ±31	2289 ±37	54.2 ±3.8	±0.0178	inf inf	inf inf	240		*Porites*	
89-A	3508 ±7	1953 ±27	2648 ±39	121.0 ±2.1	0.4801 ±0.0030	143.5 ±2.5	60.3 ±0.5	241	2	*Galaxia*	
89-B	10655 ±25	50072 ±993	1642 ±46	127.3 ±149.8	0.4674 ±0.0093	149.9 ±2.0	57.7 ±1.5	241		*favia*	
89A	3744	1715	±1807	117.7	0.5004	141.0 ±3.6	64.0 ±0.5	241	2	*Galaxia*	
89-a-1	4161	1303	±184	161.4	0.3497	191.3 ±2.0	60.1 ±0.4	241	2	*Galaxia*	
106	2724	291	1257	51.2	0.8	80.3 ±3.4	158.9 ±1.7	244	0	montipora	1.0512
98	3287 ±4	24661 ±195	1124 ±14	114.7 ±1.6	0.5108 ±0.0049	138.3 ±1.9	65.9 ±0.9	245		*Porites*	
108	3911 ±16	42924 ±365	739 ±9	122.3 ±3.7	0.4914 ±0.0051	145.6 ±4.4	61.8 ±0.9	247	22	*No ID*	
77	5736 ±15	38598 ±266	1278 ±13	117.9 ±2.3	0.5209 ±0.0041	142.8 ±2.7	67.4 ±0.8	291	21	*Galaxia*	
77	9365 ±33	76037 ±82	848 ±3	121.9 ±2.9	0.4173 ±0.0021	140.5 ±3.3	50.3 ±0.4	291	21	*No ID*	
57-a coral	2185 ±4	6071 ±35	4086 ±32	110.0 ±2.3	0.6876 ±0.0038	147.2 ±3.1	103.1 ±1.0	292		*pocillophora*	
57-b coral	2086 ±3	3773 ±30	6434 ±57	111.0 ±1.8	0.7041 ±0.0032	150.4 ±2.5	107.3 ±0.9	292		*pocillophora*	
57	2619	16644	±2002	104.0	0.7842	150.7 ±3.2	131.0 ±1.5	292	31	*Pocillifera family - Stylophora pistalata*	
38	205 ±0	50781 ±394	154 ±2	125.4 2.2	±0.0245	inf inf	inf inf	645			
33	911 ±1	35823 ±664	521 ±18	93.3 1.3	1.2395 ±0.0368	inf inf	inf inf	655			
18	1168 ±2	11024 ±36	1721 ±43	75.0 ±1.3	0.9834 ±0.0244	151.5 ±11.5	248.6 ±25.1	726	23		
15	1196 ±1	75778 ±422	259 ±3	99.2 ±1.5	0.9944 ±0.0085	192.5 ±4.7	234.7 ±6.9	733			
6	3832 ±8	18614 ±126	3603 ±39	45.9 ±2.4	1.0602 ±0.0091	242.0 inf	587.5 inf	836	11		
11	10756 ±28	153188 ±1444	1259 ±17	23.4 ±2.8	1.0855 ±0.0110	inf inf	inf inf	845			
4	15399 ±21	4560 ±43	25 ±1	-187.4 ±1.0	0.0004 ±0.0000	-187.4 --	-- --	850	2		
3	2140 ±2	5695 ±54	6105 ±90	41.6 ±1.1	0.9840 ±0.0111	95.9 ±5.6	295.3 ±16.7	853	13	*Porites*	
3d	2355	1518		42.6	1.0381	143.7 ±14.0	430 +25/-21	853	13	*Porites*	
Data for Experimemts											
fc3	308 ±1	1518 ±5	3450 ±15	43.7 ±1.9	1.0311 ±0.0039	132.8 ±8.5	393.4 +17.5/-15.7	836		*Porties*	
3ch6	2331	500		40.2	1.0521	211.0 +85/-5	587 +85/-55	853	13	*Porties*	
89-ach7	5615	18610		118.8	0.4788	140.8	60.3	241	2	*Galaxia*	
Data from Other Samples											
57-a infill	2612 ±6	7272 ±45	4221 ±34	104.4 ±2.8	0.7119 ±0.0040	142.6 ±3.8	110.3 ±1.2	292			
57-b infill	3024 ±5	10872 ±39	3152 ±16	105.1 ±2.1	0.6864 ±0.0026	140.8 ±2.8	103.6 ±0.7	292			

Data from the -1200 m reef

Sample Number	^{238}U (ppb)	^{232}Th (ppt)	^{230}Th / ^{232}Th (atomic x10^{-6})	$d^{234}U$* (measured)	^{230}Th / ^{238}U (activity)	$d^{234}U_{initial}$** (corrected)	^{230}Th Age (kv BP)*** (corrected)	Depth (m)	Percent Calcite	Species	for plotting
268	3270 ±7	56395 ±390	1172 ±13	47.8 ±2	1.2244 ±0.0104	inf inf	inf inf	1137	7.7		1.0478
290	366 ±1	2046 ±15	2692 ±3	34.0 ±2	0.9121 ±0.0066	64.6 ±3.9	226.7 ±5.7	1171	92.6		1.0340
166	116 ±2	1505 ±12	37397 ###	inf inf		±0.6223	inf inf	182.8 -±1.1	1277	0.0	Porities	
166	3201 ±6	1894 ±35	56621 ###	53.4 ±1.6		±0.0422	inf inf	inf inf	1277	0.0	Porities	
166d	3159	170		49.4	1.0434	159.0 ±8.5	413.0 ±15.5	1277	0.2	Porities	1.0494
197	709	249	48721	50.6	1.0380	151.0 ±12.0	387.1 22.4/-19.5	1285	0.5	favid	1.0506
EDTA Cleaning											
166ch5	3235	254		49.1	1.0612	223.0 +29/-21	536.0 +43/-33	1277	0.2	Porities	1.0491
193-1	3423	481	1243	46.5	1.0579	214.2 inf	540.2 inf	1288	0.8	Porities	1.0465
cleaning	709 ±2	249 ±3	48721 ###	50.6 ±3	1.0280 ±0.0052	151.0 ±12.0	387.1 +22.443/-19.	1285	0.7	Porties	1.0506
Stepwise Dissolution											
197-1	2353	29164		41.8	0.9224	79.6	338.2	1285	0.7	favid	1.0418
197-2	3310 ±9	15350 ±209	1558 ±59	48.50 ±2.1	0.4375 ±0.0154	57.2 ±2.5	58.7 ±2.7	1285	0.7	favid	1.0485
197-3	8838 ±12	80769 ±1408	1767 ±49	53.30 ±1.4	0.9781 ±0.0210	114.0 +9.6/-7.5	269.2 +27.2/-22.0	1285	0.7	favid	1.0533
197-4	3592 ±5	19260 ±285	4112 ±96	47.30 ±1.2	1.3513 ±0.0244	inf inf	inf inf	1285	0.7	favid	1.0473
197-5	5102 ±14	277 ±27	8804 ###	50.70 ±1.9	0.0289 ±0.0045	51.2 ±1.9	3.0 ±0.5	1285	0.7	favid	1.0507
197-6	2222	903	45828	57.70	1.1274	inf	587.5	1285	10.7	favid	1.0577
Grainsize Experiment											
197b	2581 ±2	11024 ±36	6982 **±43**	52.2 **±1.3**	1.0337 **±0.0244**	147.7 +16.1/-15.1	367.9 +22.3/-19.3	**1285**	0.1	favid	1.0522
197l	2485 ±1	75778 ±422	259 ±3	99.2 ±1.5	0.9944 ±0.0085	192.5 ±4.7	234.7 ±6.9	**1285**	1.0	favid	1.0992
197m								1285	1.0	favid	
197vf	4149 ±8	42565 ±322	1644 ±18	49.8 ±3	1.0214 ±0.0083	131.9 ±10.0	344.6 +21.86/-18.7	1285	1.0	favid	1.0498
Chicago Cleaning											
166	3227	209	2690	47.5	1.0506	175.7 +26.3/-20.1	463.0 +44.6/-34.6	1277	0.0	Porities	1.0475
171	550	66	1479	51.3	1.0720	394.7 inf	722.3 inf	1280	4.0	montipora	1.0513
171	2062 ±3	3169 ±20	11673 ±99	48.4 ±2.0	1.0865 ±0.0064	inf inf	inf inf	1280	4.0	Montipora	1.0484
185	1567	48	5715	47.1	1.0655	332.6 inf	691.6 inf	1287	3.2	Porities	1.0471
193	3488	612	1574	47.6	1.6713	366.4 inf	722.3 inf	1288	0.8	Porities	1.0476

Data from the -1650 m reef

Sample Number	^{238}U (ppb)	^{232}Th (ppt)	^{230}Th / ^{232}Th (atomic x10^{-6})	d^{234}U* (measured)	^{230}Th / ^{238}U (activity)	d^{234}U$_{initial}$** (corrected)	^{230}Th Age (ky BP)*** (corrected)	Depth (m)	Percent Calcite	Species	for plotting
227	6561	9375	11231	50.2	0.9720	106.6	266.4	1619	3.4	favid	±1.0502
228		193		50.2	0.8299	80.4	166.6	1621	25.0	favid	±1.0502
232	2525 ±5	182 ±12	233431 ±15708	34.4 ±2.2	1.0213 ±0.0047	107.9 ±10.0	404.9 +24.4/-20.9	1623	0.0	Porities	±1.0344
232	2471	159		35.2	1.0265	116.2 +13.8/-10.6	422.2 +36.4/-28.4	1623	0.0	Porities	±1.0352
232	2460	148	427	36.0	0.8385	59.5	587.5 +5.3/-5.1	1623	10.7	Porities	±1.0360
226d	2662	21760		36.2	1.1288	inf	inf	1624	0.7	favid	±1.0362
244	2820 ±2	11024 ±36	1721 ±43	140.3 ±1.3		313.0	287.9	1631	1.2	Porities	±1.1403
244	3021 ±1	75778 ±422	259 ±3	99.2 ±1.5	0.9944 ±0.0085	192.5 ±4.7	610.4 inf	1631	1.2	Porities	±1.0992
244	2862 ±6	353 ±5	143388 ±2390	51.2 ±2.1	1.0720 ±0.0077	394.7 inf	inf inf	1631	1.2	Porities	±1.0512
225	2557	9	218	30.9	1.0491	inf inf	inf inf	1635	35.2	echinopo	±1.0309
stepwise dissolution											
227	6561	9375	11231	50.2	0.9720	106.6	266.4	1619	3.4	favid	±1.0502
227-2	5514 ±7	22075 ±215	1747 ±24	64.0 ±1.5	0.4235 ±0.0043	74.8 ±1.8	55.1 ±0.7	1619	1.9	Favid	±1.0640
227-3	6617 ±14	6617 ±14	3179 ±161	52.3 ±1.6	0.2011 ±0.0094	55.9 ±1.7	23.1 ±1.2	1619	1.9	favid	±1.0523
227-4	7330 ±20	2035 ±58	4610 ±341	50.1 ±1.8	0.0775 ±0.0053	51.3 ±1.8	8.4 ±0.6	1619	1.9	favid	±1.0501
227-5	5947 ±17	322 ±31	8817 ±1603	50.7 ±1.9	0.0283 ±0.0045	51.2 ±1.9	3.0 ±0.5	1619	1.9	favid	±1.0507
228		193		50.2	0.8299	80.4	166.6	1621	25.0	favid	±1.0502
228-2	2792 ±4	14965 ±223	2041 ±71	27.7 ±1.5	0.6625 ±0.0209	38.0 ±2.1	112.2 ±6.0	1621	18.7	favid	±1.0277
228-3	1759 ±27	10024 ±138	3758 ±74	27.7 ±1.5	0.6625	inf inf	inf inf	1621	18.7	favid	±1.0277
228-4	424 ±2	111703 ±1003	4759 ±79	36.0 #####	75.9350 ±1.1300	inf inf	inf INF	1621	18.7	favid	±1.0360
228-5	315 ±0	93 ±1	25 ±1	-- --	0.0004 ±0.0001	-- --	0.6 ±0.0	1621	18.7	favid	#VALUE!
grainsize											
226 B	2463 ±96	23892 ±338	990 ±36	44.9 ±38.5	0.5818 ±0.0299	60.2 51!!!	103.4 +inf/-11.292	1624	0.6	favid	±1.0449
226 L	2976 ±5	43308 ±577	563 ±14	30.9 ±1.6	0.4959 ±0.0106	37.8 ±1.9	70.9 ±2.1	1624	0.6	favid	±1.0309
226 M	2676 ±3	62828 ±330	769 ±6	31.7 ±1.1	1.0929 ±0.0064	inf inf	inf in	1624	0.6	favid	±1.0317
226 F	4480 ±6	219601 ±2013	388 ±5	17.5 ±1.3	1.1505 ±0.0112	inf inf	inf inf	1624	0.6	favid	±1.0175

Data from the -1950 m reef

Sample Number	^{238}U (ppb)	^{232}Th (ppt)	^{230}Th / ^{232}Th (atomic x10^{-6})	d^{234}U* (measured)	^{230}Th / ^{238}U (activity)	d^{234}U$_{initial}$** (corrected)	^{230}Th Age (ky (corrected)	Depth (m)	Percent Calcite	Species	plotting
142	2822 ±8	4206 ±28	11388 ±99	34.1 ±2.6	1.0280 ±0.0064	117.2 -±1.3	437.3 -±1.3	1951	1	Acropora	1.0341
120	2858 ±6	22560 ±149	2494 ±6	71.4 ±2.6	1.1923 ±0.0091	inf inf	inf inf	1974	1	porites	1.0714
129	2829 ±8	258126 ±3241	350 ±7	40.3 ±3.1	±0.0273	inf inf	inf inf	1976	19	Acropora palifera	1.0403
135	2276 ±4	2321 ±21	25 ±1	30 ±1.9	0.0015 ±0.0001	30.1 ±1.9	134.0 ±15.0	1976	1	Acropora	
128	5283 ±16	11010 ±34	9308 ±39	34.2 ±3.3	1.1749 ±0.0049	inf inf	inf inf	1977	1	Acropora	1.0342
135	2272 ±4	1613 ±20	23835 ±308	29.9 ±1.9	1.0249 ±0.0030	107.5 +11/-10	452.6 +27.2/-2	1977	0	Porites	1.0299
135	3537	144		52.3		57.7	34.6	1977	0	Porities	1.0523
135d	2680	1103		31.3	1.0254	110.0 +9/-8	444.0 +20/-18	1977	0	Porities	
122	3559 ±8	53069 ±45	909 ±3	104.9 ±1.7	0.8205 ±0.0034	157.0 ±2.6	143.0 ±1.3	1992	6	Acropora	1.1049
142	2840 ±21	73231 ±1415	839 ±25	9.8 ±6.7	1.3103 ±0.0318	inf inf	inf inf	2076	15.9	Favid	1.0098
EDTA Experiment											
135ch3	2696	2690		30.2	1.0414	inf	>550	1977	0	Porities	1.0302
Dredge Samples from Geology Paper											
rd01-2a	3578	218		74.1	1.0713	226.0 ±7.0	393.0 ±10.0	1950	2	porites	1.07414
rd01-2b	3567	93		77.5	1.0661	218.0 ±7.0	365.0 ±10.0	1950	2	porites	1.07752
rd01-3b	2205	15		54.6	1.0295	146.0 ±5.0	348.0 ±10.0	1950	2	favid	1.05464

Data from the >-2000 m

Sample Number	^{238}U (ppb)	^{232}Th (ppt)	^{230}Th / ^{232}Th (atomic x10^{-6})	d^{234}U* (measured)	^{230}Th / ^{238}U (activity)	d^{234}U$_{Initial}$** (corrected)	^{230}Th Age (ky (corrected)	Depth (m)	Percent Calcite	Species
294	716 ±1	27671 ±229	585 ±8	28.9 ±2.0	1.3678 ±0.0137	inf inf	inf inf	2121		
303	2315 ±3	46775 ±305	957 ±9	9.2 ±1.7	1.1711 ±0.0082	inf inf	inf inf	2122	34.6	Porities
306	2754 ±4	1432 ±16	24098 ±36	63.3 ±2.6	0.7654 ±0.0075	93.0 ±3.9	136.1 ±2.7	2124	4.6	acropora
306	3044 ±7	7440 ±45	6707 ±6	39.7 ±2.9	0.9927 ±0.0058	96.3 ±7.9	313.1 +12.6/-11	2124	4.6	acropora
306	2701 ±7	4105 ±18	11231 ±70	32.6 ±2.6	1.0348 ±0.0054	133.8 +34.7/-20.8	499.9 +78.1/-50	2124		
312	**2701 ±7**	**4089 ±22**	**11285 ±80**	**32.6 ±2.6**	**1.0348 ±0.0054**	**133.8 +34.7/-20.8**	**499.9 +78.1/-50**	**2055**		
318	1997 ±8	8290 ±73	4806 ±60	26.8 ±4.1	1.2083 ±0.0119	inf inf	inf inf	2146	18.6	platygyra
323	1856 ±4	20731 ±113	1528 ±1	30.9 ±1.9	1.0337 ±0.0063	131.2 +46.5/-21.5	512.2 +105.9/-5	2138	8.0	Porities
324	2840	73231	839	9.8	1.3103	inf inf	inf inf	2076	5.5	Favid (massive)
327	2250 ±3	3670 ±17	10518 ±65	23.7 ±1.9	1.0393 0.0045	inf inf	inf inf	2423	15.0	Acropora
328	2126 ±4	16300 ±281	1805 ±81	26.9 ±2.1	0.8384 0.0348	45.0 ±4.5	182.1 +21.3/-17	2400+	?	?
331	1786 ±2	1494 11.0	24037 292	63.3 ±2.6	1.2177 0.0118	93 ±3.9	136.1 ±2.6	2423	19.9	Acropora
333	5476 11	140 10.6	inf inf	27.9 ±1.9	0.7179	inf inf	inf inf	2394	21.5	no id
298 ch2	2601	45500		27.5	1.0585	inf inf	inf	2121	12.6	acropora
edtacleaning										
306-edta	3161 ±7	4025 ±18	13736 ±8	52.2 ±1.8	1.0594 ±0.0048	202.0 +28.9/-20.2	478.5 +45.9/-34.7	2124	4.0	acropora
298 d	2878	30600		27.4	1.0377	inf inf	inf	2121	12.6	acropora

Table 2: Protactinium data for corals.

sample	depth (m)	231Pa/235U activity	231Pa Age (ka) uncorrected	Error on Pa age (ka)
89-a	241	0.716	59.5	1.1
3 EDTA	853	1.002		
3	853	1.000		
166 EDTA	1277	0.999		
166	1277	1.005		
226 EDTA	1624	0.839		
226	1624	0.915		
135EDTA	1977	0.984		
135	1977	0.983		
298 EDTA	2121	0.973		
298	2121	0.980		

Present Water Depth (m)	Modeled Age (ka)	Best Measured Age (ka) (sample number)	Rough Subsidence Rate (m/ka) = Depth (m)/Age (ka)
175	20 (Terrace not seen or sampled).	Not measured	
250	60 (2001 sample)	57.7 ± 1.5 (89-B) to 60.3 ± 0.5 (89-B)	250/60 = 4.2
625	112	None	625/112 = 5.6
830	145	393 +17/-16 (FC3) 587 +85/-55 (6)	830/393 = 2.1 830/587 = 1.4
1130	200	None	
1280	230	367.9 +22/-19 (197b)	1280/368 = 3.5
1640	295	404.9 +24/-21 (232) 422.2 +36/-28 (232) AVE (414 ka)	1640/414= 4.0
1950	348 ± 10 (dredge sample)	437.3 ± 1.3 (142)	1950/437 = 4.5 1950/348 = 5.6
2120	375	499.8 +78.1/-60 (312) 512.2 +106/-58 (323)	2120/500 = 4.2 2120/512 = 4.1
2390	410	No decent measurements	

Table 3. Predicted (Galewsky et al., 1996) and observed terrace locations in the Huon Gulf.

[1] J. Galewsky, Silver, E.A., Gallup, C.D., Edwards, R.L., and Potts, D.C. , Foredeep tectonics and carbonate platform dynamics in the Huon Gulf, Papua New Guinea, Geology 24(1996) 819-822.

[2] L.M. Wallace, dissertation, (2002).

[3] J.M. Webster, L. Wallace, E. Silver, B. Applegate, D. Potts, J.C. Braga, K. Riker-Coleman, C. Gallup, Drowned carbonate platforms in the Huon Gulf, Papua New Guinea, Geochemistry, Geophysics, Geosystems Volume 5(2004).

Chapter 5. Conclusion:

I studied the uranium-series isotopic composition of fossil corals from three settings: New Britain, Hawaii and the Huon Gulf. These three settings are distinct in their tectonic setting. New Britain corals are emergent as a result of tectonic uplift and the Hawaiian and Huon corals are submergent.

Corals samples from uplifted terraces in New Britain are highly altered due high rainfall rates in the area. I measured the ^{230}Th age of corals from the Holocene terrace and bracket its age to be between 4.3 ± 0.03 ka to 9.0 ± 0.16 ka. Using these ages, their present elevation and the corresponding paleo sea level, I compute an uplft rate for the Holocene terrace ranging from 0.4 to 2.1 m/ka, with an average uplift rate of 1.6 ±0.4 m/ka. Corals from other, older terraces have experienced a high degree of alteration to calcite. Corals from the pre-Holocene terraces were greater than 90% calcite and all had low uranium concentrations (< 1 ppm), suggestive of uranium loss during or after recrystallization to calcite. This recrystallization was probably due to the high amount of rainfall received in the area.

I report ^{230}Th ages of three fossil reefs from the northwestern coast of Hawaii: the -400 m reef at Mahukona (136.7 ± 0.9 ka to 151.8 ± 1.7 ka), the –1000 m terrace off eastern Kohala (377.2 +13.4/-12.2 ka and 392.5 +20.5/-17.9 ka) and the -1000 m reef off northwestern Kohala (286.5 ± 1.4 ka to 342.8 ± 1.4 ka). I was surprised to discover that submerged fossil corals from Hawaii contained large amounts of calcite. Conversion to calcite is common in emergent corals, but not thought to be as significant of a problem in submerged samples. An increase in calcite content in uplifted settings correlated with increasing elevation (and age) and suggests that calcification continues

to occur in emergent fossil corals with prolonged subaerial exposure (C. Gallup, unpublished data and Esat et al., 1999). Thus, older corals have more calcite in those settings. Submerged Hawaiian corals are altered to calcite early in their diagenetic history. Concordant ^{14}C and ^{230}Th ages of samples from Webster et al. (2004) agree to within one-percent of each other at roughly 15 ka, yet contain up to 14 percent calcite. Traditionally, we would consider these ages to be unreliable because of their high calcite content. Because the calibrated radiocarbon ages and ^{230}Th ages agree with each other, it is probable that recrystallization to calcite occurred early in the sample's diagenetic history. Unlike their subaerially exposed counterparts, calcite in submergent corals from Hawaii does not appear to be closely related to the age of a sample.

Uranium-series isotopic compositions of Hawaiian submerged corals resting on the sea bottom are not better preserved than their subaerially exposed counterparts, although their diagenetic signatures differ. From the submerged Hawaiian samples I identify three main trends in uranium-series isotopic composition: (1.) An increase in both 230Th/238U and 234U/238U; (2.) an increase in 230Th/238U with little change in 234U/238U; and (3.) low 230Th/238U with both low and high 234U/238U. The first trend is commonly observed in emergent corals and is attributed to alpha recoil (e.g. Gallup et al., 1994; Thompson et al., 2003; Villemant and Feuillet, 2003). Trend two is similar to that produced by ^{230}Th addition (Villemant and Feuillet, 2003) and I suggest that trend three is produced by ^{238}U addition. ^{230}Th addition is Hawaii may be the result of excess thorium present in seawater – that thorium may come from interaction of that seawater with nearby volcanic clastic sediments (in some cases located in horizons directly on top of the corals (J.Webster, personal communication) or from decay of

uranium in the overlying water column.

Corals from the Huon Gulf, while also submergent, do not exhibit the same trends in uranium-series isotopic composition as that observed in submerged corals from Hawaii. Measured ^{230}Th ages of coral samples from the Huon Gulf range from 60 ka to infinite age (>600 ka); however none of the measured corals were between 130 ka and 350 ka in age. The measured ^{230}Th ages of coral samples are older than we expected, but broadly increase in age with depth. Corals from three terraces (-1280 m, -1650 m, and -1950 m) represent material from Stage 11, suggesting that the model of terrace development is likely more complex than the original idea of a distinct sea-level rise event per terrace.

Like the samples from Hawaii, fossil corals from the Huon Gulf contain more calcite than expected. More than 75 percent of measured samples from the Huon Gulf contain more than 2 percent calcite. Although I am able to identify three main trends in the uranium-series isotopic compositions of the Hawaiian samples, no clear trend emerges in the Huon Gulf setting.

The subsidence rate (m/ka) computed from the most reliable ages of the deepest terraces suggests that the subsidence in the Huon Gulf averages 4 m/ka, slower than that predicted by Galewsky et al. (1996). Three terraces (1280 m, -1650 m, and -1950 m) have corals with ages broadly associated with Stage 11, indicating that preliminary modeling of the region was and current modeling remains incomplete.

Fundamentally what is the difference between the data from corals from the Huon Gulf and Hawaiian settings? The settings themselves make the difference. The distinction between the Hawaiian setting and the Huon Gulf setting is that the geologic

setting of Hawaii less complex. The island of Hawaii is subsiding as a result of loading of the oceanic lithosphere due to hot-spot related volcanic activity. The life span of one of volcano on Hawaii is likely to be 2-3 million years (Moore and Campbell, 1987) and the processes controlling the island's subsidence are likely to remain constant on a similar timescale. The Huon Gulf is forming as a result of lithospheric loading stemming from collision-related subduction. The geometry of the Huon Gulf is more complex, involving multiple lithospheric plates and the rates of motion of the involved plates are not constant and vary both in time and space. The models of Huon Gulf terrace development are inadequate to explain their present-day geomorphology.

Corals from the Huon Gulf on a gross observation are discolored in hand sample. When the samples were collected, they were bathed in sediment. Presumably that sediment comes from the volcanic-rich New Guinea Highlands, ripe with uranium and thorium, and infiltrates the water of the Gulf, adding both uranium and thorium to the water column. The sediment eventually rains down over and covers the corals. Corals that we collected were packed with sediment, probably both siliciclastic and carbonate in nature. While surficially bathed in sediment, the interior of corals from Hawaii retained their original color. In both settings, deeper corals likely gain thorium from the decay of uranium in the overlying water column.

Additionally, circulation of marine and meteoric waters throughout the reefs must be considered as a potential source term (either positive indicating gain or negative indicating loss) for uranium-series isotopes in the fossil corals. Cementation is enhanced with increased fluid circulation (Tucker and Wright, 1990). In Hawaii corals develop a calcite signature early in their diagenetic history. In the Huon Gulf the timing

of calcite cement and/or recrystallization is not as clearly defined. It may be possible (in the future) to refine the alpha-recoil models of open system behavior (Gallup et al., 1994; Thompson et al., 2003; Villemant and Feuillet, 2003) in corals to include an estimate of the water to rock ratio required to produce some of the open-system behavior I observe in the Huon samples.

Lastly a word on the differences observed between emergent and submerged corals. Uranium-series measurements of emergent corals (including those from New Britain) has focused on those corals in areas with fast enough uplift rates that they are divided into distinct terraces. Corals from these terraces tend to die as a result of subaerial exposure – suggesting that the chief diagenetic agent of these corals is meteoric water. Emergent coral terraces tend to exhibit diagenesis in the form of calcite replacement (and or sparry calcite cementation) and open-system behavior of uranium-series isotopes explained by the alpha-recoil processes. Submerged corals, while likely to have remained submerged in seawater since the time of their death, suffer from a multitude of diagenetic problems. An examination of the mineralogy of submerged corals alone identifies three chief issues: corals maybe be recrystallized to calcite, they may have develop marine aragonite cements, and/or they may develop marine calcite cements. Corals in a submerged near-shore environment also are subject to fluid circulation, bringing elements to or taking elements away from the coral skeleton. Finally sitting on the seafloor itself can be a source for diagenetic alteration: the coral skeleton can adsorb thorium from decay of uranium in the overlying water column and from siliciclastic and carbonate sediments deposited on top of the corals.

Bibliography

Abbott, L.D., Silver, E.A., and Galewsky, J., Silver, E.A., Gallup, C.D., Edwards, R.L., and Potts, D.C., 1994, Structural evolution of a modern arc-continent collision in Papua New Guinea: Tectonics, v. 13, p. 1007-1034.

Allison, N., Finch, A.A., Webster, J.M., and Clague, D.A., 2007, Palaeoenvironmental records from fossil corals: The effects of submarine diagenesis on temperature and climate estimates: Geochim. Cosmochim. Acta, v. 71, p. 4693-4703.

Amiel, A.J., Miller, D.S., and Friedman, G.M., 1973, Incorporation of uranium in modern corals: Sedimentology, v. 20, p. 523-528.

Andersen, M.B., Stirling, C.H., Potter, E.-K., Halliday, A.N., Blake, S.G., McCulloch, M.T., Aylin, B.F., and O'Leary, M., 2008, High-precision U-series measurements of more than 500,000 year old fossil corals: Earth and Planetary Science Letters, v. 265, p. 229-245.

Bard, E., Hamelin, B., and Fairbanks, R.G., 1990, U-Th ages obtained by mass spectrometry in corals from Barbados: sea level during the past 130,000 years: Nature, v. 346, p. 456-458.

Bard, E., Jouannic, C., Hamelin, B., Pirazzoli, P., Arnold, M., Faure, G., Sumosusastro, P., and Syaefudin, 1996, Pleistocene sea levels and tectonic uplift based on dating of corals from Sumba Island, Indonesia: Geophysical Research Letters, v. 23, p. 1473-1476.

Bathurst, R.G.C., 1983, Early diagenesis of carbonate sediments, in Parker, A., and Sellwood, B.W., eds., Sediment Diagenesis, D. Reidel Publishing Company, p. 349-377.

Bender, M.L., Fairbanks, R., Taylor, F.W., Matthews, R.K., Goddard, J.G., and Broecker, W., 1979, Uranium-series dating of the Pleistocene reef tracts of Barbados, West Indies: Geological Society of America Bulletin, v. 90, p. 577-594.

Berger, A., and Loutre, M.F., 1991, Insolation values for the climate of the last 10 million years: Quaternary Science Reviews, v. 10, p. 297-318.

Bloom, A.L., Broecker, W., Chappell, J., Matthews, R.K., and Mesolella, K.J., 1974, Quaternary sea level fluctuations on a tectonic coast: New 230Th/234U dates from the Huon Peninsula, New Guinea: Quat. Res., v. 4, p. 185-205.

Broecker, W., 1963, A preliminary evaluation of uranium series inequilibrium as a tool for absolute age measurements on marine carbonates: J Geophysical Research, v. 68, p. 2817-2834.

Broecker, W., and van Donk, J., 1970, Insolation changes, ice volumes and the 18O record in deep-sea cores: Rev. Geophys., Space Phys., v. 8, p. 169-197.

Broecker, W., Thurber, D., Ku, J.G.T.-l., Matthews, R.K., and Mesolella, K.J., 1968, Milankovitch Hypothesis Supported by Precise Dating of Coral Reefs and Deep-Sea Sediments: Science, v. 159, p. 297-300.

Campbell, J.F., and Erlandson, D.L., 1981, Geology of the Kohala submarine terrace, Hawaii: Marine Geology, v. 41, p. 63-72.

Chappell, J., 1974, Geology of coral terraces, Huon Peninsula, New Guinea: A study of Quaternary tectonic movements and sea-level changes: Geological Society of America Bulletin, v. 85, p. 553-570.

Chappell, J., 1996, Reconciliation of late Quaternary sea levels derived from coral terraces at Huon Peninsula with deep sea oxygen isotope records: Earth and Planetary Science Letters, v. 141, p. 227-236.

Chappell, J., and Veeh, H.H., 1978, Late Quaternary tectonic movements and sea-level changes at Timor and Atauro Island: Geological Society of America Bulletin, v. 89, p. 356-368.

Cheng, H., Edwards, R.L., Hoff, J., Gallup, C.D., Richards, D.A., and Asmerom, Y., 2000, The half-lives of uranium-234 and thorium-230: Chemical Geology, v. 169, p. 17-33.

Cheng, H., Edwards, R.L., Wang, Y., Kong, X., Ming, Y., Kelly, M.J., Wang, X., Gallup, C.D., and Liu, W., 2006, A penultimate glacial monsoon record from Hulu Cave and two-phase glacial terminations: Geology, v. 34, p. 217-220.

Clague, D.A., Reynolds, J.R., Maher, N., Hatcher, G., Danforth, W., and Gardner, J.V., 1998, High-resolution Simrad EM300 Multibeam surveys near the Hawaiian Islands: Canyons, reefs, and landslides: Eos (Transactions, American Geophysical Union), v. 79, p. F826.

Crook, K., 1989, Suturing history of an allochthonous terrane at a modern plate boundary traced by flysch-to-molasse facies transitions: Sedimentary Geology, v. 61, p. 49-79.

Cutler, K., 2003, Rapid sea-level fall and deep-ocean temperature change since the last interglacial period Earth and Planetary Science Letters, v. 206, p. 253-271.

Cutler, K.B., Edwards, R.L., Taylor, F.W., Cheng, H., Adkins, J., Gallup, C.D., Cutler, P.M., Burr, G.S., Chappell, J., and Bloom, A.L., 2003, Rapid sea-level fall and deep-

ocean temperature change since the last interglacial period: Earth and Planetary Science Letters, v. 206, p. 253-271.

Davies, H.L., Honza, E., Tiffin, D.L., Lock, J., Okuda, Y., Keene, J.B., Murakami, F., and Kisimota, K., 1987, Regional setting and structure of the western Solomon Sea: Geo-Marine Letters, v. 7, p. 153-160.

DeMets, C., Gordon, R.G., Argus, D.F., and Stein, S., 1994, Effects of recent revisions to the geomagnetic reversal time scale on estimates of current plate motions: Geophys. Res. Letters, v. 21, p. 2191-2194.

Dow, D.B., 1977, A geological synthesis of Papua New Guinea: Bur. Miner. Resour. Aust. Bull., v. 201, p. 1-41.

Edwards, R.L., Beck, J., Burr, G.S., Donahue, D.J., Chappell, J.M., Bloom, A.L., Druffel, E.R.M., and Taylor, F.W., 1993, A large drop in atmospheric 14C/12C and reduced melting in the Younger Dryas, documented with 230Th ages of corals: Science, v. 260, p. 962-968.

Edwards, R.L., Chen, J.H., and Wasserburg, G.J., 1987, U-238-U-234-Th-230-Th-232 systematics and the precise measurement of time over the past 500,000 years.: Earth and Planetary Science Letters.

Edwards, R.L., Cutler, K.B., Cheng, H., and Gallup, C.D., 2003, Geochemical evidence for Quaternary sea-level changes, in Turekian, H.D.H.a.K.K., ed., Treatise on Geochemistry: The Oceans and Marine Geochemistry, Volume 6: Oxford, Elsevier-Pergamon, p. 343-364.

Edwards, R.L., Gallup, C.D., and Cheng, H., 2003, Uranium-series dating of marine and lacustrine carbonates, in Bourdon, B., Henderson, G.M., Lundstrom, C.C., and Turner, S.P., eds., Uranium-series Geochemistry, Volume 52: Reviews in Mineralogy and Geochemistry, p. 363-405.

Edwards, R.L., Gallup, C.D., Taylor, F.W., and Quinn, T.M., 1991, 230Th/238U and 234U/238U in submarine corals: Evidence for Diagenetic Leaching of 234U: Eos (Transactions, American Geophysical Union), v. 72, p. 535.

Enmar, R., Stein, M., Bar-Matthews, M., Sass, E., Katz, A., and Lazar, B., 2000, Diagenesis in live corals from the Gulf of Aqaba I: The effect on paleo-oceanography tracers: Geochim. Cosmochim. Acta, v. 64, p. 3123-3132.

Esat, T.M., McCulloch, M.T., Chappell, J., Pillans, B., and Omura, A., 1999, Rapid fluctuations in sea level recorded at Huon Peninsula during the penultimate deglaciation: Science, v. 283, p. 197-204.

Galewsky, J., and Silver, E.A., 1997, Tectonic controls on facies transitions in an oblique collision: The western Solomon Sea, Papua New Guinea: Geological Society of America Bulletin, v. 109, p. 1266-1278.

Galewsky, J., Silver, E.A., Gallup, C.D., Edwards, R.L., and Potts, D.C. , 1996, Foredeep tectonics and carbonate platform dynamics in the Huon Gulf, Papua New Guinea: Geology, v. 24, p. 819-822.

Gallup, C.D., Cheng, H., Speed, R., Taylor, F.W., and Edwards, R.L., 2002, Direct Determination of the Timing of Sea Level Change During Termination II: Science, v. 295, p. 310-314.

Gallup, C.D., Edwards, R.L., and Johnson, R.G., 1994, The timing of high sea levels over the past 200,000 years: Science, v. 263, p. 796-800.

Goreau, T., 1959, The ecology of Jamaican coral reefs. 1. Species composition and zonation: Ecology, v. 40, p. 67-90.

Hantoro, W.S., Pirazzoli, P.A., Jouannin, C., Faure, H., Hoang, C.T., Radtke, U., Causse, C., Best, M.B., Lafont, R., Bieda, S., and Lambeck, K., 1994, Quaternary uplifted coral reef terraces on Alor Island, east Indonesia: Coral Reefs, v. 13, p. 215-223.

Hays, J., Imbrie, J., and Shackleton, N., 1976, Variations in the Earth's orbit: Pacemaker of the ice ages: Science, v. 194, p. 1121-1132.

Henderson, G., and Slowey, N., 2000, Evidence from U-Th dating against Northern Hemisphere forcing of the penultimate deglaciation: Nature, v. 404, p. 61-66.

Henderson, G.M., 2002, Seawater (234U/238U) during the last 800 thousand years.: Earth and Planetary Science Letters, v. 199, p. 97-110.

Henderson, G.M., Slowey, N.C., and Fleisher, M.Q., 2001, U–Th dating of carbonate platform and slope sediments. : Geochim. Cosmochim. Acta, v. 65, p. 2757-2770.

Hilman Natawidjaja, D., Sieh , K., Galetzka, J., Suwargadis, B.W., Cheng, H., Edwards, R.L., and Chilfeh, M., 2007, Interseismic deformation above the Sunda Megathrust recorded in coral microatolls of the Mentawai islands, West Sumatra: Journal of Geophysical Research, v. 112, p. B02404.1-B02404.27.

Hughen, K., Baillie, M., Bard, E., Bayliss, A., Beck, J., Bertrand, C., Blackwell, P., Buck, C., Burr, G., Cutler, K., Damon, P., Edwards, R., Fairbanks, R., Friedrich, M., Guilderson, T., Kromer, B., McCormac, F., Manning, S., Ramsey, C.B., Reimer, P., Reimer, R., Remmele, S., Southon, J., Stuiver, M., Talamo, S., Taylor, F., Plicht, J.v.d.,

and Weyhenmeyer, C., 2004, MARINE04 Marine radiocarbon age calibration, 0–26 cal kyr BP: Radiocarbon, v. 46, p. 1059-1086.

Johnson, R.W., 1979, Geotectonics and volcanism in Papua New Guinea: A review of the late Cainozoic: BMR Journal of Australian Geology and Geophysics, v. 4, p. 181-207.

Lambeck, K., and J. Chappell 2001, Sea level change through the last glacial cycle: Science, v. 292, p. 679-686.

Lambeck, K., Yokoyama, Y., and Purcell, T., 2002, Into and out of the Last Glacial Maximum: sea-level change during Oxygen Isotope Stages 3 and 2 Quaternary Science Reviews, v. 21, p. 343-360.

Lazar, B., Enmar, R., Schossberger, M., Bar-Matthews, M., Halicz, L., and Stein, M., 2004, Diagenetic effects on the distribution of uranium in live and Holocene corals from the Gulf of Aqaba: Geochimica et Cosmochimica Acta, v. 68, p. 4583-4593.

Ludwig, K.R., Szabo, B.J., Moore, J.G., and Simmons, K.R., 1991, Crustal subsidence rate off Hawaii determined from 234U/238U ages of drowned coral reefs: Geology, v. 19, p. 171-174.

Matsuda, F., Campbell, C., and Wallensky, E., 1994, Recent coralline algal assemblages at Huon Peninsula, in Ota, Y., ed., Study on Coral Reef Terraces of the Huon Peninsula, Papua New Guinea: establishment of Quaternary sea level and tectonic history.I GCP Contribution 274; Monbusho International Research Program Preliminary Report, p. 117-118.

McCulloch, M., Tudhpe, A.W., Esat, T.M., Mortimer, G.E., Chappell, J., Pillans, B., Chivas, A.R., and Omura, A., 1999, Coral record of equatorial sea-surface temperature during the penultimate deglaciation at Huon Peninsula: Science, v. 283, p. 202-204.
Moore, J., and Campbell, J.F., 1987, Age of tilted reefs, Hawaii: Journal of Geophysical Research, v. 92, p. 2641-2646.

Moore, J., and Fornari, D.J., 1984, Drowned reefs as indicators of the rate of subsidence of the island of Hawaii: Journal of Geology, v. 92, p. 753-759.

Moore, J.G., 1987, Subsidence of the Hawaiian Ridge, in Decker, R.W., Wright, T.L., and Staufer, P.H., eds., Volcanism in Hawaii U.S. Geological Survey Professional Paper: Washington DC, p. 85-100.

Moore, J.G., and Clague, D.A., 1987, Coastal laval flows from Mauna Loa and Hualalai volcanoes: Bulletin of Volcanology, v. 49, p. 752-764.

Moore, J.G., Ingram, B.L., Ludwig, K.R., and Clague, D.A., 1996, Coral ages and island subsidence, Hilo drill hole: Journal of Geophysical Research, v. 101, p. 11599-11606.

Moore, P.R., 1987b, Ages of the raised beaches of Turakirae Head, New Zealand: A reassement based on radiocarbon dates.: Royal Society of New Zealand Bulletin., v. 74, p. 357-375.

Nakamori, T., Campbell, C.R., and Wallensky, E., 1994, Recent hermatypic coral assemblages at Huon Peninsula., in Ota, Y., ed., Study on Coral Reef Terraces of the Huon Peninsula, Papua New Guinea: establishment of Quaternary sea level and tectonic history.I GCP Contribution 274; Monbusho International Research Program Preliminary Report, Volume 104, p. 111-117.

Nakamori, T., Matsuda, S., Omura, A., and Ota, Y., 1995, Depositional Environments of the Pleistocene Reef Limetone at Huon Peninsula, Papua New Guinea on the Basis of Hermatypic Coral Assemblages: Journal of Geography (Japan), v. 104, p. 725-742.

Nakamori, T., Wallensky, E., and Campbell, C., 1994, Recent hermatypic coral assemblages at Huon Peninsula: Contrib. Int. Geol. Correlation Prog., v. 274, p. 111-116.

Ota, Y., and J. Chappell 1996, Late Quaternary coseismic uplift events on the Huon Peninsula, Papua New Guinea, deduced from coral terrace data: Journal of Geophysical Research, B, Solid Earth and Planets, v. 101, p. 6071-6082.

Ota, Y., Chappell, J., Kelly, Yonekura, N., Matsumoto, E., Nishimura, T., and Head, J., 1993, Holocene coral reef terraces and coseismic uplift of Huon Peninsula, Papua New Guinea: Quaternary Research, v. 40.

Pandolfi, J.M., 1995, Limited membership in Pleistocene reef coral assemblages from the Huon Peninsula, Papua New Guinea: constancy during global change: Paleobiology, v. 22, p. 152-176.

Pandolfi, J.M., and Minchin, P.R., 1995, A comparison of taxanomic composition and diversity between reef coral life and death assemblages in Madang Lagoon, Papua New Guinea: Palaeogeography, Palaeoclimatology, Palaeoecology, v. 119, p. 321-341.

Pigram, C.J., and Davies, H.L., 1987, Terranes and the accretion history of the New Guinea orogen: BMR J. Aust. Geol. Geophys., v. 10, p. 193-211.

Pigram, C.J.a.D., H.L, 1987, Terranes and accretion history of the New Guinea orogen: BMR Journal of Australian Geology and Geophysics, v. 19, p. 55-76.

Pirazzoli, P.A., 1993, A one million-year-long sequence of marine terraces on Sumba Island, Indonesia: Marine Geology, v. 109, p. 221-236.

Pirazzoli, P.A., Radtke, U., Hantoro, W.S., Jouannic, C., Hoang, C.T., Causse, C., and Best, M.B., 1993, A one million-year-long sequence of marine terraces on Sumba Island, Indonesia: Marine Geology, v. 109, p. 221-236.

Potthast, I., 1992, Short-term progressive early diagenesis in density bands of recent corals:Porites Colonies, Mauritius Island, Indian Ocean: Facies, v. 27, p. 105-111.

Reeder, R.J., M. Nugent, C. D. Tait, D. E. Morris, S. M., and Heald, K.M.B., W. P. Hess, and A. Lanzirotti, 2001, Coprecipitation of uranium (VI) with calcite: XAFS, micro-XAS, and luminescence characterization: Geochim. Cosmochim. Acta, v. 65, p. 3491-3503.

Riker-Coleman, K.E., Gallup, C.D., Wallace, L.M., Webster, J.M., Cheng, H., and Edwards, R.L., 2006, Evidence of Holocene uplift in east New Britain, Papua New Guinea: Geophys. Res. Letters, v. 33, p. L18612

Riker-Coleman, K.E., Webster, J.M., Gallup, C.D., Wallace, L.M., and Silver, E.A., 2004, Evidence of rapid tectonic uplift in East New Britian, Papua New Guinea: Geological Society of America Abstracts with Programs, v. 36, p. 215-231.

Sellwood, B.W., 1994, Principles of Carbonate Diagenesis in Parker, A., and Sellwood, B.W., eds., Quantitative Diagenesis: Recent Developments and Applications to Reservoir Geology: Netherlands, Kluwer Academic Publishers, p. 1-32.

Shackleton, N.J., and Opdyke, N.D., 1973, Oxygen isotope and palaeomagnetic stratigraphy of equatorial Pacific core V28-238: Oxygen isotope temperatures and ice volumes on a 10^6 year scale: Quat. Res., v. 3, p. 39-55.

Sharp, W.D., and Renne, R.P., 2006, The 40Ar/39Ar dating of core recovered by the Hawaii Scientific Drilling Project (Phase 2), Hilo, Hawaii: Geochemistry, Geophysics, Geosystems, v. 6.

Shen, C.-C., Edwards, L.R., Cheng, H., Dorale, J.A., Thomas, R.B., Bradley, M.S., Weinstein, S.E., and Edmonds, H.N., 2002, Uranium and thorium isotopic and concentration measurements by magnetic sector inductively coupled plasma mass spectrometry: Chemical Geology, v. 185, p. 165-178.

Shen, G.T., and R. B. Dunbar 1995, Environmental controls on uranium in reef corals: Geochim. Cosmochim. Acta, v. 59, p. 2009-2024.

Sherman, C.E., Fletcher, C.H., and Rubin, K.H., 1999, Marine and meteoric diagenesis of Pleistocene carbonates from a nearshore submarine terrace, Oahu, Hawaii: J. Sed. Res., v. 69, p. 1083-1097.

Siddall, M., Rohling, E.J., Almogi-Labin, A., Hemleben, C., Meischner, D., Schmelzer, I., and Smeed, D.A., 2003, Sea-level fluctuations during the last glacial cycle: Nature, v. 423, p. 853-859.

Silver, E.A., Abbott, L.D., Kirchoff-Stein, K.S., Reed, D.L., Bernstein-Taylor, B., and Hilyard, D. , 1991, Collision propagation in Papua New Guinea and the Solomon Sea: Tectonics, v. 10, p. 863-874.

Silver, E.A., Kirchoff-Stein, L., Reed, K.S., Bernstein, B.L., and Hilyard, D., 1991, Collision propagation in Papua New Guinea and the Solomon Sea: Tectonics, v. 10, p. 863-874.

Smith, J.R., Satake, K., and Suyehiro, K., 2002, Deepwater multibeam sonar surveys along the southeastern Hawaiian Ridge: Guide to the CD-ROM in Takahashi, E., et al., ed., Hawaiian volcanoes: Deep underwater perspectives, p. 3–9.

Stein, M., Wasserburg, G.J., Aharon, P., Chen, J.H., Zhu, Z.R., Bloom, A., and Chappell, J., 1993, TIMS U-series dating and stable isotopes of the last interglacial event in Papua New Guinea: Geochimica et Cosmochimica Acta, v. 57, p. 2541-2554.

Stirling, C.H., Esat, T.M., Lambeck, K., McCulloch, M.T., 1998, Timing and duration of the Last Interglacial: Evidence for a restricted interval of widespread coral reef growth: Earth and Planetary Science Letters, v. 160, p. 745-762.

Taylor, F.W., Frohlich, C., Lecolle, J., and Strecker, M., 1987, Analysis of Partially Emerged Corals and Reef Terraces in the Central Vanuatu Arc: Comparison of Contemporary Coseismic and Nonseismic With Quaternary Vertical Movements Journal of Geophysical Research, v. 92, p. 4905-4933.

Thompson, W.G., and Goldstein, S.L., 2005, Open-system coral ages reveal persistent suborbital sea-level cycles: Science, v. 308, p. 401-404.

Thompson, W.G., Spiegelman, M.W., Goldstein, S.L., and Speed, R.C., 2003, An open-system model for U-series age determinations of fossil corals: Earth and Planetary Science Letter, v. 210, p. 365-381.

Thurber, I.D., broeker, S.W., Blanchard, R.L., and Potratz, H.A., 1965, Uranium-series ages of Pacific atoll coral.: Science, v. 149, p. 55-59.

Tregoning, P., Jackson, R.J., McQueen, H., Lambeck, K., Stevens, C., Little, R.P., Curley, R., Rosa, R., 1999, Motion of the South Bismarck plate, Papua New Guinea: Geophys. Res. Letters, v. 26, p. 3517-3520.

Tucker, M., E., and Wright, V.P., 1990, Carbonate Sedimentology: Oxford, Blackwell Science, 482 p.

Villemant, B., and Feuillet, N., 2003, Dating open systems by the 238U-234U-230Th method: application to Quaternary reef terraces: Earth and Planetary Science Letter, v. 210, p. 105-118.

Walcott, R.I., 1987, Geodetic strain and the deformational history of the North Island of New Zealand during the late Cainozoic: Philos. Trans. R. Society of London Series A, v. 321, p. 163-181.

Wallace, L.M., 2002, Tectonics and arc-continent collision in Papua New Guinea: Insights from geodetic, geophysical and geologic data: Santa Cruz, California, University of California.

Wallace, L.M., Stevens, C., Silver, E., McCaffrey, R., Loratung, W., Hasiata, S., Stanaway, R., Curely, R., Rosa, R., Taugaloidi, J., 2004, GPS and seismological constraints on active tectonics and arc-continent collision in Papua New Guinea: Implications for mechanics of microplate rotations in a plate boundary zone: Journal of Geophysical Research, v. 109, p. B05404.

Webster, J.M., Braga, J.C., Clague, D.A., Gallup, C.D., hein, J.R., Potts, D.C., Renema, W., Riding, R., Riker-Coleman, K., Silver, E., and Wallace, L.M., accepted, in revision, Coral Reef Evolution on Rapidly Subsiding Margins: Global and Planetary Change, Special Issue.

Webster, J.M., Clague, D.A., Riker-Coleman, K., Gallup, C., Braga, J.C., Potts, D., Moore, J.G., Winterer, E.L., and Paull, C.K., 2004a, Drowning of the -150 m reef off Hawaii: A casualty of global meltwater pulse 1A?: Geology, v. 32, p. 249-252.

Webster, J.M., Wallace, L., Silver, E., Applegate, B., Potts, D., Braga, J.C., Riker-Coleman, K., and Gallup, C., 2004b, Drowned carbonate platforms in the Huon Gulf, Papua New Guinea: Geochemistry, Geophysics, Geosystems, v. Volume 5.

Webster, J.M., Wallace, L., Silver, E., Potts, D., Braga, J.C., Renema, W., Riker-Coleman, K., and Gallup, C., 2004, Coralgal composition of drowned carbonate platforms in the Huon Gulf, Papua New Guinea ; implications for lowstand reef development and drowning Marine Geology, v. 204, p. 59-89.

Webster, J.M., Wallace, L.M., Clague, D.A., and Braga, J.C., 2007, Numerical modeling of the growth and drowning of Hawaiian coral reefs during the last two glacial cycles (0–250 kyr): Geochemistry, Geophysics, Geosystems, v. 8, p. Q03011.

Wilson, J.T., 1963, A possible origin of the Hawaiian Islands: Canadian Journal of Physics, v. 41, p. 863-870.

From: Michael Connolly <MConnolly@agu.org>
Subject: **Re: copyright**
Date: December 18, 2008 10:27:10 AM CST
To: Kristin Riker-Coleman <krikerco@tc.umn.edu>

We are pleased to grant permission for the use of the material requested for inclusion in your thesis. The following non-exclusive rights are granted to AGU authors:

- All proprietary rights other than copyright (such as patent rights).
- The right to present the material orally.
- The right to reproduce figures, tables, and extracts, appropriately cited.
- The right to make hard paper copies of all or part of the paper for classroom use.
- The right to deny subsequent commercial use of the paper.

Further reproduction or distribution is not permitted beyond that stipulated. The copyright credit line should appear on the first page of the article or book chapter. The following must also be included, "Reproduced by permission of American Geophysical Union." To ensure that credit is given to the original source(s) and that authors receive full credit through appropriate citation to their papers,
we recommend that the full bibliographic reference be cited in the reference list. The standard credit line for journal articles is: "Author(s), title of work, publication title, volume number, issue number, citation number (or page number(s) prior to 2002), year. Copyright [year] American Geophysical Union."

If an article was placed in the public domain, in which case the words "Not subject to U.S. copyright" appear on the bottom of the first page or screen of the article, please substitute "published" for the word "copyright" in the credit line mentioned above.

Copyright information is provided on the inside cover of our journals. For permission for any other use, please contact the AGU Publications Office at AGU, 2000 Florida Ave., N.W., Washington, DC 20009.

Michael Connolly
Journals Publications Specialist

On 12/18/2008 11:25 AM, Kristin Riker-Coleman wrote:

> Hi,
> We just spoke on the phone. I'm putting together the final document that will be my PhD dissertation for the University of Minnesota. I have to include a letter authorizing use of the material from the publisher to include the material in my dissertation.
> This letter must state that "the copyright owner is aware that ProQuest may supply single copies on demand. If permissions are not supplied, ProQuest will not publish copyright materials".
> This is the article's citation:
> Riker-Coleman, K. E., C. D. Gallup, L. M. Wallace, J. M. Webster, H. Cheng, and R. L. Edwards (2006),
> Evidence of Holocene uplift in east New Britain, Papua New Guinea,
> Geophys. Res. Lett., 33, L18612, doi:10.1029/2006GL026596
> Thanks,
> Kristin
> *Kristin Riker-Coleman*
> PhD. Candidate
> Geology Department
> University of Minnesota
> Duluth, MN 55812
> phone: 218-341-3251
> krikerco@umn.edu <mailto:krikerco@umn.edu>